Universität für Bodenkultur Wien

Department of Biotechnology

Institute of Applied Microbiology

Supervised by O. Univ. Prof. Dipl. –Ing. Dr. nat. techn.Hermann Katinger

Title of Doctoral Thesis:

Characterization of membrane protein complexes including neurotransmitter receptors and transporters in mouse hippocampus

Dissertation for obtaining a doctorate degree at the University of Natural Resources and Applied Life Sciences Vienna

Submitted By

Gangsoo Jung

Vienna, May 2015

I. Acknowledgement

I would like to thank Prof. Gert Lubec, who excellently supervised me during this work. He continuously supported me in all aspects and trusted my ability to work on this project that was performed in a collaborating laboratory.

The results of my thesis have been published in a total of 2 papers as a partial requirement for this thesis. These papers are attached as Appendix 1 and 2.

In paper one, I performed the gel based proteomic experiments from membrane fractionation from mouse hippocampus to analysis of the protein in native gels, Western blot and mass spectrometry with critical advices of Seok Heo under supervision of Gert Lubec. All animal experiments were carefully performed by Tamara beuk and Harald Hoeger on Himberg. All experiments were designed and written by Gert Lubec.

In paper two, I have performed genotyping of drebrin knockout mice with great helps of Manuella in Johannes Berger's supervision and native gel based analysis of neuro transmitter receptors complex in mouse hippocampus. Moreover, I participated in brain preparation of imaging works with Eungjung and Sunetra. Electrophysiological works were performed by Francisco J. Monje and Cicvaric in the Department of Neurophysiology and Neuropharmacology, Medical University of Vienna.

I appreciate all my international colleagues in the lab including, my senior Korean Doctors, Sungung, Narkhyun, Seok, Eunjung and Jaewon, Hungarian cigarette smoking team Edit, peter, Indian best chiefs, sunetra, saras, and their husbands and other lab members. They kept me working in stable condition and gave many valuable advices. Moreover, I gave many thanks to my brother DDGSJ Seungjun, Geunyoung, Jaehyun, Haesol and Vienna fam.

Lastly, I dedicate this work to my mom and dad. Without their supporting and sacrifice, I couldn't manage my works and life in Vienna.

Table of contents

Appendix 1 Article:

Hippocampal glutamate transporter 1 (GLT-1) complex levels are paralleling memory training in the Multiple T-maze in C57BL/6J mice. Seok Heo*, Gangsoo Jung*, Tamara Beuk, Harald Hoeger, Gert Lubec, Brain Struct Funct (2012) 217:363–378

Appendix 2 Article:

Drebrin depletion alters neurotransmitter-receptor levels in protein-complexes, dendritic spine morphogenesis and memory-related synaptic plasticity in the mouse hippocampus. Gangsoo Jung*, Eun-Jung Kim*, Ana Cicvaric, Sunetra Sase, Arnold Pollak, Marion Gröger, Harald Höger, Sialana Fernando, Johannes Berger, Francisco J. Monje and Gert Lubec, J Neurochem. (2015)

I. Introduction

I. 1. Hippocampus

The hippocampus belongs to the limbic system which has a fundamental site in mammalian memory. Functions of the hippocampus in memory were first researched in the patient named as Henry Gustav Molaison by Scoville and Milner (Scoville & Milner, 2000). In an attempt to remove epileptic seizures, patient H.M. was under an operation, which leads destruction of hippocampus. H.M. suffered from serious anterograde and partial retrograde amnesia. The case was fascinating since H.M. could not remember new memories that have formed after surgery but his long-term memories were undamaged and especially he could recall the events happened in his childhood. In later, many studies in patients with damage on the hippocampus and amnesia were investigated and the numbers of animal experiments have been performed in order to discover functions and working mechanisms of the hippocampus. Extensively evidences suggested that the hippocampus closely related to the formation of episodic memories in humans and in consolidating information into long-term declarative memory.

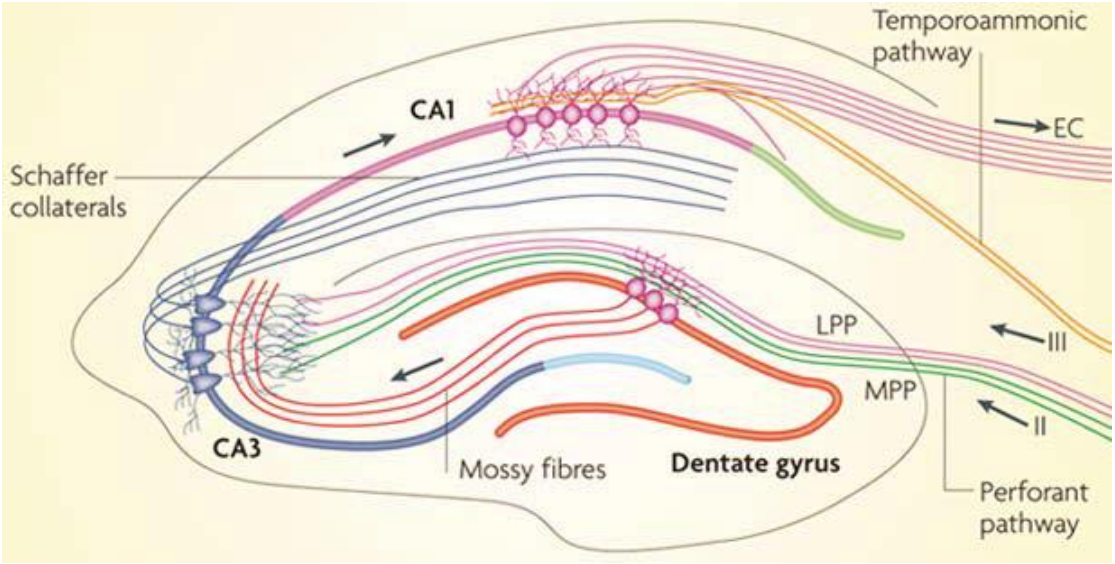

Figure 1. Diagram of the hippocampal neural network. (Deng. et al., *Nat Rev Neurosci*. 2010)

In structural property, hippocampus is a curved tube shape, divided into regions as dentate gyrus and cornu ammonis (CA). The dentate gyrus expands from entorhinal cortex and thus, definition of hippocampus is used to describe the CA and along with the dentate gyrus. The CA is segregated into CA1, CA2, CA3 and CA4 (Andersen, 2007) A diagram of

the hippocampal neural network is shown in Figure 1. Input signal starts from the axons of layer II neurons in Entorhinal cortex (Shim & Lubec), and it forms connections with the dentate gyrus (Collingridge et al) and CA3 pyramidal neurons via the perforant path including lateral (LPP) and medial perforant path (MPP). CA3 neurons also receive input from the DG via the Mossy fibers (MF). Afterwards, this information is sent to CA1 pyramidal neurons through the Schaffer Collateral pathway (SC). CA1 pyramidal neurons send back projections into deep-layer neurons of the EC (Deng et al, 2010). Dentate gyrus projections are mainly towards CA3 area. There are three layers of neurons as molecular, granular, and polymorphic. Granule cells are principal excitatory neurons and are projecting to interneurons and pyramidal neurons (Andersen, 2007).

As discussed above, since H.M. case proved that the hippocampus influence in the memory and many studies have determined the structural and functional role of hippocampus in learning and memory. In addition to studies in human, the studies involving hippocampus in animal learning and memory models have been shown that the hippocampal lesion yields impairment of learning in animal learning paradigms. Several tasks as delayed non-matching to sample (Clark et al, 2001; Zola-Morgan & Squire, 1986), radial arm maze (Hudon et al, 2002), water maze (Morris, 1984) and contextual fear conditioning in rodents (Li et al, 1999) showed that the hippocampus plays pivotal roles in memory and learning.

I.1.1. Dendritic spine

Small protrusions, called dendritic spines, arising from shaft in dendritic region which were first described by Ramón y Cajal, with almost all (>95%) of excitatory synaptic inputs to pyramidal neurons being received by spines. Dendritic spines contain postsynaptic structure such as post synaptic density (PSD), cytoskeletal proteins and their binding proteins (Colgan & Yasuda, 2014). Spines consist of three fundamental components: a delta shaped base at the junction with the dendritic shaft, a constricted neck in middle and head containing an axon. Their lengths are varying from 0.2 to 2 um and volumes from 0.001 to 1 um^3 (Bosch et al, 2014). Dendritic protrusions are very thin and long; these protrusions are called dendritic filopodia. (Figure 2A) In contrast, at the mature stage (Figure 2B) dendrites are covered by dendritic spines, which commonly have an expanded head and a narrow neck.

Based on electron microscopy (Hollmann & Heinemann), morphologies of dendritic spines are generally classified into three categories according their size and head shapes; (1) thin, filopodia-like protrusions (thin spines) which composed of small head and elongated

neck, (2) short spines without a well-defined spine neck (stubby spines), and (3) spines with a relatively large bulbous head (mushroom spines) which are associated with mature and stable synapses (Figure.2C) (Sekino et al, 2007). Before the appearance of dendritic spines, dendrites exhibit long, thin filopodia like protrusion. As the brain matures, the number of dendritic filopodia is reduced and stable dendritic spines with mushroom and stubby shapes are increased (Calabrese et al, 2006; Svitkina et al, 2010). Interestingly, three shapes are not static but the structures can interchange among the shapes according to activity and plasticity. (Hotulainen & Hoogenraad, 2010) Live imaging studies showed shapes and size of dendritic spines are highly dynamic in response to synaptic transmission in vitro and experience in vivo. (Roberts et al, 2010) The morphological changes are closely correlated with the size of post synaptic density, and glutamate evoked responses leading to changes in the strength of excitatory synapse and synaptic activities. So, functional and structural changes of spines are thought to be core of learning and memory in brain.

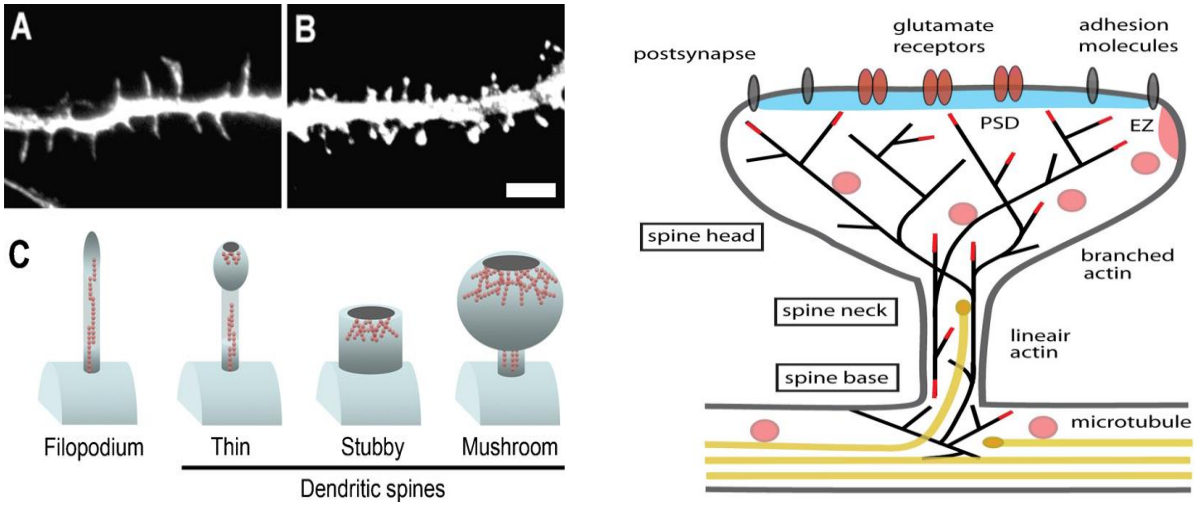

Figure 2. Morphology of dendritic protrusions, filopodia and spines (Sekino Y., *Neurochem Int.* 2007)

Indeed, the studies of spine morphologies in dementia patients showed loss or alteration of spine structures along with neurodegenerative disorders such as Alzheimer's disease, Parkinson's disease and Huntingtun disease (Dickstein et al, 2013; Knobloch & Mansuy, 2008). Moreover, the reduced density of spines is one of observed features have been found in schizophrenia and depression (Moyer et al, 2014).

An important structural component in dendritic spines is the postsynaptic density (PSD), which positions glutamate receptors including, alpha amino-3-hydroxy-5-methyl-4-isoxazolepropionic acid receptor (AMPA), N-methyl-D-aspartate (NMDA), and metabotropic

subtype, and voltage-gated Ca2+ channels, PSD-95, Shank, and calcium/calmodulin-dependent kinase II (CaMKII) in close to the pre-synaptic region and provides scaffold proteins for synaptic signaling molecules (Bosch et al, 2014). The size of PSD is closely correlated with morphologies of spine head, and the number of synaptic AMPA receptors and additionally, docked synaptic vesicles are proportional to the size of PSD (Hanley, 2014).

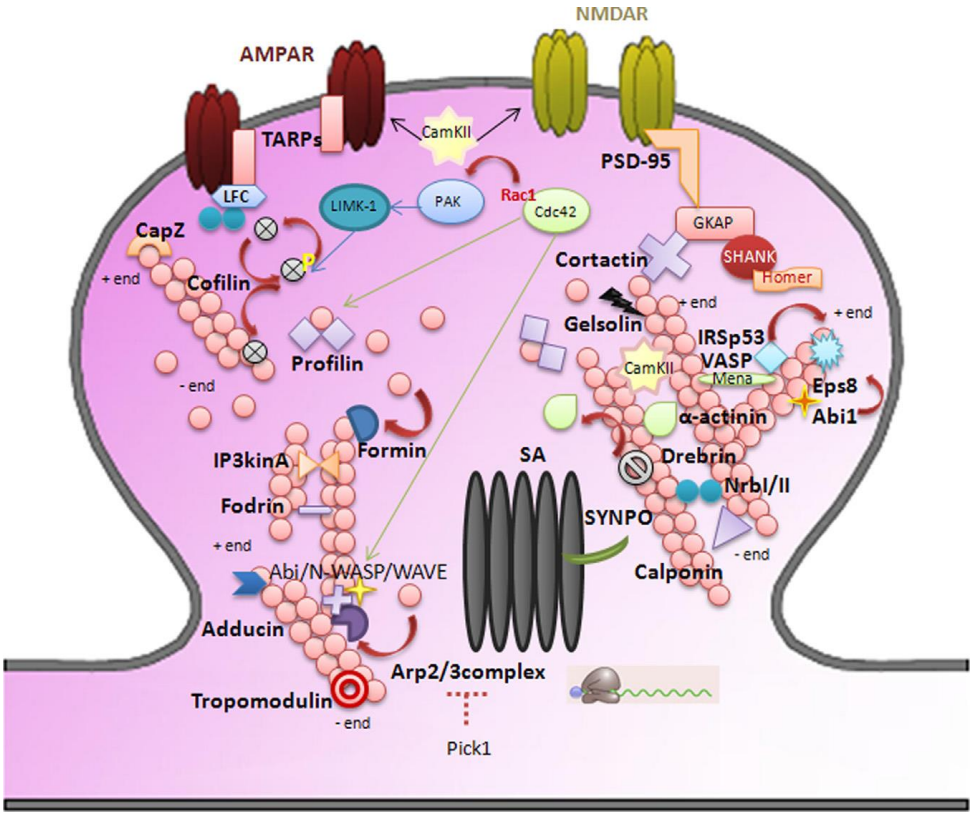

Figure 3. Various actin associating molecules in dendritic spines (Bellot A., *Brain Res.* 2014)

I.1.2. Actin filament

Actin is the most abundant cytoskeletal protein in eukaryotic cell and facilitates a various cellular processes are driven by assemble of monomeric form (G-actin) into two twisted strands and fibrous form (F-actin) and disassembly of F-actin to G-actin (Hotulainen & Hoogenraad, 2010). In nature of actin dynamics, actin filaments have polarity and tread-milling reaction, actin protomers are continuously added at the barbed (plus) end removed at the pointed (minus) end (Schubert & Dotti, 2007). In migrating cells, actin cause different cell shape in form of sheet and rod-like extensions, termed lamellipodia and filopodia which consists of long, un-brunched actin filaments arranged in tight, unipolar, and parallel bundles (Frost et al, 2010).

Actin filament is the major component of dendritic spines (Figure 3), reflecting the highly plastic nature of this subcellular component. In the spines, long and short branching actin filaments consist of the spine neck and short branched form is presenting in the spine head just underneath the PSD. It has been reported that actin polymerization is associated with spine enlargement and depolymerization with spine shrinkage (Bellot et al, 2014). Mainly, roles of actin in spines are to stabilize the PDS proteins and remodel the spine head in response to synaptic transmission. Actin filaments are associated with PSD by directly connection. Inhibition of polymerization reduces stability of synapses in age dependent manner and enhances dissociation of AMPA receptors from the PSD proteins (Chater & Goda, 2014; Yokoi et al, 2012). While NMDA receptors attach to actin filaments via single actin binding protein called alpha-actinin, AMPA receptors in the synapses generally contact the cytoskeleton through PSD scaffold proteins (Kantamneni, 2015).

I.1.3. Drebrin

Actin associating proteins, including CaMKII, cortactin, drebrin A, and neurabin I, have been found in PSD fraction by mass spectrometry analysis (Hotulainen & Hoogenraad, 2010). Reduced expression level of the proteins induces abnormal formation and immature spines in several neuronal diseases (Bernardinelli et al, 2014). As mentioned above, polymerization and depolymerization of actin filament is central core in morphological changes of dendritic spine, affecting the synaptic activity and transmission. A set of actin binding proteins determine the characteristic organizations of F-actins, such as bundles or networks. In spines, F-actin is presenting various structures for examples, networks and straight or tangled bundles in a different subcellular location. The composition of actin binding proteins determines region specific organization of F-actin. Interestingly, localization of actin binding protein can be modified according to synaptic signals.

Drebrin is an F-actin bundling protein which was first cloned by Shirao T. a decade ago and two isoforms, drebrin E and A, have been found (Shirao et al, 1988). Whereas drebrin E is an embryonic isoform and expressed in developmental cells, drebrin A expressed is adult form and spatially expressed in adult brain.(Shirao et al, 1990) Recently, many studies have investigated functions of drebrin using by knocking out of drebrin in neuronal cell line e.g. hippocampal neuron and mouse brain (Aoki et al, 2009; Kojima et al, 2010). According to the studies, it has been reported that location and expression level of drebrin is closely related to dynamics of dendritic spine morphologies on synaptic activities via

organization of actin filaments. Inhibition of drebrin in neuronal development down regulates spine morphogenesis and reduces spine density. Moreover, the suppression of drebrin expression results in immature thin spine structures and a reduced glutamatergic and GABAenergic synaptic activities in primary hippocampal neurons (Ivanov et al, 2009). The abnormalities of drebrin level in spines also found in neuronal disease including Alzheimer's disease and down-syndrome. (Dun & Chilton, 2010; Shim & Lubec, 2002)

Previous studies demonstrated that drebrin expression is involved in localization and trafficking of neurotransmitter membrane receptors on dendritic spines, which contain the machinery for receiving the majority of glutamatergic inputs (Merriam et al, 2013)

I.2. Membrane proteins in brain; neurotransmitter receptors and transporter

The human brain consists of a hundred billion neurons are linked into functional neuronal circuits based on all our behaviors, thoughts, emotions, dreams and memories. Synapses are gap regulating the electric communication within brain network and passing the information from pre-synaptic axon terminal to post-synaptic dendritic regions. Neurotransmitters such as glutamate are messengers transferring the information via synapse, generating synaptic transmission and plasticity. Therefore, the receptors and transporters are considered as critical molecules for brain activities by regulation of neurotransmitters transport in synapse. Thus, I described structure and function of the major receptors and transporter which have pivotal roles in synaptic activities and plasticity in below.

I.2.1. AMPA receptor

AMPA receptor (AMPAR), an ionotrophic transmembrane receptor, forms a heterotetramer, with 4 known subunits as GluA1, GluA2, GluA3 and GluA4 wherein they consist of GluA2 dimer along with the dimer of GluA1, GluA3 and GluA4. It is known as one of the most excitatory receptors in the mammalian CNS and responsible for the fast synaptic transmission (Bats et al, 2007; Coombs & Cull-Candy, 2009). Several AMPAR binding proteins have been identified such as SAP 97, PICK1, Stargazin, GRIP and transmembrane AMPA receptor regulatory protein (TARP) as auxiliary subunits (Nicoll et al, 2006).

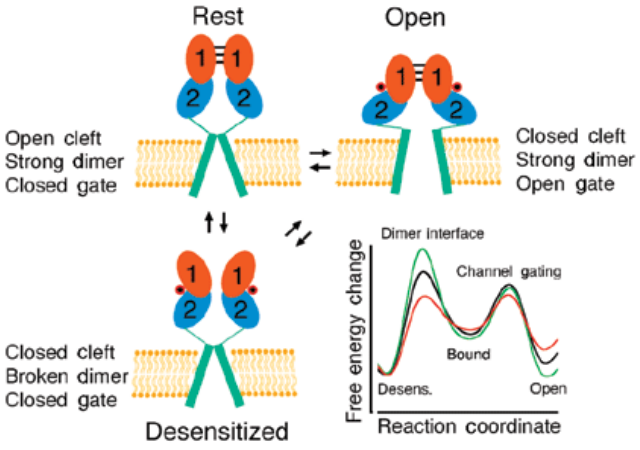

Figure 4. AMPA receptor (Mayer ML. *Nat Struct Mol Biol*. 2005)

Once the agonist, such as glutamate, binds to AMPAR tetrameric complex, the two loops become closer leading to conformational change and opening the channel to allow the currents to through in (Rosenmund et al, 1998). After the opening, AMPAR functions as fast excitatory receptor which rapidly opens and closes and then, desensitization of receptor results from reorganization of the dimer which comes up closing of channel immediately even though glutamate is bound to the receptor. (Figure 4) GluA2 subunit determines permeability of AMPARs and blocks the flow of calcium ions (Burnashev et al, 1992; Granger et al, 2011).

I.2.2. NMDAR

NMDAR is an ionotrophic glutamate receptor, which is named because it binds to N-methyl-d-aspartate as an agonist. In this voltage dependent ion channel, the ion action is blocked by extracellular magnesium and zinc ions. In addition, NMDAR allows influx of sodium ions, small amount of potassium ions into the cell (Dingledine et al, 1999). The influx of calcium ion forms the basis of synaptic plasticity (Paoletti et al, 2013)

In structural property, NMDAR structure is heterotetrameric consists of diverse subunits, containing GluN1 subunit, four GluN2 subunits which are sub-typed as GluN2A, GluN2B, GluN2C and GluN2D and two GluN3 subunits which are sub-typed as GluN3A and GluN3B (Cull-Candy & Leszkiewicz, 2004). It has been proposed that there are obligatory two GluN1 subunits in a receptor complex and then other subunits forms di-heterotetrameric and tri-heterotetrameirc NMDARs (Paoletti, 2011). In common, complex of NMDAR is

formed as GluN1-GluN2B and GluN1-2A in adult NMDAR, while GluN1-2A-2B is present in cortex and hippocampus as tri-heterotetrameic form.

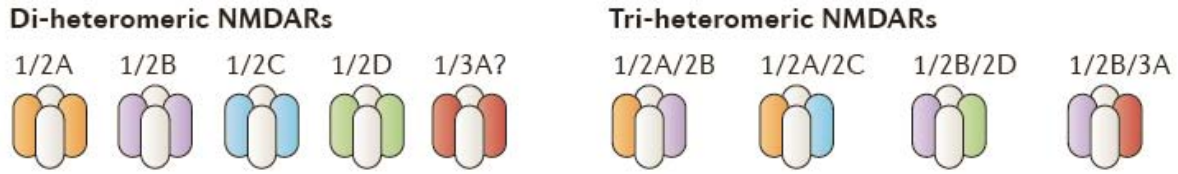

Figure 5. Complexity of NMDA receptors (Paoletti P., *Nat Rev Neurosci*. 2013)

It requires binding of two ligands glutamate and either D-serine or glycine in addition of or removal of a voltage-dependent block by magnessium ion which then lead to opening of channel allowing calcium ions influx.

In pharmacological studies, NMDAR has several agonists like NMDA, glutamic acid, homo-quinolinate, cis-2, 3-Piperidinedicarboxylic acid, tetrazolylglycine etc. Examples of antagonists are D,L-2-amino-5-phosphonovaleric acid (APV), conantokins, dextromethorphan, dexanabinol, dizocilpine (MK-801), ketamine, memantine, nitrous oxide, phencyclidine (Monaghan & Jane, 2009).

I.2.3. Dopamine receptor

3-hydroxytyramine (dopamine), a metabolite of the amino acid tyrosine, functions on neuronal circuitry through a relatively slow regulation of the fast neurotransmission that is regulated by glutamate and GABA (Beaulieu & Gainetdinov, 2011). It has been identified that foul major dopaminerginc pathways, the nigrostriatal, mesolimbic, mesocortical and tuberoinfundibular system, are seriously implicated in various pivotal roles in brain activities, including voluntary movement, reward, sleep, working memory, and learning. Moreover, several human diseases are related to dopaminergic dysfunctions such as Parkinson's disease, Huntington's disease, schizophrenia, ADHD and Tourette's syndrome (Beaulieu & Gainetdinov, 2011).

G protein-coupled dopamine receptors, five receptors D1 to D5, are activated by dopamine released from presynaptic terminals. Five dopamine receptors are divided into two groups: D1 and D2 classes based on biochemical property that dopamine is able to regulate adenylyl cyclase (AC) activity. Generally D1 class receptors stimulate cAMP production by AC whereas D2 class receptors induce suppression of AC. The two groups are also divided

according to their structural and pharmacological properties, D1-class dopamine receptors (D1 and D5) and D2 (D2, D3 and D4), with high level of homology of their transmembrane domains in subfamilies.

The most studied role involves the effects of dopamine on locomotor activity. Multiple lines of evidence indicate that locomotor activity is primarily controlled by D1, D2, and D3 dopamine receptors (Missale et al, 1998; Sibley, 1999). The activation of D1 dopamine receptors that are exclusively expressed on the postsynaptic neurons has a moderate stimulatory effect on locomotor activity. The roles of the D2 and D3 dopamine receptors are much more complex than D1 dopamine receptors because they result from both presynaptic and postsynaptic expression of these subtypes of receptors. In addition to role in locomotor activity, other vital functions depend on the activation of brain dopamine receptors. D1, D2, and, to a lesser degree, D3 dopamine receptors are critically involved in reward and reinforcement mechanisms. In learning and memory, both D1 and D2 dopamine receptors seems to be critical, espatially, working memory that are induced by the profrontal cortex. Clinical approches were developed by blocking D2 dopamine receptors in patients suffering from schizophrenia and bupolar disease. At the same time, D3, D4 and D5 dopamine receptors have a minor regulatory effects in some cognitive functions that are linked in hippocampal regions. The studies of complexity among the receptors have been reported that D1 dopamine receptors are able to form not only homo-oligomers (O'Dowd et al, 2011) but also D1–D2 dopamine receptors hetero-oligomers (O'Dowd et al, 2012) that are co-activated on the cell surface and mouse hippocampus (So et al, 2009). Moreover, these hetero-oligomers have even been mediated to regulation by calcium signalling in the brain (George & O'Dowd, 2007).

I.2.4. Glutamate transporter 1

Extracellular glutamate concentrations are maintained exclusively within physiological levels by members of a family of sodium-dependent glutamate transporters (O'Shea, 2002). GLT-1, the excitatory amino acid transporter 2 (EAAT2, syn.: sodium-dependent glutamate/aspartate transporter 2;solute carrier family 1 member 2), is essential for neural transmission in brain and spinal cord, responsible for up to 95% of all glutamate transporting activity (Danbolt, 2001). GLT-1 is a symporter which up-takes one molecule of L-glutamate coupled with transporting three Na+ and one H+, during one K+ is moving out of the cell to re-exposure the substrate-binding domains (Kanai & Hediger, 2004; Robinson, 1998). In structural property, GLT-1 contains 572 amino acids and eight transmembrane

domains and forms a homotrimer, and three splice variants were discovered (Peacey et al, 2009; Raunser et al, 2005; Williams et al, 2005). Posttranslational modifications have been identified including four phosphorylation sites at S21, Y493, Y537, S562 (Ballif et al, 2008); (Munton et al, 2007), and two glycosylation sites at N205 and N215.

Functional properties of excitatory amino acid transporters functions in the brain is a role of ensuring a high signal-to-noise ratio on synaptic transmission and prevent neuronal damage by over excitation of the glutamate receptors resulting in excess of glutamate. (Amara & Fontana, 2002; Campbell & Hablitz, 2004). GLT-1 expression and activity are regulated by substrate and non-transportable analogues (Munir et al, 2000), signaling cascades (Li et al, 2006; Sitcheran et al, 2005) and hormones (Autry et al, 2006; Pawlak et al, 2005). Many studies which were modulating GLT-1 expression have been reported that down regulation of GLT-1 using antisense oligonucleotides induced oligodendrocyte death and axonal damage (Domercq et al, 2005), and genetic inactivation of GLT-1 has been found in neurodegenerative characteristic of excitotoxicity (Rao & Sari, 2012) and increased expression of GLT-1 in multiple sclerosis along with GLT-2 and 3 (Vallejo-Illarramendi et al, 2006). In pharmacological studies, GLT-1 was up-regulated and damages induction of LTD and down regulation in induction of LTP, suggesting that GLT-1 may have a pivotal role in normal cognition and memory consolidation (Katagiri et al, 2001; Omrani et al, 2009). Furthermore, GLT-1 is involved in human disease including schizophrenia and neuro-degenerative disease (Sheldon & Robinson, 2007).

I.3. Synaptic plasticity

Synaptic plasticity is the ability of the synapse to modify the strength of synaptic transmission and is thought to be the main mechanism in learning and memory. Synaptic transmission is changed dependent neural activities at pre-existing synapses and it leads the growth of new synaptic connections or the pruning away of existing ones. Furthermore, it modulates the excitability properties of individual neurons by changing of the number of receptors located at a synapse (Gerrow & Triller, 2010).

In an enormous amount of work, many forms of synaptic plasticity have been reported including changes in the quantity of neurotransmitters released into a synapse, and changes in how effectively cells respond to those neurotransmitters. (Gaiarsa et al, 2002) Synaptic plasticity has been shown to play a critical role in the outstanding capacity of the brain to translate transient experiences into infinite numbers of memories that can last for decades.

Synaptic transmission can either be enhanced or depressed by activity. These changes prolong from milliseconds to continuing modifications lasting for few days or weeks and possibly even longer. Transient forms of synaptic plasticity associate with short-term memory and more enduring alterations are regarded to play pivotal roles in the organization of neural circuits during development, and with long-term memory in the mature nervous system.

I.3.1. Long Term Potentiation (LTP)

Long-term potentiation (LTP), an alteration of synaptic strength for a long period, is one of main factors in synaptic plasticity. It is widely believed that LTP is one of the main neural mechanisms by storing memory in the brain and collaborating memory consolidation and recall. In 1966, LTP was first originally descripted by Terje Lomo, examined the functions of short term memory using anesthetized rabbits. Actually, he measured excitatory postsynaptic potentials (EPSPs) in response to single pulses generated by electrical stimulation in the perforant pathway in dentate gyrus. During these experiments, he unexpectedly found that enhanced excitatory postsynaptic potentials (EPSPs) were observed over a long period of time that was provoked by high frequency stimulation in the presynaptic fibers. (Bliss & Lomo, 1973)

In 1975, Douglas and Goddard named this new phenomenon of long-lasting potentiation as long term potentiation (LTP). After its initial discovery in the rabbit hippocampus, LTP has been shown in different brain areas such as cerebral cortex, cerebellum, amygdala and so on. Robert Malenka has suggested that LTP could be exhibited at all excitatory synapses in the mammalian brain (Douglas & Goddard, 1975; Malenka & Bear, 2004).

Because of well-known organization and an easily inducible LTP, CA1 region in hippocampus, particularly NMDA receptor dependent Schaffer collateral pathway, has become the most popular brain region for studying LTP in mammals. In common, memory storage consists of at least two distinct stages, which are an early and short term stage of LTP (E-LTP) and a late stage of LTP (L-LTP) in the mammalian brain. E-LTP which lasts for minutes involves localized, transient changes in synaptic efficacy and is independent of new protein synthesis and RNA synthesis whereas, L-LTP is persistent form of memory, lasts longer, for up to 8 hr in hippocampal slices and for days in the intact animal. L-LTP requires an elevation of cAMP, recruitment of the cAMP-dependent protein kinase A (PKA), and ultimately the activation of transcription and translation for new RNA and protein synthesis

(Frey et al, 1993). L-LTP shares with long term memory the requirement for the synthesis of new RNA and protein. It has been shown that brief inhibition of either protein synthesis or transcription selectively blocks induction of long term memory without affecting short term memory (Crow & Forrester, 1990; Nguyen et al, 1994).

LTP has been the object of intense investigation because it is widely believed that LTP provides a critical key to understanding the molecular mechanisms by which memories are generated and, more generally, by which experience modifies behavior. At molecular level, several studies showed that AMPARs play an important role in integral process of LTP formation (Collingridge et al, 1983). Binding glutamate to AMPAR results in sodium influx into the postsynaptic membrane. This influx leads to release of magnesium ions on NMDAR at depolarization. As magnesium ion is removed from NMDAR, channel opens and causes calcium and potassium ion influx, which is necessary for LTP induction. This results in the activation of kinases like CamKII which in turn phosphorylates NMDAR and GluA2 AMPAR subunit. It is believed to be the major contribution to the sharp efficiency of glutamatergic synapses in CA1 area of hippocampus during LTP (Lee & Kirkwood, 2011; Malenka & Nicoll, 1999). In addition to the roles of AMPAR in LTP, NMDAR functions in LTP induction. The co-incidence detector can best explain NMDAR synaptic plasticity and its role in learning and memory.(Aksoy-Aksel & Manahan-Vaughan, 2015) The co-incidence detection phenomenon can be described by the Donald Hebb's postulation, proposed in 1949, wherein he postulated that synaptic connections are underwired when the presynaptic and the post synaptic neurons are activated concurrently. To maintain the hippocampal LTP for long time, sustained depolarization is necessary which can remove the magnesium block on the NMDARs allowing calcium ions influx in cell activating protein kinases, which in turn activates AMPA receptors(Aksoy-Aksel & Manahan-Vaughan, 2015). The prolonged depolarization needs stronger stimulus and thus associativity and thus co-incidence detector acts a factor where then two simultaneous inputs activate LTP. Thus NMDAR acts a molecular coincidence detector which executes Hebb's rule at the synapses for detecting concurrent events (Sanhueza & Lisman, 2013).

II. Articles (Appendix)

Appendix 1 Article:

Hippocampal glutamate transporter 1 (GLT-1) complex levels are paralleling memory training in the Multiple T-maze in C57BL/6J mice. Seok Heo*, Gangsoo Jung*, Tamara Beuk, Harald Hoeger, Gert Lubec, Brain Struct Funct (2012) 217:363–378

Appendix 2 Article:

Drebrin depletion alters neurotransmitter-receptor levels in protein-complexes, dendritic spine morphogenesis and memory-related synaptic plasticity in the mouse hippocampus. Gangsoo Jung*, Eun-Jung Kim*, Ana Cicvaric, Sunetra Sase, Arnold Pollak, Marion Gröger, Harald Höger, Sialana Fernando, Johannes Berger, Francisco J. Monje and Gert Lubec, J Neurochem. (2015)

III. Summary (English)

The work presented in this cumulative thesis reflects my efforts in studying the identification and characterization of glutamate transporter in mouse hippocampus. Furthermore by investigation of drebrin knockout mice, I discovered functional effects of drebrin on the conformational changes of several major receptors complex, spine morphologies and synaptic plasticity.

In first paper, I found differential conformation of GLT-1 complexes, which were detected at apparent molecular weights of 242, 480 and 720 kDa on BN-PAGE Western blotting in the spatial memory training C57BL/6J mice hippocampus. Moreover, high sequence coverage of GLT-1 and glycosylation sites were observed in mass spectrometry (nano-LC-ESI-MS/MS). The detected posttranslational modifications were identified by several glycosidases. GLT-1 complex levels were significantly higher in the trained group as compared to yoked controls, thus, it is revealed that increased GLT-1 complex levels are paralleling and are linked to spatial memory training. Additionally, antibody specificity was verified by immunoblotting on multi-dimensional gels (BN-SDS/SDS-PAGE).

In the second article, we examined the effects of genetic deletion of drebrin on dendritic spine and on the level of complexes containing major brain receptors. Level of protein complexes containing dopamine receptor D1/dopamine receptor D2, 5-hydroxytryptamine receptor 1A (5-HT1A R), and 5-hydroxytryptamine receptor 7 (5-HT7R) were significantly reduced in hippocampus of drebrin knockout mice whereas no significant changes were detected for GluR1, 2, and 3 and NR1 as examined by native gel-based immunoblotting. Drebrin depletion also reduced dendritic spine density, morphogenesis, and reduced levels of dopamine receptor D1 in dendritic spines as evaluated using immunohistochemistry/confocal microscopy. Furthermore, memory-related hippocampal synaptic plasticity was significantly decreased upon drebrin depletion in electrophysiology. These findings provide unprecedented experimental support for a role of drebrin in the regulation of memory-related synaptic plasticity and neurotransmitter receptor signaling

IV. Zusammenfassung (German)

Die präsentierte Thesis reflektiert meine Bemühungen an der Arbeit der Identifikation undCharakterisierung der Glutamattransporter im Maus Hippocampus. Des Weiteren habe ich, durch Studien an der Drebrin knock-out Mäusen, funktionelle Effekte von drebrinonten Konfomationsänderungen von einigen Rezeptorkomplexen, Wirbelsäulenmorphologien und synaptischen Plastizitäten herausgefunden.

In der ersten Abhandlung fand ich verschiedene Konformationen von GLT-1 Komplexen, welche bei Molekularmassen von 242, 480 und 720 kDa sichtbar waren und durch BN-PAGE Western-blotting an räumlichen Gedächtnis trainierten C57BL/6J Maushippocampus detektiert wurden. Eine hohe Sequenzabdeckung von GLT-1 und Glykosylierungsseiten wurden außerdem durch Massenspektroskopie (nano-LC-ESI-MS/MS) entdeckt. Die detektierten Glykosylierungen wurden durch viele Glykosidasen identifiziert. GLT-1 Komplexlevels waren in der trainierten Gruppe signifikant höher verglichen mit der yoked Kontrolle, daher ist gezeigt, dass zunehmende GLT-1 Levels zusammenhängend sind mit dem räumlichen Gedächtnistraining. Zusätzlich wurde die Antikörperspezifität geprüft durch immunoblotting auf mehrdimensionalen Gelen (BN-PAGE/SDS-PAGE).

Im zweiten Artikel haben wir die Effekte von genetischen Deletionen von Drebrin auf dem Dorn und auf dem Level von Komplexen welche wichtige Gedächtnisrezeptoren besitzen beobachtet. Das Level von Proteinkomplexen welche über Dopaminrezeptor D1/Dopaminrezeptor D2, 5-hydroxytryptamine-Rezeptor 1A (5-HT1A R), und 5-hydroxytryptamine-ReZeptor 7 (5-HT7R) verfügten waren signifikant reduziert im Hippocampus von Drebrin knock-out Mäusen. Bei GluR1, 2 und 3 und NR1 hingegen wurde kein signifikanter Unterschied bemerkt. Debrin Abbau hat außerdem auch die Dichte vom Dorn und die Morphogenesis reduziert und reduzierte Levels von Dopamine rezeptor D1 im Dorn. Dies wurde durch immunohistochemistry/confocoal Mikroskopie evaluiert. Des Weiteren war die Gedächtnis verbundene hippocampe synaptische Plastizität signifikant reduziert auf Grund von Debrin Abbau in Elektrophysiologie. Diese Entdeckungen bieten beispiellos experimentelle Unterstützung für die Rolle von Debrin in der Regulation von Gedächtnis-verbundener synaptischer Plastizität und von Neurotransmitterrezeptor-signaling.

V. References

Aksoy-Aksel A, Manahan-Vaughan D (2015) Synaptic strength at the temporoammonic input to the hippocampal CA1 region in vivo is regulated by NMDA receptors, metabotropic glutamate receptors and voltage-gated calcium channels. *Neuroscience*

Amara SG, Fontana AC (2002) Excitatory amino acid transporters: keeping up with glutamate. *Neurochem Int* **41:** 313-318

Andersen P (2007) *The hippocampus book*, Oxford ; New York: Oxford University Press.

Aoki C, Kojima N, Sabaliauskas N, Shah L, Ahmed TH, Oakford J, Ahmed T, Yamazaki H, Hanamura K, Shirao T (2009) Drebrin a knockout eliminates the rapid form of homeostatic synaptic plasticity at excitatory synapses of intact adult cerebral cortex. *J Comp Neurol* **517:** 105-121

Autry AE, Grillo CA, Piroli GG, Rothstein JD, McEwen BS, Reagan LP (2006) Glucocorticoid regulation of GLT-1 glutamate transporter isoform expression in the rat hippocampus. *Neuroendocrinology* **83:** 371-379

Ballif BA, Carey GR, Sunyaev SR, Gygi SP (2008) Large-scale identification and evolution indexing of tyrosine phosphorylation sites from murine brain. *J Proteome Res* **7:** 311-318

Bats C, Groc L, Choquet D (2007) The interaction between Stargazin and PSD-95 regulates AMPA receptor surface trafficking. *Neuron* **53:** 719-734

Beaulieu JM, Gainetdinov RR (2011) The physiology, signaling, and pharmacology of dopamine receptors. *Pharmacol Rev* **63:** 182-217

Bellot A, Guivernau B, Tajes M, Bosch-Morato M, Valls-Comamala V, Munoz FJ (2014) The structure and function of actin cytoskeleton in mature glutamatergic dendritic spines. *Brain Res* **1573:** 1-16

Bernardinelli Y, Nikonenko I, Muller D (2014) Structural plasticity: mechanisms and contribution to developmental psychiatric disorders. *Front Neuroanat* **8:** 123

Bliss TV, Lomo T (1973) Long-lasting potentiation of synaptic transmission in the dentate area of the anaesthetized rabbit following stimulation of the perforant path. *J Physiol* **232:** 331-356

Bosch M, Castro J, Saneyoshi T, Matsuno H, Sur M, Hayashi Y (2014) Structural and molecular remodeling of dendritic spine substructures during long-term potentiation. *Neuron* **82:** 444-459

Burnashev N, Khodorova A, Jonas P, Helm PJ, Wisden W, Monyer H, Seeburg PH, Sakmann B (1992) Calcium-permeable AMPA-kainate receptors in fusiform cerebellar glial cells. *Science* **256:** 1566-1570

Calabrese B, Wilson MS, Halpain S (2006) Development and regulation of dendritic spine synapses. *Physiology (Bethesda)* **21:** 38-47

Campbell SL, Hablitz JJ (2004) Glutamate transporters regulate excitability in local networks in rat neocortex. *Neuroscience* **127:** 625-635

Chater TE, Goda Y (2014) The role of AMPA receptors in postsynaptic mechanisms of synaptic plasticity. *Front Cell Neurosci* **8:** 401

Clark RE, West AN, Zola SM, Squire LR (2001) Rats with lesions of the hippocampus are impaired on the delayed nonmatching-to-sample task. *Hippocampus* **11:** 176-186

Colgan LA, Yasuda R (2014) Plasticity of dendritic spines: subcompartmentalization of signaling. *Annu Rev Physiol* **76:** 365-385

Collingridge GL, Kehl SJ, McLennan H (1983) Excitatory amino acids in synaptic transmission in the Schaffer collateral-commissural pathway of the rat hippocampus. *J Physiol* **334:** 33-46

Coombs ID, Cull-Candy SG (2009) Transmembrane AMPA receptor regulatory proteins and AMPA receptor function in the cerebellum. *Neuroscience* **162:** 656-665

Crow T, Forrester J (1990) Inhibition of protein synthesis blocks long-term enhancement of generator potentials produced by one-trial in vivo conditioning in Hermissenda. *Proc Natl Acad Sci U S A* **87:** 4490-4494

Cull-Candy SG, Leszkiewicz DN (2004) Role of distinct NMDA receptor subtypes at central synapses. *Sci STKE* **2004:** re16

Danbolt NC (2001) Glutamate uptake. *Prog Neurobiol* **65:** 1-105

Deng W, Aimone JB, Gage FH (2010) New neurons and new memories: how does adult hippocampal neurogenesis affect learning and memory? *Nat Rev Neurosci* **11:** 339-350

Dickstein DL, Weaver CM, Luebke JI, Hof PR (2013) Dendritic spine changes associated with normal aging. *Neuroscience* **251:** 21-32

Dingledine R, Borges K, Bowie D, Traynelis SF (1999) The glutamate receptor ion channels. *Pharmacol Rev* **51:** 7-61

Domercq M, Etxebarria E, Perez-Samartin A, Matute C (2005) Excitotoxic oligodendrocyte death and axonal damage induced by glutamate transporter inhibition. *Glia* **52:** 36-46

Douglas RM, Goddard GV (1975) Long-term potentiation of the perforant path-granule cell synapse in the rat hippocampus. *Brain Res* **86:** 205-215

Dun XP, Chilton JK (2010) Control of cell shape and plasticity during development and disease by the actin-binding protein Drebrin. *Histol Histopathol* **25:** 533-540

Frey U, Huang YY, Kandel ER (1993) Effects of cAMP simulate a late stage of LTP in hippocampal CA1 neurons. *Science* **260:** 1661-1664

Frost NA, Kerr JM, Lu HE, Blanpied TA (2010) A network of networks: cytoskeletal control of compartmentalized function within dendritic spines. *Curr Opin Neurobiol* **20:** 578-587

Gaiarsa JL, Caillard O, Ben-Ari Y (2002) Long-term plasticity at GABAergic and glycinergic synapses: mechanisms and functional significance. *Trends Neurosci* **25:** 564-570

George SR, O'Dowd BF (2007) A novel dopamine receptor signaling unit in brain: heterooligomers of D1 and D2 dopamine receptors. *ScientificWorldJournal* **7:** 58-63

Gerrow K, Triller A (2010) Synaptic stability and plasticity in a floating world. *Curr Opin Neurobiol* **20:** 631-639

Granger AJ, Gray JA, Lu W, Nicoll RA (2011) Genetic analysis of neuronal ionotropic glutamate receptor subunits. *J Physiol* **589:** 4095-4101

Hanley JG (2014) Actin-dependent mechanisms in AMPA receptor trafficking. *Front Cell Neurosci* **8:** 381

Hollmann M, Heinemann S (1994) Cloned glutamate receptors. *Annu Rev Neurosci* **17:** 31-108

Hotulainen P, Hoogenraad CC (2010) Actin in dendritic spines: connecting dynamics to function. *J Cell Biol* **189:** 619-629

Hudon C, Dore FY, Goulet S (2002) Spatial memory and choice behavior in the radial arm maze after fornix transection. *Prog Neuropsychopharmacol Biol Psychiatry* **26:** 1113-1123

Ivanov A, Esclapez M, Pellegrino C, Shirao T, Ferhat L (2009) Drebrin A regulates dendritic spine plasticity and synaptic function in mature cultured hippocampal neurons. *J Cell Sci* **122:** 524-534

Kanai Y, Hediger MA (2004) The glutamate/neutral amino acid transporter family SLC1: molecular, physiological and pharmacological aspects. *Pflugers Arch* **447:** 469-479

Kantamneni S (2015) Cross-talk and regulation between glutamate and GABAB receptors. *Front Cell Neurosci* **9:** 135

Katagiri H, Tanaka K, Manabe T (2001) Requirement of appropriate glutamate concentrations in the synaptic cleft for hippocampal LTP induction. *Eur J Neurosci* **14:** 547-553

Knobloch M, Mansuy IM (2008) Dendritic spine loss and synaptic alterations in Alzheimer's disease. *Mol Neurobiol* **37:** 73-82

Kojima N, Hanamura K, Yamazaki H, Ikeda T, Itohara S, Shirao T (2010) Genetic disruption of the alternative splicing of drebrin gene impairs context-dependent fear learning in adulthood. *Neuroscience* **165:** 138-150

Lee HK, Kirkwood A (2011) AMPA receptor regulation during synaptic plasticity in hippocampus and neocortex. *Semin Cell Dev Biol* **22:** 514-520

Li HH, Yu WH, Rozengurt N, Zhao HZ, Lyons KM, Anagnostaras S, Fanselow MS, Suzuki K, Vanier MT, Neufeld EF (1999) Mouse model of Sanfilippo syndrome type B produced by targeted disruption of the gene encoding alpha-N-acetylglucosaminidase. *Proc Natl Acad Sci U S A* **96:** 14505-14510

Li M, Liu RM, Timblin CR, Meyer SG, Mossman BT, Fukagawa NK (2006) Age affects ERK1/2 and NRF2 signaling in the regulation of GCLC expression. *J Cell Physiol* **206:** 518-525

Malenka RC, Bear MF (2004) LTP and LTD: an embarrassment of riches. *Neuron* **44:** 5-21

Malenka RC, Nicoll RA (1999) Long-term potentiation--a decade of progress? *Science* **285:** 1870-1874

Merriam EB, Millette M, Lumbard DC, Saengsawang W, Fothergill T, Hu X, Ferhat L, Dent EW (2013) Synaptic regulation of microtubule dynamics in dendritic spines by calcium, F-actin, and drebrin. *J Neurosci* **33:** 16471-16482

Missale C, Nash SR, Robinson SW, Jaber M, Caron MG (1998) Dopamine receptors: from structure to function. *Physiol Rev* **78:** 189-225

Monaghan DT, Jane DE (2009) Pharmacology of NMDA Receptors.

Morris R (1984) Developments of a water-maze procedure for studying spatial learning in the rat. *J Neurosci Methods* **11:** 47-60

Moyer CE, Shelton MA, Sweet RA (2014) Dendritic spine alterations in schizophrenia. *Neurosci Lett*

Munir M, Correale DM, Robinson MB (2000) Substrate-induced up-regulation of Na(+)-dependent glutamate transport activity. *Neurochem Int* **37:** 147-162

Munton RP, Tweedie-Cullen R, Livingstone-Zatchej M, Weinandy F, Waidelich M, Longo D, Gehrig P, Potthast F, Rutishauser D, Gerrits B, Panse C, Schlapbach R, Mansuy IM (2007) Qualitative and quantitative analyses of protein phosphorylation in naive and stimulated mouse synaptosomal preparations. *Mol Cell Proteomics* **6:** 283-293

Nguyen PV, Abel T, Kandel ER (1994) Requirement of a critical period of transcription for induction of a late phase of LTP. *Science* **265:** 1104-1107

Nicoll RA, Tomita S, Bredt DS (2006) Auxiliary subunits assist AMPA-type glutamate receptors. *Science* **311:** 1253-1256

O'Dowd BF, Ji X, Alijaniaram M, Nguyen T, George SR (2011) Separation and reformation of cell surface dopamine receptor oligomers visualized in cells. *Eur J Pharmacol* **658:** 74-83

O'Dowd BF, Ji X, Nguyen T, George SR (2012) Two amino acids in each of D1 and D2 dopamine receptor cytoplasmic regions are involved in D1-D2 heteromer formation. *Biochem Biophys Res Commun* **417:** 23-28

O'Shea RD (2002) Roles and regulation of glutamate transporters in the central nervous system. *Clin Exp Pharmacol Physiol* **29:** 1018-1023

Omrani A, Melone M, Bellesi M, Safiulina V, Aida T, Tanaka K, Cherubini E, Conti F (2009) Up-regulation of GLT-1 severely impairs LTD at mossy fibre--CA3 synapses. *J Physiol* **587:** 4575-4588

Paoletti P (2011) Molecular basis of NMDA receptor functional diversity. *Eur J Neurosci* **33:** 1351-1365

Paoletti P, Bellone C, Zhou Q (2013) NMDA receptor subunit diversity: impact on receptor properties, synaptic plasticity and disease. *Nat Rev Neurosci* **14:** 383-400

Pawlak J, Brito V, Kuppers E, Beyer C (2005) Regulation of glutamate transporter GLAST and GLT-1 expression in astrocytes by estrogen. *Brain Res Mol Brain Res* **138:** 1-7

Peacey E, Miller CC, Dunlop J, Rattray M (2009) The four major N- and C-terminal splice variants of the excitatory amino acid transporter GLT-1 form cell surface homomeric and heteromeric assemblies. *Mol Pharmacol* **75:** 1062-1073

Rao PS, Sari Y (2012) Glutamate transporter 1: target for the treatment of alcohol dependence. *Curr Med Chem* **19:** 5148-5156

Raunser S, Haase W, Bostina M, Parcej DN, Kuhlbrandt W (2005) High-yield expression, reconstitution and structure of the recombinant, fully functional glutamate transporter GLT-1 from Rattus norvegicus. *J Mol Biol* **351:** 598-613

Roberts TF, Tschida KA, Klein ME, Mooney R (2010) Rapid spine stabilization and synaptic enhancement at the onset of behavioural learning. *Nature* **463:** 948-952

Robinson MB (1998) The family of sodium-dependent glutamate transporters: a focus on the GLT-1/EAAT2 subtype. *Neurochem Int* **33:** 479-491

Rosenmund C, Stern-Bach Y, Stevens CF (1998) The tetrameric structure of a glutamate receptor channel. *Science* **280:** 1596-1599

Sanhueza M, Lisman J (2013) The CaMKII/NMDAR complex as a molecular memory. *Mol Brain* **6:** 10

Schubert V, Dotti CG (2007) Transmitting on actin: synaptic control of dendritic architecture. *J Cell Sci* **120:** 205-212

Scoville WB, Milner B (2000) Loss of recent memory after bilateral hippocampal lesions. 1957. *J Neuropsychiatry Clin Neurosci* **12:** 103-113

Sekino Y, Kojima N, Shirao T (2007) Role of actin cytoskeleton in dendritic spine morphogenesis. *Neurochem Int* **51:** 92-104

Sheldon AL, Robinson MB (2007) The role of glutamate transporters in neurodegenerative diseases and potential opportunities for intervention. *Neurochem Int* **51:** 333-355

Shim KS, Lubec G (2002) Drebrin, a dendritic spine protein, is manifold decreased in brains of patients with Alzheimer's disease and Down syndrome. *Neurosci Lett* **324:** 209-212

Shirao T, Kojima N, Kato Y, Obata K (1988) Molecular cloning of a cDNA for the developmentally regulated brain protein, drebrin. *Brain Res* **464:** 71-74

Shirao T, Kojima N, Terada S, Obata K (1990) Expression of three drebrin isoforms in the developing nervous system. *Neurosci Res Suppl* **13:** S106-111

Sibley DR (1999) New insights into dopaminergic receptor function using antisense and genetically altered animals. *Annu Rev Pharmacol Toxicol* **39:** 313-341

Sitcheran R, Gupta P, Fisher PB, Baldwin AS (2005) Positive and negative regulation of EAAT2 by NF-kappaB: a role for N-myc in TNFalpha-controlled repression. *EMBO J* **24:** 510-520

So CH, Verma V, Alijaniaram M, Cheng R, Rashid AJ, O'Dowd BF, George SR (2009) Calcium signaling by dopamine D5 receptor and D5-D2 receptor hetero-oligomers occurs by a mechanism distinct from that for dopamine D1-D2 receptor hetero-oligomers. *Mol Pharmacol* **75:** 843-854

Svitkina T, Lin WH, Webb DJ, Yasuda R, Wayman GA, Van Aelst L, Soderling SH (2010) Regulation of the postsynaptic cytoskeleton: roles in development, plasticity, and disorders. *J Neurosci* **30:** 14937-14942

Vallejo-Illarramendi A, Domercq M, Perez-Cerda F, Ravid R, Matute C (2006) Increased expression and function of glutamate transporters in multiple sclerosis. *Neurobiol Dis* **21:** 154-164

Williams SM, Sullivan RK, Scott HL, Finkelstein DI, Colditz PB, Lingwood BE, Dodd PR, Pow DV (2005) Glial glutamate transporter expression patterns in brains from multiple mammalian species. *Glia* **49:** 520-541

Yokoi N, Fukata M, Fukata Y (2012) Synaptic plasticity regulated by protein-protein interactions and posttranslational modifications. *Int Rev Cell Mol Biol* **297:** 1-43

Zola-Morgan S, Squire LR (1986) Memory impairment in monkeys following lesions limited to the hippocampus. *Behav Neurosci* **100:** 155-160

VI. Curriculum vitae

NAME Gangsoo Jung
CONTACT gsjung0402@gmail.com
MOBILE +43 676 7092145

PERSONAL INFORMATION
Date of Birth April 2, 1982
Place of Birth Seoul, South of Korea

EDUCATION
2010-2015 Ph.D., Department of Biotechnology, Prof. Hermann Katinger
University of National Resources and Applied Life Sciences
2008-2010 Master, Biochemistry laboratory of Prof. Sungyul Hong
Department of Genetic engineering, University of Sungkyunkwan
2001-2008 Bachelor, Department of Genetic engineering, University of Sungkyunkwan

Language skills
Korean, English

Certificates
2013. September. Late Summer Practical Proteomics Seminar from IMP/IMBA
2012. April. Hands On Proteomics Workshop from Austrian proteomics association

Comprehensive List of publications
1. Amphetamine action at the cocaine- and antidepressant sensitive serotonin transporter is modulated by αCaMKII
Thomas Steinkellner, Therese Montgomery, Tina Hofmaier, Oliver Kudlacek, Jae-Won Yang, Matthias Rickhag, Gangsoo Jung, Gert Lubec, Ulrik Gether, Michael Freissmuth, and Harald Sitte., *J Neurosci*.(2015) – Impressed

2. Drebrin depletion alters neurotransmitter-receptor levels in protein-complexes, dendritic spine morphogenesis and memory-related synaptic plasticity in the mouse hippocampus.

Jung G, Kim EJ, Cicvaric A, Sase S, Gröger M, Höger H, Sialana FJ, Berger J, Monje FJ, Lubec G., *J Neurochem*. (2015)

3. Radiation protection from whole-body gamma irradiation (6.7 Gy): behavioural effects and brain protein-level changes by an aminothiol compound GL2011 in the Wistar rat.
Ganesan MK, Jovanovic M, Secerov B, Ignjatovic M, Bilban M, Andjus P, Refaei AE, Jung G, Li L, Sase A, Chen W, Bacic G, Lubec G., *Amino Acids.* 46:1681-96 (2014)

4. Characterization of α-l-Iduronidase (Aldurazyme®) and its complexes.
Jung G, Pabst M, Neumann L, Berger A, Lubec G. *J Proteomics*. 80:26-33 (2013)

5. Hippocampal levels and activity of the sodium/potassium transporting ATPase subunit α-3 (AT1A3) are paralleling memory training in the multiple T-maze in the C57BL/6J mouse.
Heo S, Csaszar E, Jung G, Beuk T, Höger H, Lubec G. *Neurochem Int.* 61:702-12 (2012)

6. Hippocampal glutamate transporter 1 (GLT-1) complex levels are paralleling memory training in the Multiple T-maze in C57BL/6J mice.
Heo S, Jung G, Beuk T, Höger H, Lubec G. *Brain Struct Funct.* 217:363-78 (2012)

7. A serotonin receptor 1A containing complex in hippocampus of PWD/PhJ mice is linked to training effects in the Barnes maze.
Heo S, Patil SS, Jung G, Höger H, Lubec G. *Behav Brain Res*. 216:389-95 (2011)

8. Protein L-isoaspartyl O-methyltransferase inhibits amyloid beta fibrillogenesis in vitro.
Jung G, Ryu J, Heo J, Lee SJ, Cho JY, Hong S. *Pharmazie.* 66:529-34 (2011)

Brain Struct Funct (2012) 217:363–378
DOI 10.1007/s00429-011-0362-5

ORIGINAL ARTICLE

Hippocampal glutamate transporter 1 (GLT-1) complex levels are paralleling memory training in the Multiple T-Maze in C57BL/6J mice

Seok Heo · Gangsoo Jung · Tamara Beuk · Harald Höger · Gert Lubec

Received: 27 June 2011 / Accepted: 8 November 2011 / Published online: 24 November 2011

Abstract The glutamate transporter 1 (GLT-1) is essential for glutamate uptake in the brain and associated with various psychiatric and neurological disorders. Pharmacological inhibition of GLT-1 results in memory deficits, but no study linking native GLT-1 complexes was published so far. It was therefore the aim of the study to associate this highly hydrophobic, eight transmembrane spanning domains containing transporter to memory training in the Multiple T-maze (MTM). C57BL/6J mice were used for the spatial memory training experiments, and trained mice were compared to untrained (yoked) animals. Mouse hippocampi were dissected out 6 h after training on day 4, and a total enriched membrane fraction was prepared by ultracentrifugation. Membrane proteins were separated by blue native polyacrylamide gel electrophoresis (BN-PAGE) with subsequent Western blotting against GLT-1 on these native gels. Moreover, GLT-1 complexes were identified by mass spectrometry (nano-LC-ESI-MS/MS). Animals learned the MTM task and multiple GLT-1 complexes were detected at apparent molecular weights of 242, 480 and 720 kDa on BN-PAGE Western blotting. GLT-1 complex levels were significantly higher in the trained group as compared to yoked controls, and antibody specificity was verified by immunoblotting on multidimensional gels. Hippocampal GLT-1 was unambiguously identified by mass spectrometry with high sequence coverage, and glycosylation was observed. It is revealed that increased GLT-1 complex levels are paralleling and are linked to spatial memory training. We provide evidence that signal termination, represented by the excitatory amino acid transporter GLT-1 complexes, is involved in spatial memory mechanisms.

Keywords Excitatory amino acid transporter 2 · Gel-based proteomics · Multidimensional gel electrophoresis · Spatial memory

Seok Heo and Gangsoo Jung contributed equally to this work.

Electronic supplementary material The online version of this article (doi:10.1007/s00429-011-0362-5) contains supplementary material, which is available to authorized users.

S. Heo · G. Jung · T. Beuk · G. Lubec (✉)
Department of Pediatrics and Adolescent Medicine, Medical University of Vienna, Währinger Gürtel 18, 1090 Vienna, Austria
e-mail: gert.lubec@meduniwien.ac.at

H. Höger
Core Unit of Biomedical Research, Division of Laboratory Animal Science and Genetics, Medical University of Vienna, Brauhausgasse 34, 2325 Himberg, Austria

Introduction

Extracellular glutamate concentrations are maintained exclusively within physiological levels by members of a family of sodium-dependent glutamate transporters (O'Shea 2002).

GLT-1, the excitatory amino acid transporter 2 (EAAT2, syn.: sodium-dependent glutamate/aspartate transporter 2; solute carrier family 1 member 2), is an essential element for neural transmission in brain and spinal cord, accounting for up to 95% of all glutamate transport activity (Danbolt 2001).

GLT-1 is a symporter uptaking one molecule of L-glutamate coupled with transporting three Na^+ and one H^+, while one K^+ is moving outward of the cell to re-orient the substrate-binding domains (Kanai and Hediger 2004; Robinson 1998; Rose et al. 2009; Zerangue and Kavanaugh 1996). GLT-1 contains 572 amino acids and eight

transmembrane domains and is a homotrimer, and three splice variants were described (Hediger et al. 1995; Kirschner et al. 1994; Meyer et al. 1997, 1998; Mukainaka et al. 1995; Peacey et al. 2009; Raunser et al. 2005; Suchak et al. 2003; Sutherland et al. 1995; Williams et al. 2005). Post-translational modifications include phosphorylations at S21, Y493, Y537, S562 (UniProtKB P43006) (Ballif et al. 2008; Gonzalez et al. 2005; Munton et al. 2007), and GlcNAC at N205 and N215. This carrier is pivotal for terminating the postsynaptic action of glutamate by removing released glutamate from the synaptic cleft (Takatsuru et al. 2007). The expression patterns of GLT-1 subunits rather than GLT-1 complexes were described by several groups (Brooks-Kayal et al. 1998; Furuta et al. 1997; Maragakis et al. 2004; Mennerick et al. 1998; Regan et al. 2007; Sims and Robinson 1999; Utsunomiya-Tate et al. 1997).

Functions of excitatory amino acid transporters in the brain pointing to a role of ensuring a high signal-to-noise ratio during synaptic transmission and prevention of neuronal damage by overexcitation of the glutamate receptors by excess of glutamate have been reviewed by Tanaka (2000), Amara and Fontana (2002), Campbell and Hablitz (2004), Huang et al. (2004) and Robinson (1998).

Regulation of GLT-1 expression and activity has been reported by Swanson et al. (1997) and was reviewed by Sattler and Rothstein (2006): neuronal activity is regulating GLT-1 (Perego et al. 2000) as well as synaptic activity (Zhang et al. 2009). Basically, substrate and nontransportable analogues (Munir et al. 2000; Qu and Kanner 2008), signaling cascades (Li et al. 2006; Sitcheran et al. 2005), hormones (Autry et al. 2006; Pawlak et al. 2005; Dunlop et al. 1999a) and a series of pharmacological agents (Chu et al. 2007; Dunlop et al. 1999b; Fattorini et al. 2008) regulate GLT-1 expression and activity.

Inactivation of GLT-1 by antisense oligonucleotides or pharmacological inhibition leads to oligodendrocyte death and axonal damage (Domercq et al. 2005). Genetic inactivation of GLT-1 is followed by neurodegeneration characteristic of excitotoxicity and progressive paralysis (Rothstein et al. 1996) or seizures and increased susceptibility to cortical injury (Tanaka et al. 1997). Pharmacological up-regulation of GLT-1, however, severely impairs long-term depression in hippocampus (Omrani et al. 2009). Blockade of astrocytic glutamate uptake by dihydrokainic acid, a GLT-1 inhibitor (Anderson and Swanson 2000; Arriza et al. 1994), induces signs of anhedonia and impairs spatial memory in rats (Bechtholt-Gompf et al. 2010). Induction of long-term potentiation, a possible molecular correlate with learning and memory by tetanic stimulation in the CA1 region, is impaired in GLT-1 knockout mice, suggesting that GLT-1 may have an important role in normal cognition (Katagiri et al. 2001).

Moreover, GLT-1 was proposed to be involved in human disease including patients with schizophrenia (Matute et al. 2005; McCullumsmith and Meador-Woodruff 2002; Ohnuma et al. 2000; Schmitt et al. 2003; Smith et al. 2001), mood disorders (Lee et al. 2007) and neurodegenerative disease (Sheldon and Robinson 2007).

So far, this transporter has not been unambiguously identified in mouse hippocampus at the protein level. This information, however, is needed because in addition to immunochemical information, chemical identification and characterization by mass spectrometry are mandatory reflecting the state of the art technology. Moreover, there is limited information on GLT-1 complexes, and although the existence of several GLT-1 complexes including formation of homo- and heteropolymers has been reported (Gebhardt et al. 2010; Gonzalez–Gonzalez et al. 2009; Haugeto et al. 1996), it is not known whether and which GLT-1 complex levels are paralleling training in a spatial memory paradigm and this question formed the aim of the study. It has been shown that major transporter systems in the brain use complex formation forming homo- or heterooligomers (e.g., Agnati et al. 2005; Baucum et al. 2004; Bauman et al. 2000; Genedani et al. 2005; Gonzalez and Robinson 2004; Hadlock et al. 2010) and that transporter activation or inactivation can be regulated by forming different complexes or monomers, and indeed, Hadlock et al. (2009) have shown a negative correlation between dopamine transporter complex formation and activity. Moreover, uncoupling the dopamine D1–D2 receptor complex led to significant behavioral changes (Pei et al. 2010). These findings formed the rationale to carry out the current study.

Given the major implication of GLT-1 in basic and clinical neurosciences, it was the aim of the study to use a method to unambiguously identify, characterize and analyze these transporter complexes in the native state from brain tissue to answer the question whether and which GLT-1 complexes are paralleling spatial memory training in the mouse.

In analogy to previous work with other membrane proteins (Ghafari et al. 2011), it was observed that native hippocampal GLT-1 complexes were paralleling spatial memory performance. This finding was obtained by the use of blue native gel technology allowing work under native conditions and therefore detection of native complexes, thus representing a major step forwards in functional neuroproteomics.

Materials and methods

Animals

C57BL/6J mice, male, aged 10–14 weeks, were used for Multiple T-maze (MTM) and protein chemical studies. Mice were bred and housed in their individual home cages

made from Makrolon and filled with autoclaved woodchips in the Core unit of Biomedical Research, Division of Laboratory Animal Science and Genetics, Medical University of Vienna. An autoclaved standard rodent diet (Altromin 1314ff) and water (acidified to pH 3 in bottles) were available ad libitum. Room temperature was 22 ± 1°C, and relative humidity was 50 ± 10%. The light/dark rhythm was 14:10. Ventilation with 100% fresh air resulted in an air change rate of 15 times per hour. The room was illuminated with artificial light at an intensity of about 200 lx in 2 m from 5 a.m. to 7 p.m. Behavioral tests were performed between 8 a.m. and 1 p.m.

Six hours after probe trials in the MTM, mice were killed by neck dislocation and hippocampi were dissected. Tissues were immediately frozen and stored at −80°C until used for protein chemical analysis. All efforts were made to minimize animal suffering and the number of animals used.

Experiments were performed under license of the federal ministry of education, science and culture, which includes an ethical evaluation of the project (Project: BMWF-66.009/0152-C/GT/2007). Housing and maintenance of animals were in compliance with European and national regulations.

Multiple T-Maze (MTM)

In this spatial learning task, animals learn to find the goal box based on their memory of previously visited arms. The MTM was constructed of wood and consisted of a wooden platform with eight choice points and the dimensions 265 cm × 202 cm × 140 cm and a path width of 8 cm.

Prior to testing, mice were deprived of food for 16 h to motivate food searching. Mice were placed in a start box in a black cylindrical start chamber. After 10 s elapsed, the chamber was lifted and the first trial was started. Mice were searching for the reward, and the trial was completed when mice had reached the goal box or, if failed, after 5 min. After mice arrived in the goal box, they were allowed to consume a small piece of a food pellet provided as reward and transferred to their home cage. Immediately after each trial, the entire maze was cleaned with 1% incidin solution. After testing, animals were given food as per body weight (120 g/kg) into the home cage, representing the amount to preserve their body weight but making them hungry for the following day for MTM tests. Mice were trained with 3 trials per day for 4 days. Trials were carried out using 20-min intervals.

Trials were recorded using the computerized tracking/image analyzer system (video camcorder: 1/3 in. SSAMHR EX VIEWHAD coupled with computational tracking system: TiBeSplit MFC application, Imagination Computer Services GmbH). The system provided the following parameters: latency, path length, speed and correct or wrong decisions (wrong means a path ending) to reach the goal box.

Yoked controls were placed in the MTM chamber to remain for the same time as their trained mates, but without rewarding food provided in the goal box. Since animals were exposed to the same spatial cues, but without rewarding food, mice did not develop an association between the extra-maze cues and the location of the food. The MTM was following the principle as published previously (Patil et al. 2009).

Total hippocampal membrane preparation

Total hippocampal cell membranes were prepared as described previously (Heo et al. 2010). All procedures were carried out at 4°C. Ten C57BL/6J mouse hippocampi per group ($n = 20$) were carefully washed with ice-cold homogenization buffer containing 10 mM HEPES, pH 7.5, containing 300 mM sucrose, 1 mM EDTA and protease inhibitor cocktail (Roche Diagnostics, Mannheim, Germany). Mouse hippocampi were homogenized in 10 mL of homogenization buffer using an Ultra-Turrax® (IKA, Staufen, Germany). The homogenate was centrifuged for 10 min at 1,000×g and the pellet was discarded. The resulting supernatant was centrifuged for 1 h at 50,000×g. The pellet was suspended in 5 mL of washing buffer (homogenization buffer without sucrose) followed by incubation in ice for 30 min. The homogenate was centrifuged for 30 min at 50,000×g.

Multidimensional gel electrophoresis

One-dimensional gel electrophoresis: blue native (BN)-PAGE

BN-PAGE was carried out as published previously with minor modifications (Kang and Lubec 2009). The 50,000×g total membrane pellets were suspended in membrane protein extraction buffer containing 1.5 M 6-aminocaproic acid and 300 mM Bis–Tris, pH 7.0. After resuspension, 10% n-dodecyl β-D-maltoside (DDM) stock solution was added to achieve a 1% DDM concentration. Membrane protein extraction was performed for 1 h at 4°C with vortexing every 10 min followed by centrifugation for 1 h at 20,800×g, 4°C. 8 µL of BN-PAGE loading buffer [5% (w/v) Coomassie G250 in 750 mM 6-aminocaproic acid] was mixed with 50 µL of resulting supernatant and loaded onto the gel. BN-PAGE was performed in a PROTEAN II xi Cell (BioRad, Germany) using a 4% stacking and a 5–18% separating gel. The BN-PAGE gel buffer contained 500 mM 6-aminocaproic acid and 50 mM Bis–Tris, pH 7.0; the cathode buffer 50 mM Tricine, 15 mM Bis–Tris and 0.05% (w/v) Coomassie G250, pH 7.0; and

the anode buffer 50 mM Bis–Tris, pH 7.0. For electrophoresis, the voltage was set to 50 V for 1 h, 75 V for 6 h, and was increased sequentially to 400 V (maximum current 15 mA/gel, maximum voltage 500 V) until the dye front reached the bottom of the gel. BN-PAGE gels were cut into lanes for use in BN/SDS-PAGE (2DE) or cut into small pieces for BN/SDS/SDS-PAGE focused on specific bands. High-molecular mass markers were obtained from Invitrogen (Carlsbad, CA, USA).

Two-dimensional gel electrophoresis: BN/SDS-PAGE

Gel pieces containing proteins of interest were separated via BN-PAGE and equilibrated for 30 min in an equilibration buffer (1% (w/v) SDS and 1% (v/v) 2-mercaptoethanol) with gentle agitation and then briefly rinsed with Milli-Q water. Gel pieces were then rinsed twice with SDS-PAGE electrophoresis buffer (25 mM Tris–HCl, 192 mM glycine and 0.1% (w/v) SDS; pH 8.3) and subsequently placed onto the SDS-PAGE gels. SDS-PAGE was performed in a PROTEAN II xi Cell using a 4% stacking and a 5–15% separating gel. Electrophoresis was carried out at 12°C with an initial current of 50 V (during the first hour). Then, voltage was increased to 100 V for the next 12 h (overnight) and increased to 150 V until the dye front reached the bottom of the gel. Colloidal Coomassie Brilliant Blue staining was used for visualization.

Three-dimensional gel electrophoresis: BN/SDS/SDS-PAGE

The three-dimensional gel electrophoresis was carried out according to a previously published protocol (Kang et al. 2009). Gel pieces (1–2 cm length) from BN-PAGE were equilibrated for 30 min in an equilibration buffer (1% (w/v) SDS and 1% (v/v) 2-mercaptoethanol). Gel pieces were then rinsed with Milli-Q water followed by SDS-PAGE electrophoresis buffer (25 mM Tris–HCl, 192 mM glycine and 0.1% (w/v) SDS; pH 8.3), and then, the gel pieces were placed onto the gels. Electrophoresis was performed in PROTEAN II xi Cell using a 4% stacking and a 5–15% separating gel for BN/SDS-PAGE (2DE). Electrophoresis was carried out at 12°C with an initial current of 50 V for the first 1 h. Then, the voltage was set to 75 V for the next 12 h and increased to 150 V until the bromophenol blue indicator moved 14–16 cm from the top of separation gel.

2DE gels were cut again into lanes and subsequently soaked for 30 min in an equilibration solution as same with equilibration for 2DE. Gel strips were then rinsed with water/SDS-PAGE electrophoresis buffer (25 mM Tris–HCl, 192 mM glycine and 0.1% (w/v) SDS; pH 8.3) and were then placed onto the BN/SDS/SDS-PAGE gels (3DE). SDS-PAGE was performed in PROTEAN II xi Cell using a 4% stacking and a 5–18% separating gel. Electrophoresis was carried out at 12°C with an initial current of 50 V for the first hour. Then, the voltage was set to 75 V for the next 12 h (overnight) and increased to 150 V until the bromophenol blue indicator reached the bottom of the gel. Colloidal Coomassie Brilliant Blue staining was used for visualization.

Immunoprecipitation of GLT-1 from mouse hippocampi

Membrane pellets from hippocampi were suspended in lysis buffer containing 1% DDM, 150 mM NaCl, 1 mM EDTA, 50 mM Tris–HCl (pH 8.0), 10 mM NaF and protease inhibitor cocktail (Roche, Mannheim, Germany) on a rotation shaker for 1 h at 4°C. After centrifugation at 15,300×*g*, 4°C for 10 min, the supernatant was incubated with affinity-purified rabbit anti-GLT1 polyclonal antibody (Abcam, Cambridge, UK) and subsequently incubated with protein A agarose beads (Roche, Mannheim, Germany) for 4 h at 4°C with gentle rotation. After six times of washing with the same lysis buffer, proteins bound were eluted with SDS sample buffer at 55°C for 12 min with vortexing and subsequently loaded on SDS-PAGE.

Enzymatic deglycosylation of GLT-1

To investigate the glycosylation status of GLT-1, samples were treated with PNGase F (peptide *N*-glycosidase F from *Flavobacterium meningosepticum*; New England Biolabs, Beverly, MA). Briefly, membrane proteins extracted with 1% DDM were partially denatured with 0.5% (w/v) SDS and 20 mM β-mercaptoethanol without heat treatment. 500 units of PNGase F were added with 50 mM sodium phosphate (pH 7.5) and 1% Nonidet P-40 to counteract SDS inactivation of PNGase F. After incubation at 37°C for 24 h, the reaction was stopped by adding 5 μL of 5× concentrated SDS sample buffer to 20 μL of the mixture.

Native membrane proteins prepared for BN-PAGE were also deglycosylated using Endoglycosidase F1, F2 or F3 from *Elizabethkingia miricola* (Endo F1, F2 or F3, recombinant, expressed in *E.coli*, Sigma, Germany). 37.5 μL of protein samples was mixed with 10 μL of reaction buffer. 2 μL of each enzyme (15 units/mg for Endo F1, 20 units/mg for Endo F2, 30 units/mg for Endo F3) was added to the reaction mixture and incubated for 1 h at 37°C. Results were monitored by SDS-PAGE followed by Western blotting to show shifts of mobility.

Western blots

Total enriched membrane protein samples were loaded onto 5–18% BN-PAGE or 10% SDS-PAGE, followed by electrophoresis with PROTEAN II xi/xL system or mini-

PROTEAN (BioRad, Germany). Proteins separated on the gel were transferred onto polyvinylidene fluoride (PVDF) membranes. After proteins were transferred from BN-PAGE to PVDF membranes, excess Coomassie Brilliant Blue G-250 dye was removed by rinsing the membranes in 100% methanol for 30 s. After blocking with 5% nonfat dry milk in 0.1% TBST, membranes were incubated with diluted primary rabbit polyclonal antibody against GLT-1 (1:50,000, Abcam, Cambridge, UK) and detected with horseradish peroxidase-conjugated anti-rabbit IgG (1:70,000, Abcam, Cambridge, UK). Membranes were developed with the GE healthcare ECL Plus Western Blotting Detection System (GE Healthcare, Buckinghamshire, UK).

Loading control: Protein contents of the lanes in all gels including BN-gels were evaluated, and the images and statistics are given in Suppl. Fig. 1 as described previously (Lomberk et al. 2006).

In-gel multi-enzymatic digestion of proteins and peptides

The gel pieces from BN/SDS/SDS-PAGE gels (3DE) were cut into small pieces to increase surface and put into a 1.5-mL tube. Gel pieces from MS compatible silver-stained gels were washed with 100 µL of destaining solution (50 mM potassium hexacyanoferrate, 300 mM sodium thiosulfate) for 10 min with vortexing. Destained gel pieces were then washed 2 times with washing solution (50% methanol, 40% water, 10% glacial acetic acid) for 5 min each with vortexing followed by washing with LC/MS water (Sigma, Germany) 4 times for 10 min each with vortexing. Gel pieces from colloidal stained gels were washed with 50 mM ammonium bicarbonate and then two times with washing buffer (50% 100 mM ammonium bicarbonate/50% acetonitrile) for 30 min each with vortexing. An aliquot of 100 µL of 100% acetonitrile was added to the tubes to cover the gel pieces completely and incubated for 10 min. The gel pieces were dried completely using a SpeedVac concentrator. Reduction in cysteine residues was carried out with a 10 mM dithiothreitol (DTT) solution in 100 mM ammonium bicarbonate pH 8.6 for 60 min at 56°C. After discarding the DTT solution, the same volume of a 55 mM iodoacetamide (IAA) solution in 100 mM ammonium bicarbonate buffer pH 8.6 was added and incubated in darkness for 45 min at 25°C to achieve alkylation of cysteine residues. The IAA solution was replaced by washing buffer (50% 100 mM ammonium bicarbonate/50% acetonitrile) and washed twice for 15 min each with vortexing. Gel pieces were washed and dried in 100% acetonitrile followed by drying in the SpeedVac.

The dried gel pieces were re-swollen with 12.5 ng/µL trypsin (Promega, Germany) solution reconstituted with 25 mM ammonium bicarbonate and 12.5 ng/µL chymotrypsin (Roche, Germany) solution buffered in 25 mM ammonium bicarbonate. The gel pieces were incubated for 16 h (overnight) at 37°C (trypsin) or 25°C (chymotrypsin). The supernatant was transferred to new 0.5-mL tubes, and the peptides were extracted with 50 µL of 0.5% formic acid/20% acetonitrile for 20 min in a sonication bath. This step was repeated two times. Samples in extraction buffer were pooled in 0.5-mL tubes and evaporated in a SpeedVac concentrator. The volume was reduced to approximately 15 µL, and then, 15 µL LC/MS water (Sigma, Germany) was added for nano-LC-ESI-(CID/ETD)-MS/MS analysis by high-capacity ion trap (HCT; Bruker, Germany).

Endoproteinase AspN (Roche Diagnostics) digestion was performed in 25 mM ammonium bicarbonate at 37°C for overnight. Pepsin (Sigma) digestion was performed in 0.1 M HCl (pH 1.0) and kept for 1 h at 37°C. For subtilisin digestion, the gel pieces were covered with 30 µL of 10 ng/µL subtilisin (proteinase from *Bacillus subtilis* var. *biotecus* A, Sigma) in a digestion buffer consisting of a final concentration of 6 M urea and 100 mM Tris, pH 8.5 and then rehydrated for 10 min at 4°C. The supernatant was removed and replaced by 50 mM ammonium bicarbonate. Gel pieces were incubated for 1 h at 37°C. Enzymatic reaction was stopped by adding 10% formic acid (a final concentration of 1% formic acid). The supernatant was transferred to new 0.5-mL tubes. Peptides were extracted by adding 30 µL of 5% formic acid followed by 20 min of sonication. This step was repeated once. The extracted peptides were subsequently analyzed by nano-LC-ESI-(CID/ETD)-MS/MS.

Peptide analysis by Nano-LC-ESI-(CID/ETD)-MS/MS HCT

For GLT-1 identification and posttranslational modification (PTM) search, trypsin-, chymotrypsin-, subtilisin-, AspN- or pepsin-digested peptides were separated by biocompatible Ultimate 3000 nano-LC system (Dionex, Sunnyvale, CA, USA) equipped with a PepMap100 C-18 trap column (300 µm id × 5 mm long cartridge, from Dionex) and PepMap100 C-18 analytic column (75 µm id × 150 mm long, from Dionex). The gradient consisted of (A) 0.1% formic acid in water and (B) 0.08% formic acid in ACN: 4–30% B from 0 to 105 min, 80% B from 105 to 110 min and 4% B from 110 to 125 min. The flow rate was 300 nL/min from 0 to 12 min, 75 nL/min from 12 to 105 min and 300 nL/min from 105 to 125 min. An HCT ultra-PTM discovery system (Bruker Daltonics, Bremen, Germany) was used to record peptide spectra over the mass range of m/z 350–1500 Th, and MS/MS spectra in information-dependent data acquisition over the mass range of m/z 100–2800 Th. Repeatedly, MS spectra were recorded followed by three data-dependent collision-induced dissociation (CID)

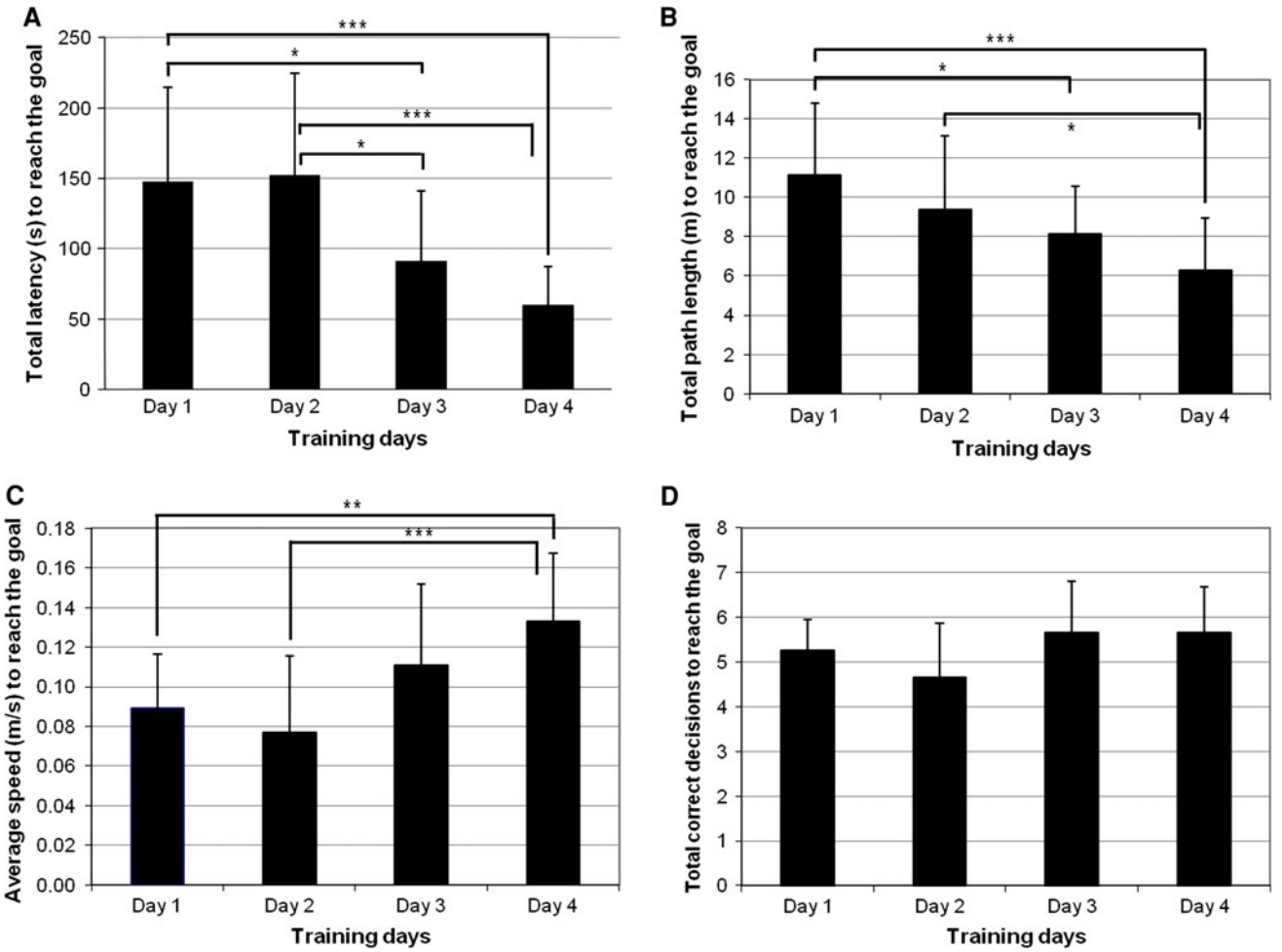

Fig. 1 Results of Multiple T-maze are given as mean ± SD. **a** During training days, there was a gradual reduction in total latency (s) in C57BL/6J. **b** Total path length (m) was reduced along with training in MTM. **c** Average speed was reduced significantly along the training period. **d** Total number of correct decisions did not show any difference between training days. *Asterisks* indicate the level of significance of difference in repeated measurement of ANOVA analysis (*$P < 0.05$, **$P < 0.01$, ***$P < 0.005$, ****$P < 0.001$). These results indicate that mice learned the spatial learning task

MS/MS spectra and three electron transfer dissociation (ETD) MS/MS spectra generated from three highest intensity precursor ions. The voltage between ion spray tip and spray shield was set to 1,500 V. Drying nitrogen gas was heated to 150°C, and the flow rate was 10 L/min. The collision energy was set automatically according to the mass and charge state of the peptides chosen for fragmentation. 2,3-charged (trypsin) or 1,2,3-charged (chymotrypsin, subtilisin, AspN, pepsin) peptides were chosen for MS/MS experiments due to their good fragmentation characteristics and specificities of hydrophobic peptides (Kang et al. 2009). MS/MS spectra were interpreted, and peak lists were generated by DataAnalysis 4.0 (Bruker Daltonics). Searches were performed by using the MASCOT v2.2.06 (Matrix Science, London, UK) and Modiro^{TM} v1.1 software (Protagen AG, Germany) against latest UniProtKB database for protein identification. Searching parameters were set as follows (1) MASCOT: enzyme selected as used with three maximum missing cleavage sites, species limited to mouse, a mass tolerance of 0.2 Da for peptide tolerance, 0.2 Da for MS/MS tolerance, ion score cutoff lower than 15, fixed modification of carbamidomethyl(C) and variable modification of oxidation (M), acetylation (K), deamidation (N, Q), methylation (C, D, E, H, K, N, Q, R, S, T) and phosphorylation (S, T, Y). Positive protein identifications were based on significant MOWSE scores. After protein identification, an error-tolerant search was performed to detect unspecific cleavage and unassigned modifications. Protein identification and modification information returned from MASCOT were manually inspected and filtered to obtain confirmed protein identification and modification lists of CID MS/MS and ETD MS/MS. (2) Modiro^{TM}: enzyme selected as used with three maximum missing cleavage sites, species limited to mouse, a peptide mass tolerance of

0.2 Da for peptide tolerance, 0.2 Da for fragment mass tolerance, modification 1 of carbamidomethyl(C) and modification 2 of methionine oxidation. Searches for unknown mass shifts, amino acid substitution and calculation of significance were selected on advanced PTM explorer search strategies. Positive protein identification was first of all listed by spectra view, and subsequently, each identified peptide was considered significant based on the 0.2 Da delta value, ion-charge status of peptide, b- and y-ion fragmentation quality, ion score (≥100) and significant scores (≥70). The Modiro software is complementary to the MASCOT software, using already identified sequences and has the advantage that also unknown mass shifts can be handled (Nuwal et al. 2011). Protein identification and modification information returned were manually inspected and filtered to obtain confirmed protein identification and modification lists (Kang et al. 2009).

Statistical analysis

Latency, total path length, average speed and total correct decisions during memory training between the trained and yoked group were compared using repeated measurement of ANOVA.

Western blotting results of GLT-1 were statistically evaluated by independent Student's *t*-test.

Correlations between latency, total path length, average speed, total correct decisions and arbitrary units of optical density of immunoreactive bands on day 4 were analyzed by Pearson correlation.

Values were expressed as mean ± SD. Statistical evaluation was made using SPSS (vers. 15.0.0; Chicago, IL, USA). In all instances, a probability level of $P < 0.05$ was considered statistically significant.

Results

Multiple T-maze

Animals trained for 4 days in the MTM learned the task as shown in Fig. 1a–d. Total latency ($P = 0.002$; Fig. 1a) was significantly decreasing in the trained group along the training period, indicating that mice learned the task.

Total path length, i.e., the distance (m) to reach the goal box in the MTM ($P = 0.002$; Fig. 1b), was also significantly decreasing along the training period.

Significantly increasing average speed was observed in trained mice along the training period ($P = 0.002$; Fig. 1c).

The numbers of total correct decisions did not show significant changes over the training period ($P = 0.092$, Fig. 1d).

BN-PAGE Western blotting for quantification

As shown in Fig. 2, three bands representing GLT-1 complexes were observed at approximately 242, 480 and 720 kDa that may be representing oligomers. Broadness of bands and smearing is a typical pattern of glycosylated proteins in native gels (Gendreau et al. 2004) or can be caused by other factors during BN-PAGE separation (Swamy et al. 2006).

Statistical analysis revealed higher levels of the three GLT-1 complexes in the trained group as shown in Fig. 3 (Band 1: $P < 0.005$, Band 1: $P < 0.001$, Band 1: $P < 0.005$).

Figure 4 shows the link between the GLT-1 complex at an apparent molecular weight of 720 kDa with the total correct decisions on day 4 ($R = 0.672$; $P = 0.033$). Pearson correlation coefficient and P values are given in Suppl. Table 2.

The loading control revealed comparable levels of proteins as shown in Suppl. Fig. 1 and Suppl. Table 1.

GLT-1 glycosylation

As shown in Fig. 5a, treatment, i.e., deglycosylation with PNGase F, resulted in a shift of GLT-1 mobility on SDS-PAGE. The probable monomer, dimer and trimer showed increased mobility in the denaturing SDS-PAGE. Bands representing GLT-1 complexes were shifted after PNGase F treatment clearly indicating *N*-glycosylation of GLT-1.

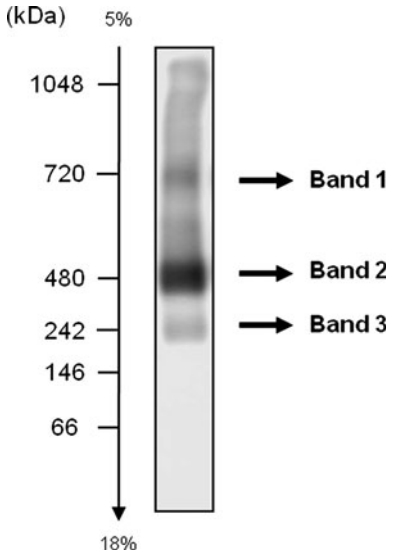

Fig. 2 Western blotting analysis of GLT-1 from C57BL/6J mice total enriched hippocampal membrane fraction. Total enriched hippocampal membrane fractions from C57BL/6J mice were subjected to BN-PAGE followed by Western blotting using an antibody recognizing GLT-1. Three GLT-1 complex bands at apparent molecular weights of 242, 480, and 720 kDa were observed

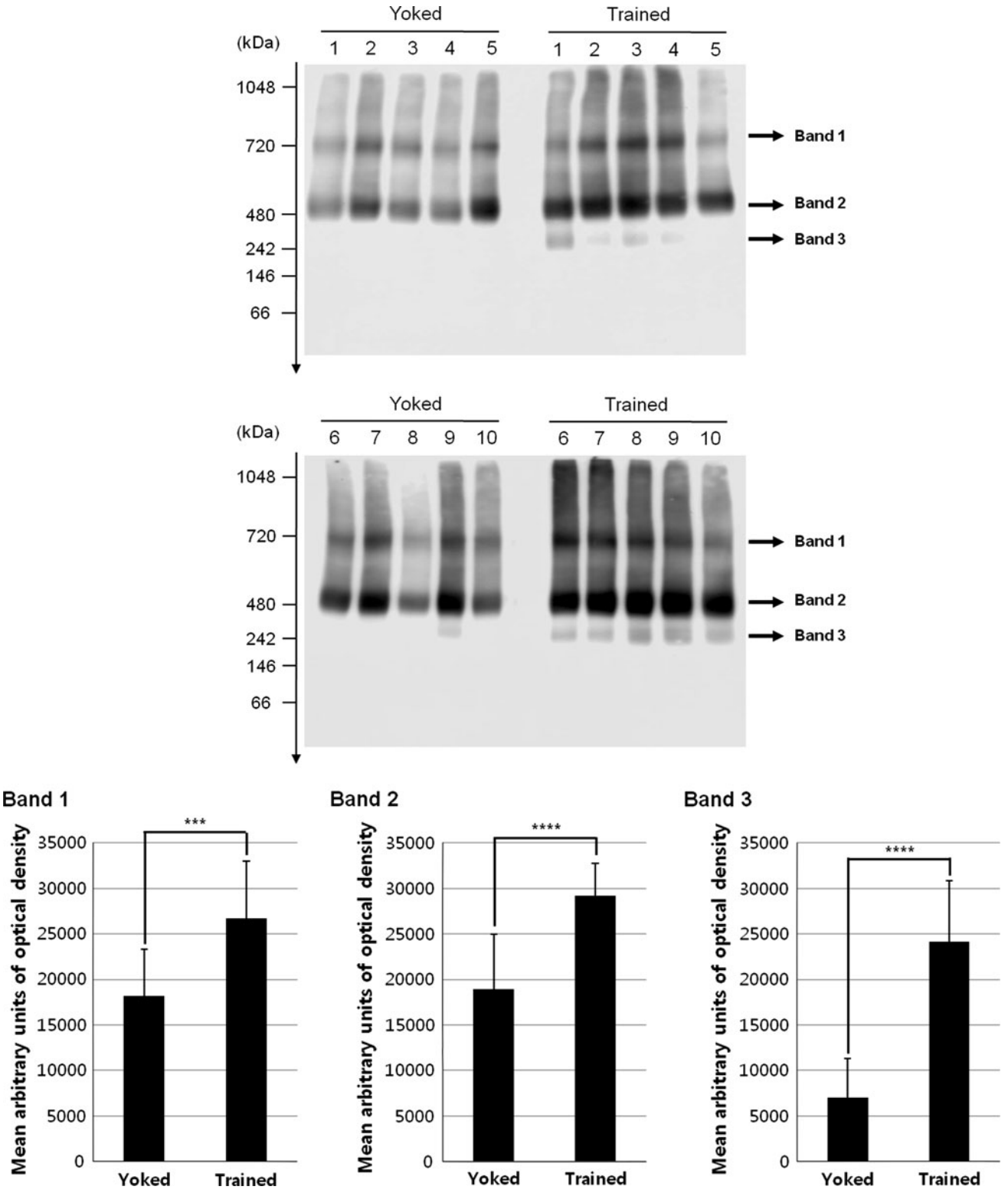

Fig. 3 BN-PAGE Western blotting and densitometric analysis of GLT-1 complexes in yoked control and trained groups. Enriched hippocampal total membrane fractions from yoked and trained C57BL/6J mice were subjected to BN-PAGE and immunoblotted using a GLT-1 antibody. Optical densities of three distinct immunoreactive bands were analyzed. Results were given as mean ± SD. The *asterisk* indicates significance (*$P < 0.05$, **$P < 0.01$, ***$P < 0.005$, ****$P < 0.001$)

Deglycosylation of GLT-1 with endoglycosidases F1, F2 or F3 did not lead to any significant shift of GLT-1 mobility in the SDS-PAGE (Fig. 5b), indicating that the complex oligosaccharide structure was not degraded by the endoglycosidases or degradation took place but did not alter electrophoretic mobility.

Mass spectrometrical assessment of GLT-1

Spots from the 3DE gel (Fig. 6a) or the SDS-PAGE gel after immunoprecipitation (Fig. 6b) were unambiguously identified as GLT-1 by nano-LC-ESI-MS/MS. Determination of the sequence coverage of GLT-1 by MS is given in Table 1 when MASCOT v2.2.06 was used and in Table 2 when Modiro ™ was v1.1 used. By summing up the peptides identified under different conditions, total sequence coverage was 88.63% from MASCOT searches and 98.95% from Modiro searches. Sequence coverage illustrations are given in Fig. 6c. Peptides identified following multi-enzyme digestion along with data on used enzymes, position of peptide, observed m/z, experimental mass, calculated (theoretical) mass, difference between experimental mass and calculated mass, number of missed cleavage sites, peptide sequence, modification, MASCOT ion score, Modiro ion score and significance score are provided in Suppl. Tables 3 and 4.

Indication for glycosylation of GLT-1 along with a representative mass spectrum is provided in Suppl. Fig. 2 and Suppl. Table 3. *N*-acetylhexosamines were observed on S3, T4, T394, T400 and N377 and hexosamine was observed on N273, thus verifying *N*-glycosylations.

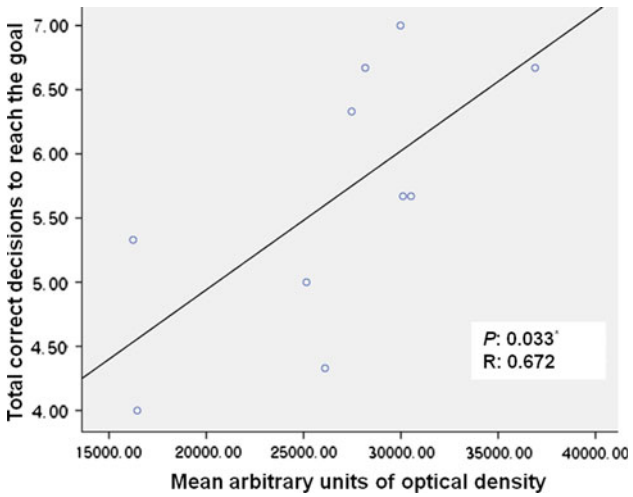

Fig. 4 Scatter plot of Pearson correlation analysis between total correct decisions on day 4 and arbitrary units of optical density of GLT-1 complex band at an apparent molecular weight of 720 kDa from BN-PAGE Western blotting analysis. Significance level (*P*) was 0.033

3DE Western blotting for antibody specificity verification

As shown in Fig. 7a, three individual bands containing GLT-1 complexes observed on BN-PAGE were processed to 3DE BN/SDS/SDS-PAGE followed by Western blotting analysis, indicating specificity of antibody recognition. Representative 3DE Western blotting results from the three individual BN-PAGE bands are shown in Fig. 7b–d. 2–3 spots were observed probably corresponding to mono-, di- and trimers.

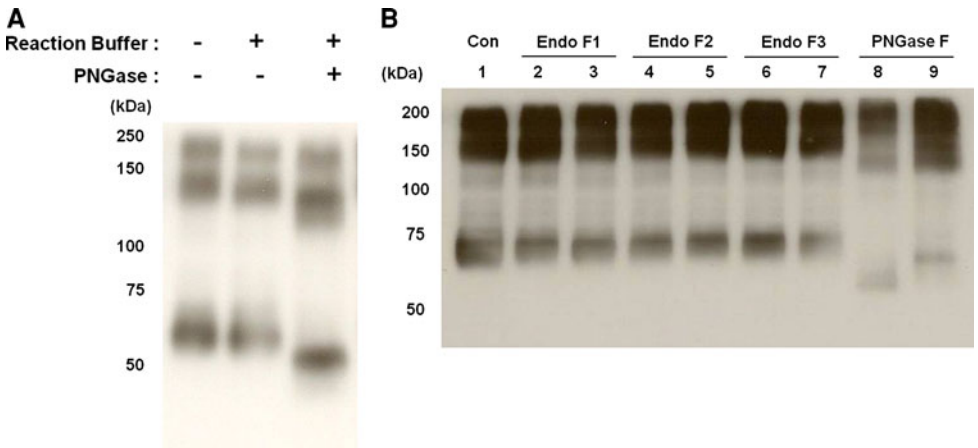

Fig. 5 Western blotting analysis of GLT-1 after deglycosylating enzyme treatment. **a** PNGase F was added to hippocampal total enriched membrane protein extracts and separated on SDS-PAGE followed by Western blotting against GLT-1. PNGase F caused obvious mobility shifts of GLT-1 on SDS-PAGE. **b** Endoglycosidase F1 (lane 2: 1-h incubation, lane 3: 2-h incubation), F2 (lane 4: 1-h incubation, lane 5: 2-h incubation) or F3 (lane 6: 1-h incubation, lane 7: 2-h incubation) were added to hippocampal total enriched membrane protein extracts, and the cleavage pattern was monitored by SDS-PAGE Western blotting against GLT-1. Crude extracts without enzyme (lane 1) and PNGase F-treated samples (lane 8: denaturing condition, lane 9: nondenaturing condition) were loaded as controls. Endo F1, F2 or F3 did not cause any significant mobility shift of GLT-1 on SDS-PAGE

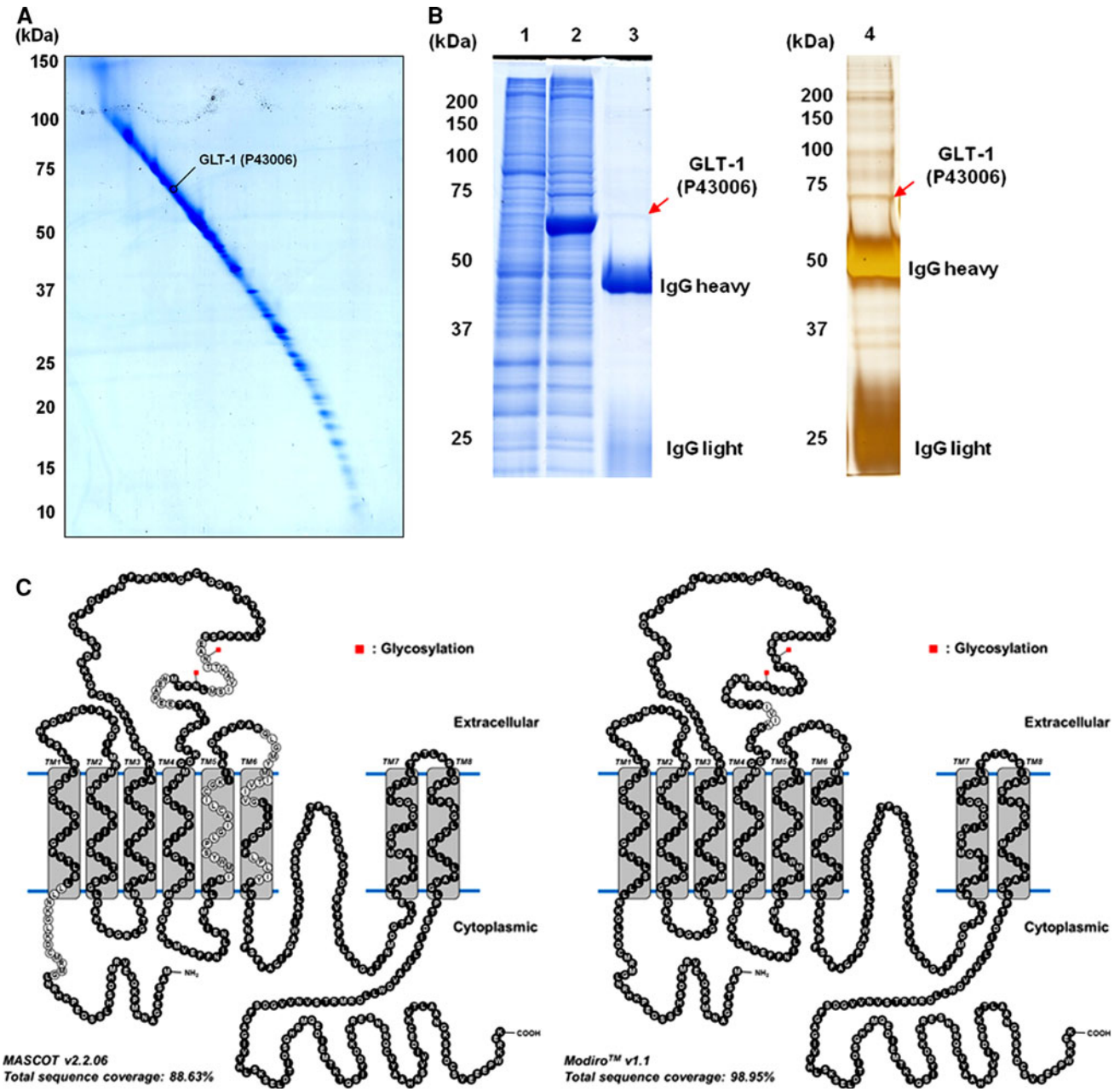

Fig. 6 **a** A representative 3DE BN/SDS/SDS-PAGE image. Gel pieces from BN-PAGE (shown in Fig. 2 marked as Band 1, 2 or 3) were equilibrated in buffer containing SDS and mercaptoethanol and loaded onto a 5–15% 2DE SDS-PAGE gel. The resulting lanes from 2DE BN/SDS-PAGE were then applied to a 5–17.5% SDS-PAGE gel. *Colloidal Blue* staining was used for protein visualization. **b** SDS-PAGE image of immunoprecipitated GLT-1 for the identification of the GLT-1 using mass spectrometry. The immunoprecipitate containing the GLT-1 was separated on SDS-PAGE, and proteins were visualized with *Colloidal Blue* (lane 1: crude extract, lane 2: flow through, lane 3: elute) or MS compatible silver staining (lane 4: elute). The indicated spots or bands were excised, and peptides were prepared by reduction/alkylation and multi-enzyme digestion. Extracted peptides were analyzed via nano-LC-ESI-MS/MS. The UniProtKB/SwissProt accession number is given. **c** Schematic illustration of sequence coverage of GLT-1 analyzed using MASCOT v2.2.06 or Modiro TM v1.1. Amino acids with closed circle are the identified residues. Total sequence coverage was 88.63% from MASCOT v2.2.06 and 98.95% from Modiro TM v1.1. Reported glycosylation sites were marked with *closed squares*

Discussion

There is only one study showing that GLT-1 is involved in memory formation in the rat, while vesicular glutamate transporters have been implicated already in memory formation (Tordera et al. 2007). Glutamate transporters (EAAT) , for example, GLT-1, serve for signal termination, while vesicular glutamate transporters regulate signal

Table 1 Identification and sequence coverage of GLT-1 from mouse hippocampal total enriched membrane fraction using multi-enzyme digestion from MASCOT v2.2.06 software

Condition Nr.	Enzyme	Database search condition with MASCOT v2.2.06	Sequence coverage (%)	Number of identified TMD	Identified TMD[a]
1	Trypsin	Database: UniProtKB/SwissProt Missed cleavage: 3 Peptide tolerance: 0.2 Da Ms/MS tolerance: 0.2 Da Peptide charge: +2, +3 Monoisotopic mass	43.53	3	pTM2, pTM4, pTM5
2	Chymotrypsin	Database: UniProtKB/SwissProt Missed cleavage: 5	76.74	8	pTM1, TM2, TM3, TM4 pTM5, pTM6, TM7, TM8
3	Subtilisin	Peptide tolerance: 0.2 Da	17.48	3	pTM3, pTM4, pTM8
4	AspN	Ms/MS tolerance: 0.2 Da	9.96	0	–
5	Pepsin	Peptide charge: +1, +2, +3 Monoisotopic mass	15.90	5	pTM1, pTM2, pTM4, pTM6, pTM8

[a] *pTM* partially identified transmembrane domain

– Not identified

Table 2 Identification and sequence coverage of GLT-1 from mouse hippocampal total enriched membrane fraction using multi-enzyme digestion from Modiro™ v1.1 software

Condition Nr.	Enzyme	Database search condition with Modiro™ v1.1	Minimum significance	Sequence coverage (%)	Number of identified TMD	Identified TMD[a]
1	Trypsin	Database: UniProtKB/SwissProt Missed cleavage: 3 Peptide tolerance: 0.2 Da Ms/MS tolerance: 0.2 Da Peptide charge: +2, +3 Monoisotopic mass	90	55.41	2	TM2, pTM5
			80	75.87	5	TM1, TM2, TM4, TM5, TM6
2	Chymotrypsin	Database: UniProtKB/SwissProt	90	86.71	8	TM1, TM2, TM4, TM4, pTM5, pTM6, TM7, TM8
		Missed cleavage: 5	80	88.71	8	TM1, TM2, TM4, TM4, TM5, TM6, TM7, TM8
3	Subtilisin	Peptide tolerance: 0.2 Da Ms/MS tolerance: 0.2 Da Peptide charge: +1, +2, +3 Monoisotopic mass	90	37.93	8	pTM1, pTM2, pTM3, pTM4, pTM5, pTM6, pTM7, pTM8
			80	41.08	8	pTM1, pTM2, pTM3, pTM4, pTM5, pTM6, pTM7, pTM8
4	AspN		90	2.09	0	–
			80	4.72	0	–
5	Pepsin		90	28.49	5	pTM1, pTM2, pTM3, pTM5, pTM6
			80	36.53	6	pTM1, pTM2, pTM3, pTM5, pTM6, pTM8

[a] *pTM* partially identified transmembrane domain

– Not identified

output through exocytotic release and glutamate receptors generate signal input (Hinoi et al. 2005).

Bechthold-Gompf et al. (Bechtholt-Gompf et al. 2010) showed that inhibition of GLT-1 by dihydrokainic acid led to impairment of spatial memory as evaluated in the Morris Water maze. Herein, we show that increased GLT-1 complex levels are paralleling memory training in a spatial memory paradigm and, moreover, that a high-molecular

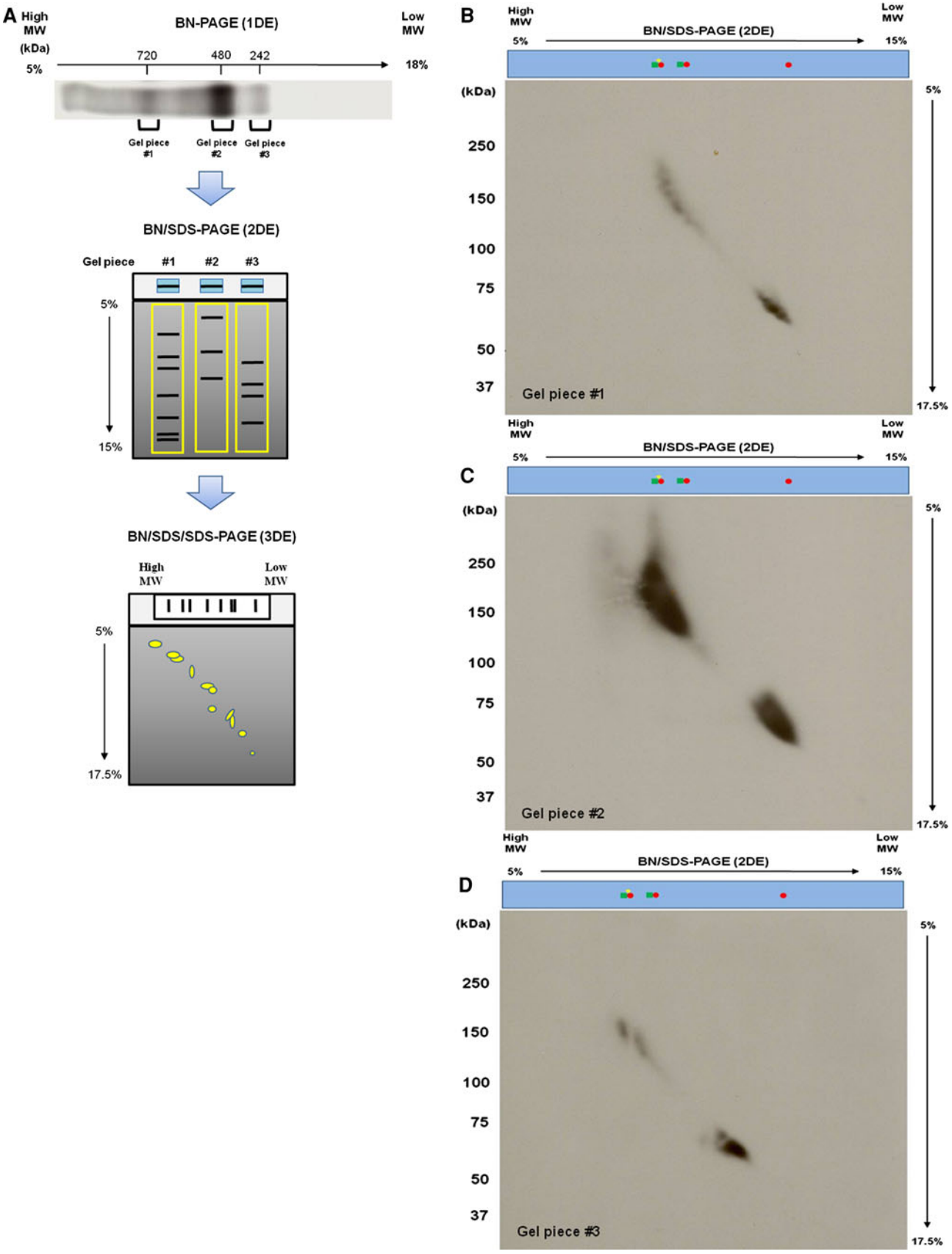
A
High MW
(kDa)
5%
BN-PAGE (1DE)
Low MW
18%
720
480
242
Gel piece #1
Gel piece #2
Gel piece #3
BN/SDS-PAGE (2DE)
Gel piece
#1
#2
#3
5%
15%
BN/SDS/SDS-PAGE (3DE)
High MW
Low MW
5%
17.5%
B
High MW
Low MW
5%
BN/SDS-PAGE (2DE)
15%
(kDa)
250
150
100
75
50
37
Gel piece #1
5%
17.5%
C
Gel piece #2
D
Gel piece #3

◀ **Fig. 7** 3DE Western blotting analysis of GLT-1 from C57BL/6J mice enriched hippocampal total membrane fraction. Enriched hippocampal total enriched membrane fractions from C57BL/6J mice were subjected to BN-PAGE and visualized by Western blotting against GLT-1 as shown in Fig. 2. **a** Three gel pieces that correspond to immunoreactive GLT-1 complexes were excised and soaked in equilibration buffer. Equilibrated BN-PAGE gel pieces were subjected to 2DE (BN/SDS-PAGE) followed by 3DE (BN/SDS/SDS-PAGE). Separated proteins on 3DE gels from Band 1 (**b**), Band 2 (**c**) and Band 3 (**d**) were transferred to PVDF membranes and subsequently visualized by Western blotting against GLT-1. Immunoreactive signals are indicating mono-, di- or trimers of GLT-1

weight GLT-1 complex is associated with the total number of correct decisions at the end of memory training in the MTM. The MTM was selected because it has been in use as a reliable paradigm as a land maze for mice in our laboratory (Patil et al. 2009).

As the monomer of GLT-1 was not detected on BN-PAGE, no correlation with parameters from the spatial memory paradigm could be evaluated. The absence may be due to undetectably low levels of the GLT-1 monomer or technical reasons. The study was designed to detect high-molecular weight complexes of GLT-1 levels: as stated in the Introduction, many transporters including the majority of brain receptors show assembly of subunits to form several functional complex units. While the GLT-1 complex at about 720 kDa was correlated with correct decisions, the other complexes observed failed to correlate, probably indicating that for generation of spatial memory in hippocampus, exactly this assembly may be functional at the time point studied. The concept and principle of complex formation of brain transporters, i.e., the reason why specific complexes are needed, has been proposed as mentioned above, but further work is needed to elucidate mechanisms of GLT-1 complex formation in the protein network of spatial memory formation. Findings herein are the first contribution to demonstrate which specific GLT-1 complex is associated with a specific function in spatial memory in a given area.

GLT-1 was unambiguously identified by mass spectrometry that was not published before, and in addition, we have shown that the antibody against GLT-1 was specifically and exclusively recognizing this transporter based upon a previously published suggestion for the validation of antibody specificity (Heo and Lubec 2010).

All bands representing GLT-1 were *N*-glycosylated as shown by the presence of electrophoretic mobility changes following incubation with PNGase F which is in agreement with previous studies on recombinant bacterial and human GLT-1 (Gendreau et al. 2004; Raunser et al. 2005). Own mass spectrometrical studies on posttranslational modifications reveal that GLT-1 is *N*-glycosylated (Suppl. Fig. 2 and Suppl. Table 3 and 4).

The high sequence coverage for protein identification obtained was due to multi-enzyme digestion and the use of two different softwares for protein identification. And indeed, GABAA receptor subunits (Kang et al. 2008, 2009, 2011) and the mitochondrial carrier Aralar1 (Heo et al. 2010) were successfully analyzed using the method used herein.

Most peptide sequences identified from subtilisin, AspN or pepsin were overlapping with peptides from trypsin or chymotrypsin digestion. As compared to other proteases, chymotrypsin was the most effective to generate peptides from transmembrane domains.

Taken together, the current findings may be relevant for subsequent studies and interpretation of previous studies on GLT-1 related to spatial memory formation. The major finding of the study is that herein GLT-1 complexes rather than a monomer were determined and characterized using BN-PAGE and that these complexes were associated with correct decisions in the MTM. Immunochemical analysis of native GLT-1 complexes was carried out by combining immunoblotting with multidimensional gel electrophoresis, and thus, antibody specificity was validated. Moreover, mass spectrometrical analysis with multi-enzyme digestion allowed to obtain high sequence coverage and verification of posttranslational modifications, i.e., *N*-glycosylation. An analytical tool for qualitative and quantitative assessment of GLT-1 containing complexes was provided that would allow further studies linking this transporter to memory formation in different settings of memory testing, and this method represents a technique for determination of GLT-1 complexes for pharmacological investigations. Our laboratory is now in the process of evaluating the concerted action of glutamate receptor complexes and glutamate transporter complexes.

Acknowledgments The authors acknowledge the contribution by the Verein zur Durchführung der wissenschaftlichen Forschung auf dem Gebiet der Neonatologie und Kinderintensivmedizin "Unser Kind".

Conflict of interest The authors declare that they have no conflicts of interest.

References

Agnati LF, Ferre S, Burioni R, Woods A, Genedani S, Franco R, Fuxe K (2005) Existence and theoretical aspects of homomeric and heteromeric dopamine receptor complexes and their relevance for neurological diseases. Neuromolecular Med 7:61–78

Amara SG, Fontana AC (2002) Excitatory amino acid transporters: keeping up with glutamate. Neurochem Int 41:313–318

Anderson CM, Swanson RA (2000) Astrocyte glutamate transport: review of properties, regulation, and physiological functions. Glia 32:1–14

Arriza JL, Fairman WA, Wadiche JI, Murdoch GH, Kavanaugh MP, Amara SG (1994) Functional comparisons of three glutamate transporter subtypes cloned from human motor cortex. J Neurosci 14:5559–5569

Autry AE, Grillo CA, Piroli GG, Rothstein JD, McEwen BS, Reagan LP (2006) Glucocorticoid regulation of GLT-1 glutamate transporter isoform expression in the rat hippocampus. Neuroendocrinology 83:371–379

Ballif BA, Carey GR, Sunyaev SR, Gygi SP (2008) Large-scale identification and evolution indexing of tyrosine phosphorylation sites from murine brain. J Proteome Res 7:311–318

Baucum AJ 2nd, Rau KS, Riddle EL, Hanson GR, Fleckenstein AE (2004) Methamphetamine increases dopamine transporter higher molecular weight complex formation via a dopamine- and hyperthermia-associated mechanism. J Neurosci 24:3436–3443

Bauman AL, Apparsundaram S, Ramamoorthy S, Wadzinski BE, Vaughan RA, Blakely RD (2000) Cocaine and antidepressant-sensitive biogenic amine transporters exist in regulated complexes with protein phosphatase 2A. J Neurosci 20:7571–7578

Bechtholt-Gompf AJ, Walther HV, Adams MA, Carlezon WA Jr, Ongur D, Cohen BM (2010) Blockade of astrocytic glutamate uptake in rats induces signs of anhedonia and impaired spatial memory. Neuropsychopharmacology 35:2049–2059

Brooks-Kayal AR, Munir M, Jin H, Robinson MB (1998) The glutamate transporter, GLT-1, is expressed in cultured hippocampal neurons. Neurochem Int 33:95–100

Campbell SL, Hablitz JJ (2004) Glutamate transporters regulate excitability in local networks in rat neocortex. Neuroscience 127:625–635

Chu K, Lee ST, Sinn DI, Ko SY, Kim EH, Kim JM, Kim SJ, Park DK, Jung KH, Song EC, Lee SK, Kim M, Roh JK (2007) Pharmacological induction of ischemic tolerance by glutamate transporter-1 (EAAT2) upregulation. Stroke 38:177–182

Danbolt NC (2001) Glutamate uptake. Prog Neurobiol 65:1–105

Domercq M, Etxebarria E, Perez-Samartin A, Matute C (2005) Excitotoxic oligodendrocyte death and axonal damage induced by glutamate transporter inhibition. Glia 52:36–46

Dunlop J, Lou Z, McIlvain HB (1999a) Steroid hormone-inducible expression of the GLT-1 subtype of high-affinity l-glutamate transporter in human embryonic kidney cells. Biochem Biophys Res Commun 265:101–105

Dunlop J, Lou Z, Zhang Y, McIlvain HB (1999b) Inducible expression and pharmacology of the human excitatory amino acid transporter 2 subtype of L-glutamate transporter. Br J Pharmacol 128:1485–1490

Fattorini G, Melone M, Bragina L, Candiracci C, Cozzi A, Pellegrini Giampietro DE, Torres-Ramos M, Perez-Samartin A, Matute C, Conti F (2008) GLT-1 expression and Glu uptake in rat cerebral cortex are increased by phencyclidine. Glia 56:1320–1327

Furuta A, Rothstein JD, Martin LJ (1997) Glutamate transporter protein subtypes are expressed differentially during rat CNS development. J Neurosci 17:8363–8375

Gebhardt FM, Mitrovic AD, Gilbert DF, Vandenberg RJ, Lynch JW, Dodd PR (2010) Exon-skipping splice variants of excitatory amino acid transporter-2 (EAAT2) form heteromeric complexes with full-length EAAT2. J Biol Chem 285:31313–31324

Gendreau S, Voswinkel S, Torres-Salazar D, Lang N, Heidtmann H, Detro-Dassen S, Schmalzing G, Hidalgo P, Fahlke C (2004) A trimeric quaternary structure is conserved in bacterial and human glutamate transporters. J Biol Chem 279:39505–39512

Genedani S, Guidolin D, Leo G, Filaferro M, Torvinen M, Woods AS, Fuxe K, Ferre S, Agnati LF (2005) Computer-assisted image analysis of caveolin-1 involvement in the internalization process of adenosine A2A-dopamine D2 receptor heterodimers. J Mol Neurosci 26:177–184

Ghafari M, Falsafi SK, Hoeger H, Lubec G (2011) Hippocampal levels of GluR1 and GluR2 complexes are modulated by training in the Multiple T-Maze in C57BL/6J mice. Brain Struct Funct (in press), doi:10.1007/s00429-011-0335-8

Gonzalez MI, Robinson MB (2004) Neurotransmitter transporters: why dance with so many partners? Curr Opin Pharmacol 4:30–35

Gonzalez MI, Susarla BT, Robinson MB (2005) Evidence that protein kinase Calpha interacts with and regulates the glial glutamate transporter GLT-1. J Neurochem 94:1180–1188

Gonzalez–Gonzalez IM, Garcia-Tardon N, Gimenez C, Zafra F (2009) Splice variants of the glutamate transporter GLT1 form hetero-oligomers that interact with PSD-95 and NMDA receptors. J Neurochem 110:264–274

Hadlock GC, Baucum AJ II, King JL, Horner KA, Cook GA, Gibb JW, Wilkins DG, Hanson GR, Fleckenstein AE (2009) Mechanisms underlying methamphetamine-induced dopamine transporter complex formation. J Pharmacol Exp Ther 329:169–174

Hadlock GC, Chu PW, Walters ET, Hanson GR, Fleckenstein AE (2010) Methamphetamine-induced dopamine transporter complex formation and dopaminergic deficits: the role of D2 receptor activation. J Pharmacol Exp Ther 335:207–212

Haugeto O, Ullensvang K, Levy LM, Chaudhry FA, Honore T, Nielsen M, Lehre KP, Danbolt NC (1996) Brain glutamate transporter proteins form homomultimers. J Biol Chem 271:27715–27722

Hediger MA, Kanai Y, You G, Nussberger S (1995) Mammalian ion-coupled solute transporters. J Physiol 482:7S–17S

Heo S, Lubec G (2010) Generation and characterization of a specific polyclonal antibody against the mouse serotonin receptor 1A: a state-of-the-art recommendation on how to characterize antibody specificity. Electrophoresis 31:3789–3796

Heo S, Kang SU, Oehler R, Pollak A, Lubec G (2010) Mass spectrometrical analysis of the mitochondrial carrier Aralar1 from mouse hippocampus. Electrophoresis 31:1813–1821

Hinoi E, Takarada T, Tsuchihashi Y, Yoneda Y (2005) Glutamate transporters as drug targets. Curr Drug Targets CNS Neurol Disord 4:211–220

Huang YH, Sinha SR, Tanaka K, Rothstein JD, Bergles DE (2004) Astrocyte glutamate transporters regulate metabotropic glutamate receptor-mediated excitation of hippocampal interneurons. J Neurosci 24:4551–4559

Kanai Y, Hediger MA (2004) The glutamate/neutral amino acid transporter family SLC1: molecular, physiological and pharmacological aspects. Pflugers Arch 447:469–479

Kang SU, Lubec G (2009) Complete sequencing of GABAA receptor subunit beta 3 by a rapid technique following in-gel digestion of the protein. Electrophoresis 30:2159–2167

Kang SU, Fuchs K, Sieghart W, Lubec G (2008) Gel-based mass spectrometric analysis of recombinant GABA(A) receptor subunits representing strongly hydrophobic transmembrane proteins. J Proteome Res 7:3498–3506

Kang SU, Fuchs K, Sieghart W, Pollak A, Csaszar E, Lubec G (2009) Gel-based mass spectrometric analysis of a strongly hydrophobic GABAA-receptor subunit containing four transmembrane domains. Nat Protoc 4:1093–1102

Kang SU, Heo S, Lubec G (2011) Mass spectrometric analysis of GABA(A) receptor subtypes and phosphorylations from mouse hippocampus. Proteomics 11:2171–2181

Katagiri H, Tanaka K, Manabe T (2001) Requirement of appropriate glutamate concentrations in the synaptic cleft for hippocampal LTP induction. Eur J Neurosci 14:547–553

Kirschner MA, Copeland NG, Gilbert DJ, Jenkins NA, Amara SG (1994) Mouse excitatory amino acid transporter EAAT2: isolation, characterization, and proximity to neuroexcitability loci on mouse chromosome 2. Genomics 24:218–224

Lee Y, Gaskins D, Anand A, Shekhar A (2007) Glia mechanisms in mood regulation: a novel model of mood disorders. Psychopharmacology (Berl) 191:55–65

Li LB, Toan SV, Zelenaia O, Watson DJ, Wolfe JH, Rothstein JD, Robinson MB (2006) Regulation of astrocytic glutamate transporter expression by Akt: evidence for a selective transcriptional effect on the GLT-1/EAAT2 subtype. J Neurochem 97:759–771

Lomberk G, Bensi D, Fernandez-Zapico ME, Urrutia R (2006) Evidence for the existence of an HP1-mediated subcode within the histone code. Nat Cell Biol 8:407–415

Maragakis NJ, Dykes-Hoberg M, Rothstein JD (2004) Altered expression of the glutamate transporter EAAT2b in neurological disease. Ann Neurol 55:469–477

Matute C, Melone M, Vallejo-Illarramendi A, Conti F (2005) Increased expression of the astrocytic glutamate transporter GLT-1 in the prefrontal cortex of schizophrenics. Glia 49:451–455

McCullumsmith RE, Meador-Woodruff JH (2002) Striatal excitatory amino acid transporter transcript expression in schizophrenia, bipolar disorder, and major depressive disorder. Neuropsychopharmacology 26:368–375

Mennerick S, Dhond RP, Benz A, Xu W, Rothstein JD, Danbolt NC, Isenberg KE, Zorumski CF (1998) Neuronal expression of the glutamate transporter GLT-1 in hippocampal microcultures. J Neurosci 18:4490–4499

Meyer T, Ludolph AC, Morkel M, Hagemeier C, Speer A (1997) Genomic organization of the human excitatory amino acid transporter gene GLT-1. Neuroreport 8:775–777

Meyer T, Munch C, Liebau S, Fromm A, Schwalenstocker B, Volkel H, Ludolph AC (1998) Splicing of the glutamate transporter EAAT2: a candidate gene of amyotrophic lateral sclerosis. J Neurol Neurosurg Psychiatry 65:954

Mukainaka Y, Tanaka K, Hagiwara T, Wada K (1995) Molecular cloning of two glutamate transporter subtypes from mouse brain. Biochim Biophys Acta 1244:233–237

Munir M, Correale DM, Robinson MB (2000) Substrate-induced up-regulation of Na(+)-dependent glutamate transport activity. Neurochem Int 37:147–162

Munton RP, Tweedie-Cullen R, Livingstone-Zatchej M, Weinandy F, Waidelich M, Longo D, Gehrig P, Potthast F, Rutishauser D, Gerrits B, Panse C, Schlapbach R, Mansuy IM (2007) Qualitative and quantitative analyses of protein phosphorylation in naive and stimulated mouse synaptosomal preparations. Mol Cell Proteomics 6:283–293

Nuwal T, Heo S, Lubec G, Buchner E (2011) Mass spectrometric analysis of synapsins in Drosophila melanogaster and identification of novel phosphorylation sites. J Proteome Res 10:541–550

Ohnuma T, Tessler S, Arai H, Faull RL, McKenna PJ, Emson PC (2000) Gene expression of metabotropic glutamate receptor 5 and excitatory amino acid transporter 2 in the schizophrenic hippocampus. Brain Res Mol Brain Res 85:24–31

Omrani A, Melone M, Bellesi M, Safiulina V, Aida T, Tanaka K, Cherubini E, Conti F (2009) Up-regulation of GLT-1 severely impairs LTD at mossy fibre–CA3 synapses. J Physiol 587:4575–4588

O'Shea RD (2002) Roles and regulation of glutamate transporters in the central nervous system. Clin Exp Pharmacol Physiol 29:1018–1023

Patil SS, Sunyer B, Hoger H, Lubec G (2009) Evaluation of spatial memory of C57BL/6J and CD1 mice in the Barnes maze, the Multiple T-maze and in the Morris water maze. Behav Brain Res 198:58–68

Pawlak J, Brito V, Kuppers E, Beyer C (2005) Regulation of glutamate transporter GLAST and GLT-1 expression in astrocytes by estrogen. Brain Res Mol Brain Res 138:1–7

Peacey E, Miller CC, Dunlop J, Rattray M (2009) The four major N- and C-terminal splice variants of the excitatory amino acid transporter GLT-1 form cell surface homomeric and heteromeric assemblies. Mol Pharmacol 75:1062–1073

Pei L, Li S, Wang M, Diwan M, Anisman H, Fletcher PJ, Nobrega JN, Liu F (2010) Uncoupling the dopamine D1–D2 receptor complex exerts antidepressant-like effects. Nat Med 16:1393–1395

Perego C, Vanoni C, Bossi M, Massari S, Basudev H, Longhi R, Pietrini G (2000) The GLT-1 and GLAST glutamate transporters are expressed on morphologically distinct astrocytes and regulated by neuronal activity in primary hippocampal cocultures. J Neurochem 75:1076–1084

Qu S, Kanner BI (2008) Substrates and non-transportable analogues induce structural rearrangements at the extracellular entrance of the glial glutamate transporter GLT-1/EAAT2. J Biol Chem 283:26391–26400

Raunser S, Haase W, Bostina M, Parcej DN, Kuhlbrandt W (2005) High-yield expression, reconstitution and structure of the recombinant, fully functional glutamate transporter GLT-1 from Rattus norvegicus. J Mol Biol 351:598–613

Regan MR, Huang YH, Kim YS, Dykes-Hoberg MI, Jin L, Watkins AM, Bergles DE, Rothstein JD (2007) Variations in promoter activity reveal a differential expression and physiology of glutamate transporters by glia in the developing and mature CNS. J Neurosci 27:6607–6619

Robinson MB (1998) The family of sodium-dependent glutamate transporters: a focus on the GLT-1/EAAT2 subtype. Neurochem Int 33:479–491

Rose EM, Koo JC, Antflick JE, Ahmed SM, Angers S, Hampson DR (2009) Glutamate transporter coupling to Na, K-ATPase. J Neurosci 29:8143–8155

Rothstein JD, Dykes-Hoberg M, Pardo CA, Bristol LA, Jin L, Kuncl RW, Kanai Y, Hediger MA, Wang Y, Schielke JP, Welty DF (1996) Knockout of glutamate transporters reveals a major role for astroglial transport in excitotoxicity and clearance of glutamate. Neuron 16:675–686

Sattler R, Rothstein JD (2006) Regulation and dysregulation of glutamate transporters. Handb Exp Pharmacol 175:277–303

Schmitt A, Zink M, Petroianu G, May B, Braus DF, Henn FA (2003) Decreased gene expression of glial and neuronal glutamate transporters after chronic antipsychotic treatment in rat brain. Neurosci Lett 347:81–84

Sheldon AL, Robinson MB (2007) The role of glutamate transporters in neurodegenerative diseases and potential opportunities for intervention. Neurochem Int 51:333–355

Sims KD, Robinson MB (1999) Expression patterns and regulation of glutamate transporters in the developing and adult nervous system. Crit Rev Neurobiol 13:169–197

Sitcheran R, Gupta P, Fisher PB, Baldwin AS (2005) Positive and negative regulation of EAAT2 by NF-kappaB: a role for N-myc in TNFalpha-controlled repression. EMBO J 24:510–520

Smith RE, Haroutunian V, Davis KL, Meador-Woodruff JH (2001) Expression of excitatory amino acid transporter transcripts in the thalamus of subjects with schizophrenia. Am J Psychiatry 158:1393–1399

Suchak SK, Baloyianni NV, Perkinton MS, Williams RJ, Meldrum BS, Rattray M (2003) The 'glial' glutamate transporter, EAAT2 (Glt-1) accounts for high affinity glutamate uptake into adult rodent nerve endings. J Neurochem 84:522–532

Sutherland ML, Delaney TA, Noebels JL (1995) Molecular characterization of a high-affinity mouse glutamate transporter. Gene 162:271–274

Swamy M, Siegers GM, Minguet S, Wollscheid B, Schamel WW (2006) Blue native polyacrylamide gel electrophoresis (BN-PAGE) for the identification and analysis of multiprotein complexes. Sci STKE 2006:pl4

Swanson RA, Liu J, Miller JW, Rothstein JD, Farrell K, Stein BA, Longuemare MC (1997) Neuronal regulation of glutamate transporter subtype expression in astrocytes. J Neurosci 17:932–940

Takatsuru Y, Iino M, Tanaka K, Ozawa S (2007) Contribution of glutamate transporter GLT-1 to removal of synaptically released glutamate at climbing fiber-Purkinje cell synapses. Neurosci Lett 420:85–89

Tanaka K (2000) Functions of glutamate transporters in the brain. Neurosci Res 37:15–19

Tanaka K, Watase K, Manabe T, Yamada K, Watanabe M, Takahashi K, Iwama H, Nishikawa T, Ichihara N, Kikuchi T, Okuyama S, Kawashima N, Hori S, Takimoto M, Wada K (1997) Epilepsy and exacerbation of brain injury in mice lacking the glutamate transporter GLT-1. Science 276:1699–1702

Tordera RM, Totterdell S, Wojcik SM, Brose N, Elizalde N, Lasheras B, Del Rio J (2007) Enhanced anxiety, depressive-like behaviour and impaired recognition memory in mice with reduced expression of the vesicular glutamate transporter 1 (VGLUT1). Eur J Neurosci 25:281–290

Utsunomiya-Tate N, Endou H, Kanai Y (1997) Tissue specific variants of glutamate transporter GLT-1. FEBS Lett 416:312–316

Williams SM, Sullivan RK, Scott HL, Finkelstein DI, Colditz PB, Lingwood BE, Dodd PR, Pow DV (2005) Glial glutamate transporter expression patterns in brains from multiple mammalian species. Glia 49:520–541

Zerangue N, Kavanaugh MP (1996) Flux coupling in a neuronal glutamate transporter. Nature 383:634–637

Zhang H, Xin W, Dougherty PM (2009) Synaptically evoked glutamate transporter currents in Spinal Dorsal Horn Astrocytes. Mol Pain 5:36

Journal of Neurochemistry

JOURNAL OF NEUROCHEMISTRY | 2015

doi: 10.1111/jnc.13119

ORIGINAL ARTICLE

Drebrin depletion alters neurotransmitter receptor levels in protein complexes, dendritic spine morphogenesis and memory-related synaptic plasticity in the mouse hippocampus

Gangsoo Jung,*,[1] Eun-Jung Kim,*,[1] Ana Cicvaric,† Sunetra Sase,* Marion Gröger,‡ Harald Höger,§ Fernando Jayson Sialana,* Johannes Berger,¶ Francisco J. Monje† and Gert Lubec*

*Department of Pediatrics, Medical University of Vienna, Vienna, Austria

†Department of Neurophysiology and Neuropharmacology, Center for Physiology and Pharmacology, Medical University of Vienna, Vienna, Austria

‡Core Facility Imaging, Medical University of Vienna, Vienna, Austria

§Core Unit of Biomedical Research, Division of Laboratory Animal Science and Genetics, Medical University of Vienna, Himberg, Austria

¶Department of Pathobiology of the Nervous System, Center for Brain Research, Medical University of Vienna, Vienna, Austria

Abstract

Drebrin an actin-bundling key regulator of dendritic spine genesis and morphology, has been recently proposed as a regulator of hippocampal glutamatergic activity which is critical for memory formation and maintenance. Here, we examined the effects of genetic deletion of drebrin on dendritic spine and on the level of complexes containing major brain receptors. To this end, homozygous and heterozygous drebrin knockout mice generated in our laboratory and related wild-type control animals were studied. Level of protein complexes containing dopamine receptor D1/dopamine receptor D2, 5-hydroxytryptamine receptor 1A (5-HT1$_A$R), and 5-hydroxytryptamine receptor 7 (5-HT7R) were significantly reduced in hippocampus of drebrin knockout mice whereas no significant changes were detected for GluR1, 2, and 3 and NR1 as examined by native gel-based immunoblotting. Drebrin depletion also altered dendritic spine formation, morphology, and reduced levels of dopamine receptor D1 in dendritic spines as evaluated using immunohistochemistry/confocal microscopy. Electrophysiological studies further showed significant reduction in memory-related hippocampal synaptic plasticity upon drebrin depletion. These findings provide unprecedented experimental support for a role of drebrin in the regulation of memory-related synaptic plasticity and neurotransmitter receptor signaling, offer relevant information regarding the interpretation of previous studies and help in the design of future studies on dendritic spines.

Keywords: dendritic spines, drebrin knockout, hippocampus, receptor complex, synaptic plasticity.

J. Neurochem. (2015) 10.1111/jnc.13119

Received December 15, 2014; revised manuscript received March 16, 2015; accepted March 27, 2015.

Address correspondence and reprint requests to Gert Lubec, Department of Pediatrics, Medical University of Vienna, A-1090 Vienna, Austria. E-mail: gert.lubec@meduniwien.ac.at

[1]These authors contributed equally to this work.

Abbreviations used: 5-HT1$_A$R, 5-hydroxytryptamine receptor 1A; 5-HT7R, 5-hydroxytryptamine receptor 7; ADF, actin depolarization factor; AMPA, α-amino-3-hydroxy-5-methyl-4-isoxazolepropionic acid; BN-PAGE, Blue native PAGE; D1R, dopamine receptor D1; D2R, dopamine receptor D2; fEPSPs, field excitatory post-synaptic potentials; NMDA, *N*-methyl-D-aspartate; PSD, post-synaptic density.

Dendritic spines are small membranous protrusions that consist of the majority of excitatory inputs in the central nervous system. According to spine shape and size, their morphologies are classified into three categories which are thin, stubby, and mushroom spines (Adrian *et al.* 2014). Morphological changes of the spine are highly dynamic and closely related to synaptic function and plasticity which are crucial for development and higher functions of the brain such as memory and learning (Holtmaat and Svoboda 2009). The actin filament is the major skeletal element of the dendritic spine architecture required for sustaining its form and size. It is widely known that actin is dynamic in nature which mainly determines spine morphologies (Schubert and Dotti 2007; Sekino *et al.* 2007). Therefore, many studies investigated effects in regulation of actin filaments on neuronal development (Urbanska *et al.* 2012), neuronal degenerative diseases (Goellner and Aberle 2012), synaptic plasticity (Colgan and Yasuda 2014), and psychiatric disorders (Wong *et al.* 2013). Moreover, actin-binding proteins are considered regulators of dendritic spine morphogenesis and synaptic activities (Hering and Sheng 2001).

Drebrin is an F-actin-binding protein that is highly expressed in the brain and localized at dendritic spines of mature cortical neurons (Shirao 1995; Hayashi *et al.* 1996; Sekino *et al.* 2007). It has been reported that two drebrin isoforms are found in mammals. Drebrin E is expressed in developing brains and various cells, whereas drebrin A is spatially dominant in adult brains and neuronal cells (Shirao *et al.* 1990; Hayashi *et al.* 1996). Drebrin regulates changes in the shape and density of dendritic spines via the reorganization of cytoskeletal actin filaments (Shirao *et al.* 1994; Hayashi and Shirao 1999). Inhibition of drebrin expression during neuronal development suppresses spine morphogenesis (Takahashi *et al.* 2003), reduces spine density, and causes thin immature spines to form (Takahashi *et al.* 2006). Moreover, downregulation of drebrin causes a decrease in both glutamatergic and GABAergic synaptic activities in mature cultured hippocampal neurons (Ivanov *et al.* 2009). In human disorders, decreased drebrin was observed in brains of patients with Alzheimer's disease (Harigaya *et al.* 1996; Hatanpaa *et al.* 1999) or Down syndrome (Shim and Lubec 2002).

It has been demonstrated that dendritic spine morphogenesis is modulated by several membrane receptors (Shirao and Gonzalez-Billault 2013). The density of puncta and spines are decreased by an agonist of the 5-$HT1_AR$ (Yoshida *et al.* 2011) and stimulation of the hippocampal 5-$HT1_AR$ caused a dramatic increase in PSD95 expression and dendritic spine and synapse formation (Mogha *et al.* 2012). The α-amino-3-hydroxy-5-methyl-4-isoxazolepropionic acid receptor activity regulates drebrin clustering in spine morphogenesis during development via the stabilization of drebrin in spines (Takahashi *et al.* 2009). In the hippocampus, synaptic *N*-methyl-D-aspartate (NMDA) receptors are involved in the induction of long- term potentiation, which entails a long-lasting increase in excitatory post-synaptic transmission and modification of dendritic spine morphology (Merriam *et al.* 2011) and also, NMDA receptor composition modulates dendritic spine morphology as, e.g., NR2A (NMDA receptors 2A) or antagonism induces an enhanced spine head width as does dopamine receptor D1 (D1R) activation (Vastagh *et al.* 2012). Proper expression of D2R on the cell surface is linked to the actin filament via interaction with filamen A (Lin *et al.* 2001) and dopamine facilitates dendritic spine formation by cultured striatal medium spiny neurons through both D1R and D2R (Fasano *et al.* 2013).

Here, we generated a novel drebrin knockout (KO) mouse and examined the effects of drebrin depletion on dendritic spine numbers and morphology in the hippocampus. We also examined the effects on the levels of major hippocampal receptor complexes. Genetic ablation of drebrin resulted in a significant inhibition of dendritic spine numbers, altered dendritic spine morphology and reduction in the levels of complexes containing D1R and D2R. Functional *ex vivo* analysis further revealed that drebrin depletion significantly alters memory-related synaptic strengthening as examined electrophysiologically in hippocampal slices. Taken together, these observations shed new light on the molecular mechanisms regulated by drebrin in the hippocampus, a brain structure critical for the formation and maintenance of memory.

Materials and methods

Construction of drebrin knockout mice

Genetic ablation of drebrin was carried out at the Ozgene company (Bentley DC, Australia). The design of the Dbn1 targeting vector was based on the exon structure of transcript ENSMUST00000109923. Exons 4–7 were flanked with loxP sites for Cre-mediated recombination to create a frame shift mutation (Fig. 1). An FRT-flanked PGK-neomycin selection cassette was inserted into intron 7–8. Targeting vector fragments and hybridization probes were amplified by PCR from C57BL/6 genomic DNA (gDNA). The 5′ probe (482 bp) was generated using primers P147_27 (CAACATTACAAATCCCTGTGGTGC, forward) and P147_28 (CTAGCCCACCTCTCCAAAATGAC, reverse). The 3′ probe (655 bp) was amplified with primers P147_03 (CGGAGCCCATCTGATTCCAGCA, forward) and P147_04 (ATGTCCACCC ACTGAAGAGTGACG, reverse). Probe clones and the final targeting construct were verified by DNA sequencing. The targeting vector was linearized with AclI and electroporated into Bruce4 (C57BL/6) ES cells as described (Koentgen *et al.*, 1993). Neomycin-resistant colonies (n = 672) were screened by Southern hybridization to identify homologous recombinants. Two correctly targeted clones were injected into BALB/c blastocysts. Thirteen high percentage (> 50%) chimaeras were obtained, of which two sired ES cell-derived offspring. Both germ line chimeras were derived from the same ES cell clone. Pups were genotyped by PCR of tail biopsy DNA (Fig. 2a). Heterozygous targeted mutant mice (Dbn1<flox>/+) were out crossed to B6.C-Tg (CMV-cre) 1Cgn/J

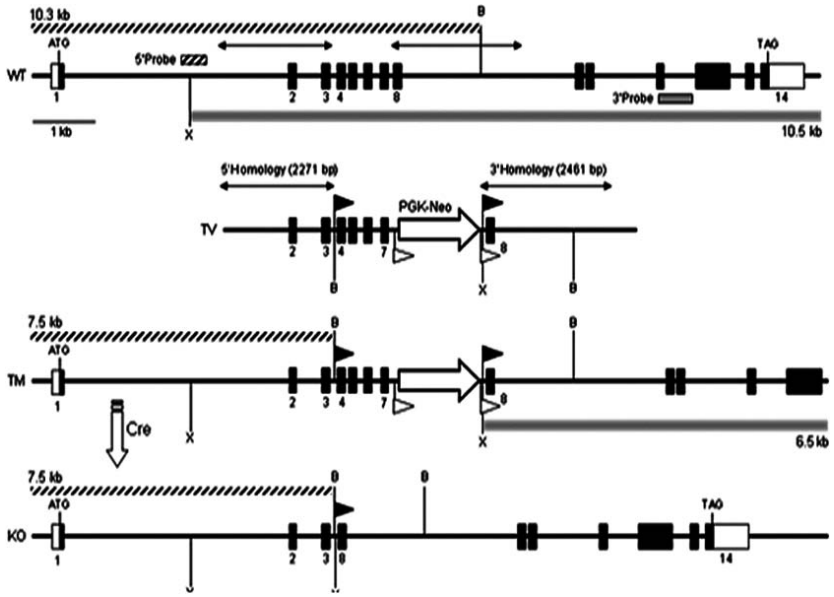

Fig. 1 Gene Targeting Design. Wild-type (WT) Dbn1 contains 14 exons. Protein coding segments are shown as black rectangles. Double arrows indicate targeting vector homology arms. Southern hybridization probes flanking the 5′ and 3′ homology arms are indicated as hatched and grey rectangles, respectively. The targeting vector (TV) contained a PGK-neomycin (PGK-Neo) selection cassette in intron 7–8. The selection marker was flanked with FRT sites (white triangles). LoxP sites (black triangles) were placed upstream of exon 4 and downstream of the selection marker. Diagnostic *Bam*HI (B) and *Xba*I (X) sites flanking the loxP sites were included. The 5′ probe recognized a 10.3 kb *Bam*HI wild-type fragment, which decreased to 7.5 kb in the targeted mutant (TM) and knockout (KO) alleles. The *Xba*I band sizes with the 3′ probe were 10.5 kb for wild type and 6.5 kb for TM. Cre-mediated recombination excised the selection marker and exons 4–7, thereby creating a frameshift mutation (KO).

deleter animals (Schwenk *et al.*, 1995) to generate carriers of the Dbn1<KO> (null) allele. In-crossing produced homozygous null (Dbn1 < KO/KO>) mice at Mendelian frequencies.

Genotyping of drebrin knockout mice

For obtaining gDNA from mice, snipped tails were incubated with 100 μL of direct PCR lysis reagent (PeqLAB, Polling, Austria) and 2 μL of proteinase K (PeqLAB) in 55°C water bath for 16 h. The resulting mixtures were inactivated in 85°C for 45 min. After centrifugation for 10 s, gDNA was isolated in supernatant. PCR amplification was performed by using following primers: for WT, 5′-CAAGCTGCCCTGCCAAAATA-3′ (forward Primer, Exon 3) and 3′-ACCAGCATCGATGTCTTCCA-5′ (reverse Primer, Exon 5); for KO, 5′-AGCTTCCAGACTCTGCTGTTT C-3′ (reverse Primer, Exon 8) and reverse primer was same as WT. The condition of PCR is shown in Appendix S1.

Determination of major brain receptor complexes

Animals

Six male mice per group [WT, heterozygous (HET) and KO mice], 11 weeks old, weighing 21± g, were bred and kept under a day/night rhythm of 14 : 10, with free access to water and food *ad libitum* at an ambient temperature of 22 ± 1°C and 50 ± 10% humidity and illumination of about 200 lux in 2 m from 5 a.m. to 7 p.m. Animals were genotyped by PCR. All animal experiments were performed under license of the federal ministry of education, science and culture, which includes an ethical evaluation of the project (Project: GZ 66.009/0017-II 10b 2009). All efforts were made to minimize animal suffering and to reduce the number of animals used.

Sample preparation

Six hippocampi per group (11 weeks old, total $n = 18$) were carefully washed with ice-cold homogenization buffer containing 10 mM HEPES, pH 7.5, containing 300 mM sucrose, 1 mM EDTA and protease inhibitor cocktail (Roche Diagnostics, Mannheim, Germany). Mouse hippocampi were homogenized in 6 mL of homogenization buffer using an Ultra-Turrax® (IKA, Staufen, Germany). The homogenate was centrifuged for 10 min at 1000 *g* and the pellet was discarded. The resulting supernatant was centrifuged for 1 h at 50 000 *g*. The pellet was suspended in 1 mL of washing buffer (homogenization buffer without sucrose) followed by incubation in ice for 30 min. The homogenate was centrifuged for 30 min at 50 000 *g*. The total membrane pellets were suspended in membrane protein extraction buffer containing 1.5 M 6-aminocaproic acid, 300 mM Bis–Tris, pH 7.0. After resuspension, 10% Triton-X 100 (Promega, Madison, CA, USA) stock solution was added to achieve 1% DDM (n-Dodecyl β-D-maltoside) concentration. Membrane protein extraction was performed for 1 h at 4°C with vortexing every 10 min followed by centrifugation for 30 min at 20 800 *g*, 4°C. An aliquot of 8 μL of Blue native PAGE (BN-PAGE) loading buffer (5% (w/v) Coomassie G250 in 750 mM 6-aminocaproic acid) was mixed with 50 μL of resulting supernatant and loaded onto the gel.

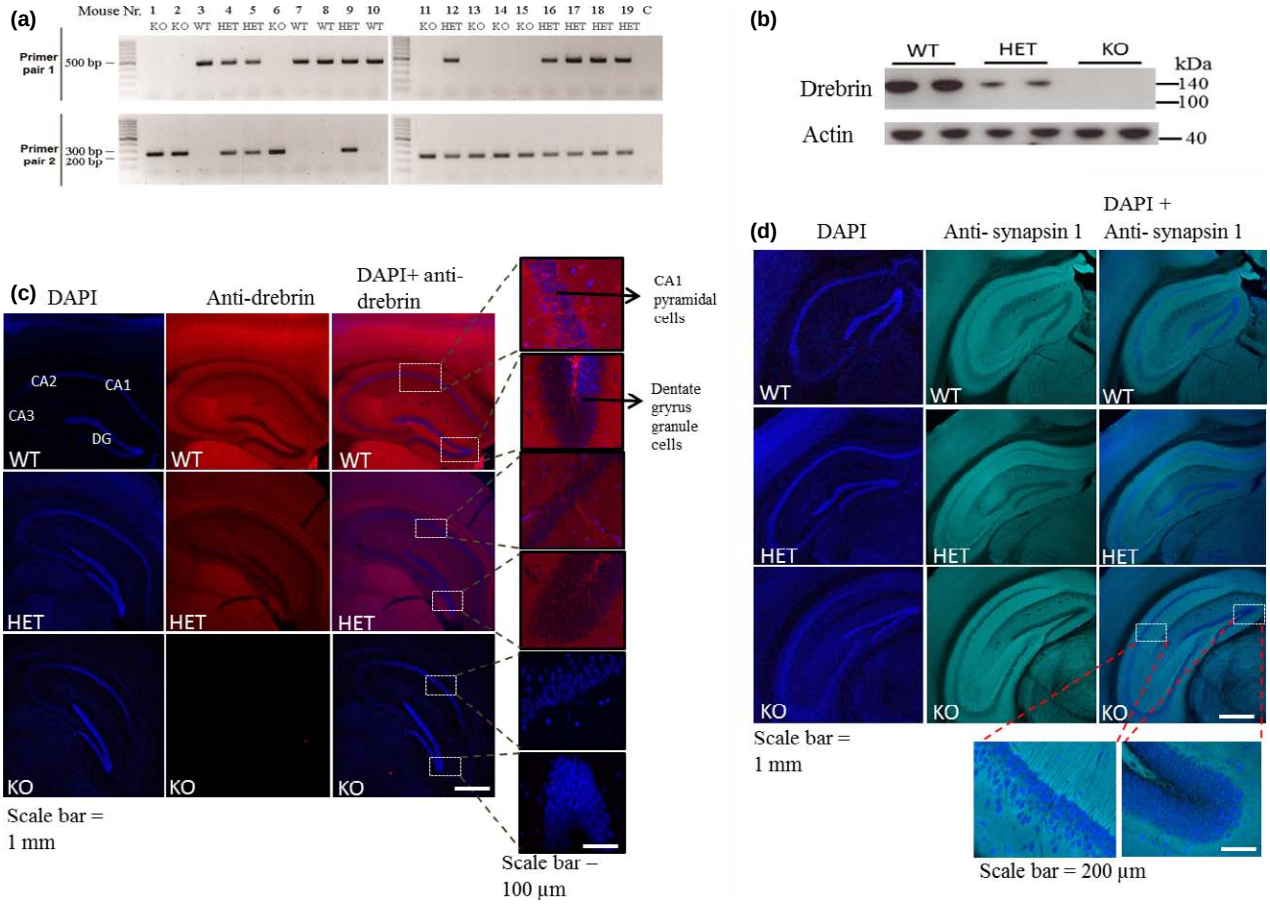

Fig. 2 (a) Mice genotyping. By using two different forward primers, for wild type (WT) in exon 5, for knockout (KO) in exon 3 and reverse primer in exon 8 (Primer pair 1 and Primer pair 2, respectively), PCR resultants were containing wild allele that showed 488 bp in upper two images and with knockout allele that was shown in 200 bp in lower two images. Heterozygous mice presented bands both PCR condition. M; 100 bp DNA ladder marker, C; negative control. (b) Representative western blot images showing expression of drebrin. A strong signal was observed in WT, lower signal in heterozygous (HET) and the absence of a band indicated genetic ablation of drebrin. (c) Immunohistochemistry data representing drebrin expression in WT, HET and KO. Hippocampal slices (representing CA1, CA2, CA3, and dentate gyrus) were examined after immunostaining and photographs were taken at 5× and 20× magnification. (d) Synapsin 1 staining represented as positive control.

Blue native PAGE

BN-PAGE was performed in a PROTEAN II xi Cell (Bio-Rad, München, Germany) using a 4% stacking and a 5–18% separating acrylamide gel. The BN-PAGE gel buffer contained 500 mM 6-aminocaproic acid, 50 mM Bis–Tris, pH 7.0; the cathode buffer 50 mM Tricine, 15 mM Bis–Tris, 0.05% (w/v) Coomassie G250, pH 7.0; and the anode buffer 50 mM Bis–Tris, pH 7.0. For electrophoresis, the voltage was set to 50 V for 1 h, 75 V for 2 h, and was increased sequentially to 200 V (maximum current 15 mA/gel, maximum voltage 300 V) until the dye front reached the bottom of the gel.

Western blotting from BN-PAGE or SDS–PAGE gels

Total membrane fraction samples were loaded onto 5–18% BN-PAGE or 10% sodium dodecyl sulfate–polyacrylamide gel electrophoresis (SDS–PAGE), followed by electrophoresis with PROTEAN II xi/xL system or mini-PROTEAN (Bio-Rad). Proteins separated on the gels were transferred onto polyvinylidene fluoride membranes. After proteins were transferred from BN-PAGE to polyvinylidene fluoride membranes, excess Coomassie Brilliant Blue G-250 dye was removed by rinsing the membranes in 100% methanol for 30 s. After blocking with 5% non-fat dry milk in 0.1% TBST, membranes were incubated overnight at 4°C with primary antibodies with gentle agitation (Appendix S2). Membranes were subsequently washed with TBST and probed with horseradish peroxidase-conjugated anti-mouse IgG (1 : 20 000; Abcam, Cambridge, UK) or anti-rabbit IgG (1 : 40 000; Abcam). Membranes were developed with the enhanced chemiluminescence Plus Western Blotting Detection System (GE Healthcare, Buckinghamshire, UK). After flatbed scanning the films, the arbitrary optical density of the immunoreactive bands was measured using ImageJ software (NIH Image, the Research Services Branch, National Institute of Mental Health, Bethesda, Maryland, USA).

Loading control

For the loading control of BN-PAGE, after immunodetection, membranes were washed twice with 0.1% TBST, stained for 1 min

with 0.1% Coomassie R-350 (GE Healthcare) prepared in methanol: water, 1 : 1, destained for 5 min with aqueous solution containing 7% methanol and 50% acetic acid, washed with water, air dried (Appendix S3) (Welinder and Ekblad 2011).

Antibody shift assay

About 0.1 μg of anti-D1R (ab1749833; Abcam) was added to 50 μg of membrane protein in the membrane extraction buffer (1.5 M 6-aminocaproic acid, 300 mM Bis–Tris, pH 7.0). The antibody–protein mixture was incubated at 4°C for 2 h in a rotator. After incubation, 10% Triton X-100 (Promega) was diluted in the mixture to achieve a final 1% concentration and mixture was incubated at 4°C for 1 h in a rotator. The resulting mixture was subjected to BN/SDS–PAGE and immunoblotting.

Two-dimensional gel electrophoresis: BN/SDS–PAGE

Gel pieces from BN-PAGE equilibrated for 30 min in an equilibration buffer (1% (w/v) SDS and 1% (v/v) 2-mercaptoethanol) with gentle agitation and then briefly rinsed with Milli-Q water. Gel pieces were then rinsed twice with SDS–PAGE electrophoresis buffer (25 mM Tris–HCl, 192 mM glycine and 0.1% (w/v) SDS; pH 8.3) and subsequently placed onto the SDS–PAGE gels. SDS–PAGE was performed in a PROTEAN II xi Cell using a 4% stacking and a 5–15% separating gel. Electrophoresis was carried out at 10°C with an initial current of 50 V (during the first hour). Then, voltage was increased to 100 V for the next 12 h (overnight) and increased to 150 V until the dye front reached the bottom of the gel.

Co-Immunoprecipitation

Co-Immunoprecipitation (co-IP) was performed using the Pierce Direct IP Kit (26148; Thermo Fisher Scientific, Wyman Street Waltham, MA, USA), coupling the 20 μL of resin with 5μl of anti-D1R (ab174938; Abcam) was incubated for 2 h at 25°C and washed the resin three times on rotator. About 1 mg of membrane fraction from mouse hippocampus, followed by the given protocol in sample preparation, was incubated in resin coupled antibody at 4°C, overnight on rotator. Elution was carried out by adding 0.2 M glycine buffer pH 2.5 after washing the resin 3–4 times to remove unbound protein. 1 M Tris base pH 10.4 was added for neutralization. The eluate was analyzed by SDS–PAGE and western blotting against anti-D1R and anti-D2R. All buffers were provided from Pierce Direct IP Kit.

Immunohistochemical analysis

Preparation of hippocampal slices

Hippocampal slices were prepared from perfusion-fixed brains of WT, HET, and KO mice. Five mice per group were taken. In brief, mice were anesthetized and perfused transcardially first with 0.9% saline and then with 1.5% paraformaldehyde in 0.1 M sodium phosphate buffer, pH 7.4. After perfusion, the brains were taken and horizontal slices were cut into 100 μm thick sections using a Vibratome 1000 Plus tissue sectioning system (Vibratome Company, St. Louis, MO, USA).

Immunohistochemistry

Immunohistochemistry was performed on 2–3 sections of hippocampal regions from each animal. Tissue was processed free-floating as follows: Briefly, slices were pre-incubated in 0.2% Tween in 0.02 M Tris-buffered saline for 1 h at 40°C and non-specific binding was blocked with 10% normal donkey serum in 0.1% Tween, 0.02 M Tris-buffered saline for 1 h at 25°C. Slices were incubated overnight in 0.5% bovine serum albumin (BSA), 0.1% Tween, 0.02 M Tris-buffered saline containing the primary antibody (rabbit anti-drebrin antibody; 1 : 100; Abcam) at 4°C. Slices were then rinsed in blocking solution and were incubated with secondary antibodies (anti-rabbit IgG Alexa Fluor 488, 1 : 1000; Cell Signaling Technology, Boston, MA, USA) for 1 h at 25°C. Counterstaining of cell nuclei was achieved with DAPI (1 μg/mL, 4′,6-diamidino-2-phenylindole; Invitrogen, Carlsbad, CA, USA). After rinsing in 0.1 M phosphate-buffered saline, slices were dried and cover-slipped with fluorescence mounting medium (DAKO, Glostrup, Denmark).

Diolistic labeling and immunostaining of the dopamine receptor on dendritic spines

To visualize the dendritic spines, the powdered Dil dye (Invitrogen) was placed over a bundle of axons in hippocampal slices with the aid of a thin histological needle manually. Slices were kept in a humid chamber at 40°C for 48 h. After rinsing with water, slices were dried and cover slipped with fluorescence mounting medium (DAKO).

For the diolistic labeling with immunofluorescence staining of dopamine receptors, the powdered Dil dye was placed on hippocampal slices after following steps (Chen *et al.* 2010; Golden *et al.* 2013): Hippocampal slices from the vibratome were placed in 0.2% Tween, 0.02 M Tris-buffered saline for 6 h at 40°C. Non-specific binding was blocked with 10% normal donkey serum in 0.1% Tween, 0.02 M Tris-buffered saline for 1 h at 25°C. Slices were incubated overnight in 0.5% BSA, 0.1% Tween, 0.02 M Tris-buffered saline containing the primary antibody (rabbit anti-Dopamine 1 receptor antibody, 1 : 100; Alomone Labs, Jerusalem, Israel) at 40°C. Slices were then rinsed with 0.5% BSA, 0.1% Tween in Tris-buffered saline solution and incubated with secondary antibodies (anti-rabbit IgG Alexa Fluor 488, 1 : 1000; Cell Signaling Technology) for 2 h at 40°C. Slices were subsequently rinsed with Tris-buffered saline. Counterstaining of cell nuclei was achieved with DAPI (3 μg/mL, 4′,6-diamidino-2-phenylindole, Invitrogen).

Confocal laser scanning microscopy

Slices were examined by Zeiss LSM 700 confocal laser scanning microscope (LSM 700; Carl Zeiss GmbH, Jena, Germany) using 20–63× oil immersion objectives (1.4 NA) with the pinhole set at 1 Airy unit. Images were acquired using LSM 700 software (Carl Zeiss GmbH) at 1024 × 1024 pixel resolution.

Spines were imaged at 63× magnifications with 2.5 zoom, collecting z-optical sections at 0.1–0.3 μm intervals. Three-dimensional reconstruction of dendritic spines was performed from confocal maximum projections using a Zen software package (Zeiss, Oberkochen, Germany). Contrast and sharpness of the images were adjusted by using the levels and sharpness commands in Adobe Photoshop CS 5 (Adobe Systems, San Jose, CA, USA). Specificity of immunostaining was confirmed by control experiments with omission of primary antibody.

Spine analysis

Dendritic spine analysis was performed using the National Institutes of Health ImageJ software and NeuronStudio semimanually (Chen

et al. 2013; Golden *et al.* 2013). To qualify for spine analysis, dendritic segments were chosen by the following requirements: the segment had to be completely filled and could not be overlapping with other dendritic branches.

Dendritic spines were counted per branch and per unit distance blinded to treatment. Spine density was expressed as the number of spines per 1 μm of dendrite length. Spine shapes were classified as thin, mushroom, stubby and others by NeuronStudio on the basis of the aspect ratio, head-to-neck ratio and head diameter. Spines with a neck can be classified as either thin or mushroom and those without a neck are classified as stubby. Spines with a neck are labeled as thin or mushroom on the basis of head diameter. Spines on apical dendritic branches in CA1 stratum lacunosum-moleculare (slm) of hippocampus were measured: 1475 spines from 32 pyramidal neurons were examined using 5 wild-type, 1120 spines from 34 pyramidal neurons were examined using 5 HET and 1027 spines, from 34 pyramidal neurons were examined using 5 KO mice. For quantitative analysis of receptor expression on dendritic segments, *z*-stack images of dendritic branches were acquired and co-localized. Dopamine 1 receptor puncta were shown on a LSM-700 confocal microscope using same parameters of spine analysis. Co-localized Dopamine1 receptor puncta were manually identified on merged RGB images (ImageJ Software) and verified with 3-dimensional reconstruction using Zen software. Data are presented as means ± SEM acquired from multiple images from five mice per group. Statistical significance between two means was calculated using Student's unpaired *t*-test (Prism; GraphPad, San Diego, CA, USA).

Statistics analysis

ANOVA was used to reveal complex level of receptors between two groups (wild and drebrin-KO) differences, followed by unpaired Student's *t*-test and data are given as means ± SEM. A probability level of $p < 0.001$ was set as statistically significant. Pearson correlation coefficients were calculated using Graph Pad prism (http://www.graphpad.com/scientific-software/prism/).

Electrophysiology studies

Acute hippocampal slices preparation

Slices were prepared as others have previously described (Simon *et al.* 2001; Rammes *et al.* 2009; Kim *et al.* 2012; Monje *et al.* 2012) with minor modifications. Briefly, the mice (C57BL/6, 11 weeks) were narcotized with CO_2 and swiftly sacrificed by instantaneous cervical dislocation and quick sharp-blade decapitation. Brains were removed and immersed in artificial cerebrospinal fluid (aCSF) solution at 4°C containing 125 mM NaCl, 2.5 mM KCl, 25 mM $NaHCO_3$, 2 mM $CaCl_2$, 1 mM $MgCl_2$, 25 mM D-glucose, and 1.25 mM NaH_2PO_4 (all compounds were purchased from Sigma-Aldrich, Vienna, Austria). Hippocampi were isolated and transverse slices (400 μm) were prepared using a McIlwain Tissue Chopper (Mickle Laboratory Engineering, Guildford, UK). Slices were transferred to a home-customized nylon-mesh submerged in aCSF and maintained at 32 ± 1°C for at least 1 h before the beginning of the electrophysiological recordings, which were performed in aCSF at 32°C. aCSF solutions were continuously bubbled with a saturating carbogen mixture (95% O_2/5% CO_2) that adjusted the pH of the solutions to a value of 7.4.

Electrophysiology and data analysis

Hippocampal field excitatory post-synaptic potentials (fEPSPs) were evoked after stimulation of the Schaffer collateral pathway. Stimulation was delivered through a home-made bipolar tungsten electrode insulated to the tip (50 μm tip diameter) using an ISO-STIM 01D isolator stimulator (NPI Electronics, Tamm, Germany). fEPSPs were recorded at the CA1 area using conventional glass micropipettes (2–5 MΩ when filled with aCSF). Strength of synaptic transmission was resolved from the decaying slope of the fEPSPs. Measurements of basal synaptic transmission were obtained for at least 20 min preceding the induction of synaptic potentiation. Baseline synaptic transmission was determined by delivering single stimulating pulses (80 ms each) at 0.03 Hz. The intensity of these stimulating pulses was set to elicit ~ 40% of the maximal peak amplitude of the fields. To obtain this value, input–output ratios were evaluated by delivering pulses of voltage with increases of 1 volt. Synaptic potentiation was induced by delivering five trains of 100 pulses (80 ms each) at 100 Hz with an inter-train interval of 5 s applied to the Schaffer collateral pathway. Changes in fEPSPs slopes, determined by normalization to baseline values, were examined for at least 1 h. Recordings were made using an AxoClamp-2B amplifier (in the Bridge mode configuration) and a Digidata-1440 interface (Axon Instruments, Sunnyvale, CA, USA). Data were analyzed using the pClamp-10 Program software (CA/Molecular Devices, Sunnyvale, CA, USA).

Results

In order to examine the impact of the genetic depletion of drebrin in the mouse brain, we generated drebrin-KO mice (Fig. 1) and studied the morphological and functional properties of brain neurons as well as the levels of protein complexes containing neurotransmitter receptors in the adult mice. As depicted in Fig. 2(a), PCR experiments were conducted using two different forward primers [one targeting exon 5 for wild type (WT) and another targeting exon 3 for KO] each in addition its corresponding reverse primer in exon 8. Results from this PCR assay reflected the predicted absence of drebrin in the samples obtained from drebrin-KO mice. In agreement with these observations, western blot analysis using a drebrin antibody allowed the detection of a band with the molecular weight expected for the drebrin in WT animals, lower expression level in HET than WT, whereas no band was detected in drebrin-KO mice (Fig. 2b). Further immunohistochemical analysis using the drebrin antibody validated the absence of drebrin in the brain of drebrin-KO mice and low expression level in HET mice in contrast to WT mice which allowed the detection of a strong signal compatible with the hippocampal localization of drebrin (Fig. 2c). The synapsin 1 antibody was used as a positive staining control in WT, HET, and KO as shown in Fig. 2(d). Additionally, to confirm whether the truncated form, which is encoded on exon 1–3, expressed in drebrin-KO, we used a specific drebrin antibody against amino acids 22–42 in the exon region. As immunohistochemical data have shown, the truncated drebrin was not expressed in KO

mice as well as the full length of drebrin (Appendix S6b). These observations thus validated the use of our genetically modified mice as a proper tool for the study of the morphological and physiological effects of drebrin depletion.

We next examined the levels of protein complexes containing neurotransmitter receptors in drebrin-KO mice and compared to related WT animals. In drebrin-KO mice, western blot and subsequent densitometry analysis revealed a significant decrease in the levels of protein complexes containing D1R, D2R, 5-HT1AR and 5HT7R. The effects on these neurotransmitter receptor seem to be specific, as no detectable changes in the levels of protein complexes containing NR1(GluN1) and AMPA GluR1, 2 and 3 receptors (GluA1–3) were observed between drebrin-KO and related WT animals (Fig. 3).

We then performed co-IP and antibody shift assays in order to examine whether D1R and D2R were co-localized in the same protein complex. Effectively, as shown in Fig. 4(a) (first lane), D1R-antibody immunoreactivity in the input was observed in several bands including at the expected band at 50 kDa. Lane 2 of Fig. 4(a) depicts how the specific D1R-antibody resulted in the detection of a band with same, as predicted, molecular weight for D1R when protein extracts from the eluate were immunoblotted. Accordingly, lane 3 of Fig. 4(a) shows a band with the expected molecular weight for D2R after incubation also using the elute protein samples. As shown in Fig. 4(b) (upper panel, upper lane), the antibody directed against D1R gave rise to the detection of two bands for the predicted D1R complex, while pre-incubation of the membrane fraction with an antibody against D1R (upper panel, lower lane) led to a shift of mobility to a higher molecular weight. These data provide experimental indications for the establishment of physical interactions and the formation of receptor complexes likely to be responsible for the partial offsets from the theoretical molecular weights observed after incubation with specific antibodies and suggest the presence of the D1R subunit in the complex in the BN-PAGE. Likewise, incubation of the membrane fraction with an antibody against D1R led to a shift of the D1R and D2R-containing complex when developed with an antibody against the D2R (Fig. 4(b), lower panel, upper lane D2R containing complex without pre-incubation with antibody against D1R). Correspondingly, Fig. 4(b), lower panel (lower lane), shows the antibody shift of the D1R and D2R-containing complex following incubation with a D1R antibody. Taken together, all these findings demonstrate that the protein complexes examined contained both D1R as well as D2R. As shown in Fig. 5(a) and (b), the number of D1R on dendritic spines was significantly decreased in drebrin-KO as compared to the WT mice, whereas the number of D1R on the shaft was not affected.

We then examined the effects of drebrin depletion on the genesis and morphological properties of dendritic spines in hippocampal neurons. To determine whether drebrin expression was affecting dendritic spine numbers, we also performed dendritic spine analysis after diolisitc labeling with DIL dye. Spine densities on apical dendrites of CA1 pyramidal cells were examined as shown in Appendix S4, S5. As shown in Fig. 6, dendritic spine density was significantly lower in neurons from the drebrin-KO and HET when compared to levels evaluated in neurons from their related WT mice. Moreover, spine densities on

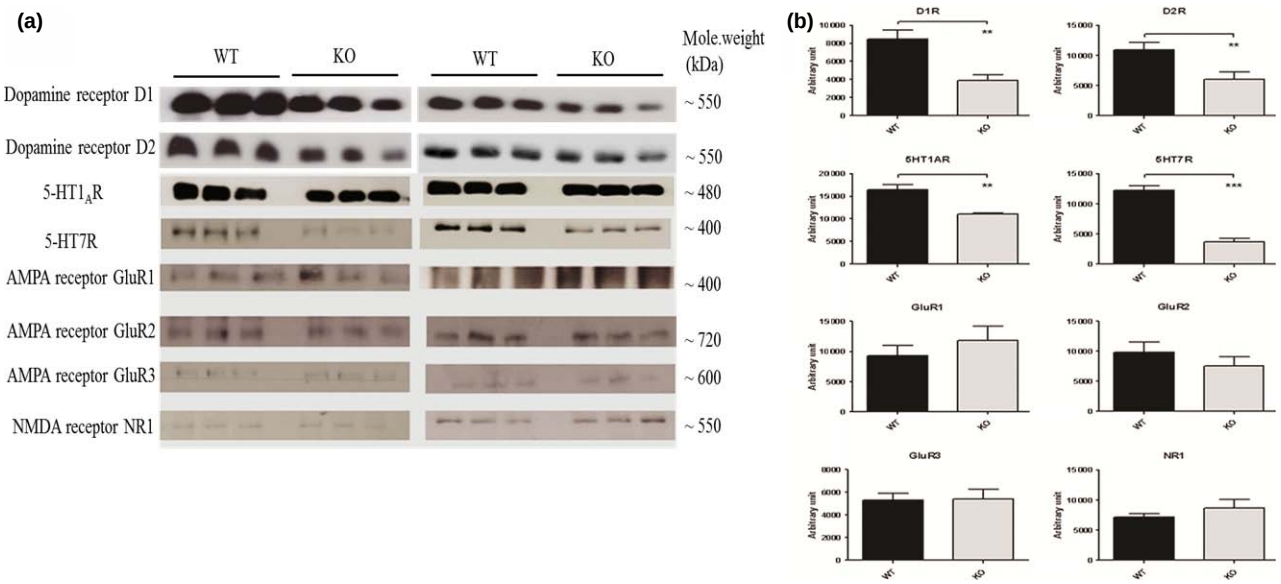

Fig. 3 (a) Levels of major receptor complexes in blue native PAGE (BN-PAGE) were represented by single bands. 45 μg of membrane fraction proteins were loaded in each lane. The loading control is shown in supplementary material 3. (b) Densitometric analysis of the different receptor complex levels in wild-type (WT) and drebrin-knockout mice (KO). $^{**}p < 0.01$, $^{***}p < 0.001$.

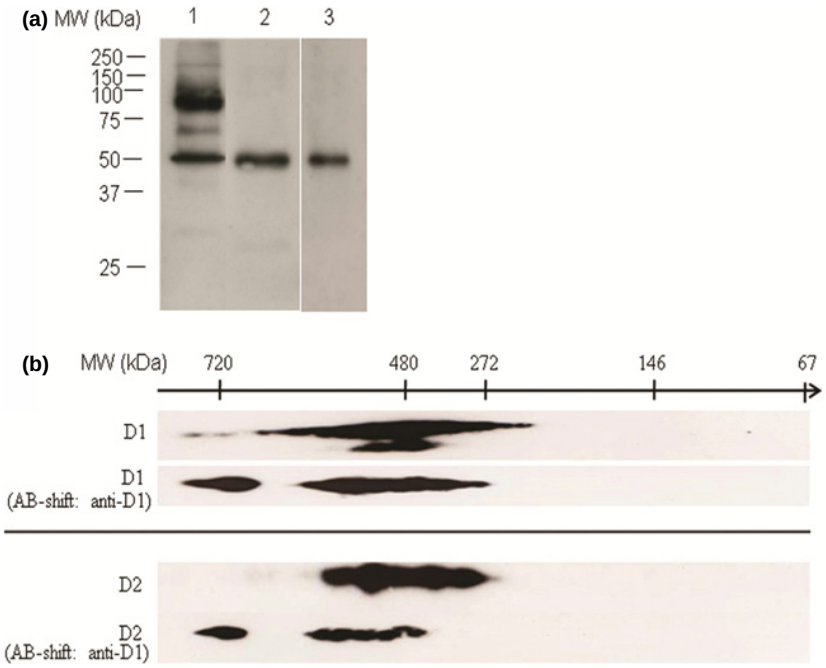

Fig. 4 Dopamine D1R and D2R were co-localized in the complex. (a) Co-immunoprecipitation (co-IP) showing that the D2R was co-eluting with the D1R from an immobilized antibody against the D1R. Western blotting from a sodium dodecyl sulfate–polyacrylamide gel electrophoresis (SDS–PAGE): Lane 1: Hippocampal protein extract (Input) showing several bands for the D1R. Lanes 2 and 3 represent the eluted fractions. Eluted fractions contained the D1R (lane 2) and the D2R (lane 3). (b) Antibody shift assays. Two-dimensional gel (BN/SDS–PAGE) separation of D1R and D2R (upper panel); western blotting using an antibody against the D1R indicates shifts of mobility of the D1R and D2R containing complex when the membrane fraction was pre-incubated with an antibody against the D1R. Pre-incubation of the membrane fraction with an antibody against D1R with subsequent development with an antibody against the D2R resulted in a shift of the D1R and D2R-containing complex (lower panel).

drebrin-KO mice neurons were significantly decreased in comparison the HET mice.

We additionally evaluated the morphological properties of dendritic spines in neurons from drebrin-KO, HET and WT mice. As illustrated in Fig. 7, we observed that neurons from the drebrin-KO presented with a pronounced, statistically significant, reduction in the number of mushroom, thin and stubby types of dendritic spines, whereas no differences in the levels of other un classified morphological types were detected when compared to neurons from wild-type animals. In case of HET mice, mushroom and stubby spines were decreased on pyramidal neurons when compared with the neurons of the WT mice significantly.

These data indicate that drebrin is involved not only in the regulation of the total number of hippocampal dendritic spines but also on the modulation of the morphological properties in dendritic spine maturation.

Finally, we evaluated the effects of genetic depletion of drebrin on memory-related hippocampal synaptic plasticity by performing electrophysiological recordings in acutely dissociated hippocampal slices (Bliss and Lomo 1973; Bliss and Collingridge 1993; Kandel 2001, 2012; Bailey *et al.* 2004). We observed no statistical differences (ANOVA, $p > 0.5$) in basal synaptic transmission of hippocampal slices obtained from WT control and drebrin-KO mice ($n = 4–6$) as examined by obtaining input–output measurement curves in the hippocampal CA3 region in response to stimulation of the Schaffer collateral pathway (Fig. 8a). However, when hippocampal synaptic plasticity was examined, a moderate, yet statistically significant difference was found (ANOVA, $p = 0.02$) with drebrin-KO mice presenting with inhibited memory-related high-frequency-induced synaptic strengthening (Fig. 8b and c).

Discussion

Here, we studied the effects of drebrin genetic depletion on dendritic spines and on the levels of neurotransmitter receptors by using a newly generated and previously uncharacterized drebrin-KO mouse. Significant inhibition in the levels of D1R-containing protein complex in drebrin-KO mice were observed together with reduced levels of D2R, which paralleled the inhibition in dendritic spine numbers and alterations in cell morphology. The inhibition effects were also observed in HET. Electrophysiological studies using hippocampal slices obtained from our generated

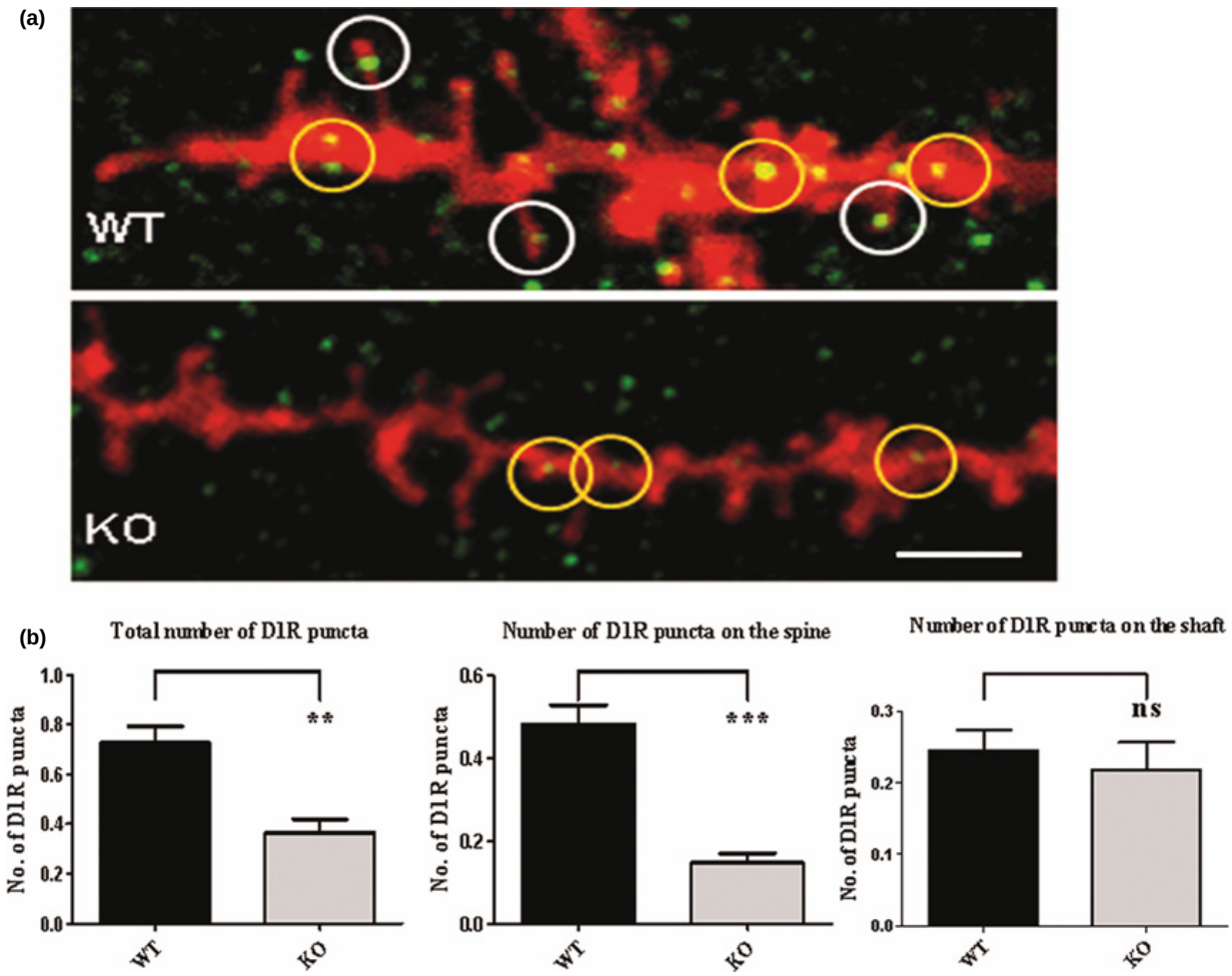

Fig. 5 Representative ×63 confocal *z*-stack images of dendritic segments of hippocampal neurons from wild-type (WT) and drebrin knockout (KO) mice. D1R expressed in dendrites. (a) Diolistic labeling (Redondo *et al.* 2010) with immunostaining of D1R (green) revealed the expression pattern of the D1R on hippocampal dendritic segments. White circles in the merge images highlight co-localization of dendritic spines and D1R puncta, and yellow circles indicate co-localized D1R on the dendritic shaft. Scale bar, 2 μm. (b) Quantification of puncta immunoreactive for D1R. In contrast to the number of puncta on the shaft, the total number of puncta (dendritic shaft and dendritic spines) and number of puncta on spines was significantly reduced in drebrin-KO mice as compared to WT. $^{**}p < 0.01$, $^{***}p < 0.001$.

drebrin-KO mice further revealed that drebrin depletion results in inhibited memory-related high-frequency-induced synaptic strengthening.

Previous reports have shown that drebrin expression is related to localization of membrane receptors on dendritic spines, which contain the machinery for receiving the majority of glutamatergic inputs (Merriam *et al.* 2013). Several receptors have been shown to regulate spine physiology. For example, Kobayashi and coworkers have demonstrated that NMDA receptor subunit NR2A is prominent in drebrin-immunopositive spines (Kobayashi *et al.* 2007). Similarly, Aoki and coworkers revealed that a NMDA antagonist, D-APV, increased the proportion of NR2A-immunolabeled spines within 30 min (Aoki *et al.* 2009). On the other hand, Nawabuisi-Heath and coworkers have also shown co-localization of AMPAR GluR1 and GluR2 with drebrin clusters and proposed a role for spine changes underlying neuronal maturation (Nwabuisi-Heath *et al.* 2012). And Takahashi *et al.* (2009) proposed that AMPAR-mediated stabilization of drebrin spines is an activity-dependent cellular mechanism for spine morphogenesis. It has also been shown that down-regulated drebrin leads to decreased glutamatergic and GABAergic synaptic activity and dendritic spine morphology, thus suggesting a role in regulation of the corresponding receptor system (Ivanov *et al.* 2009). However, besides all these preceding molecular and functional studies, only this work has comprehensively characterized the effect of drebrin deletion on the levels of major receptor complexes. Decreased levels of D1R and D2R- containing complexes in drebrin-KO mice

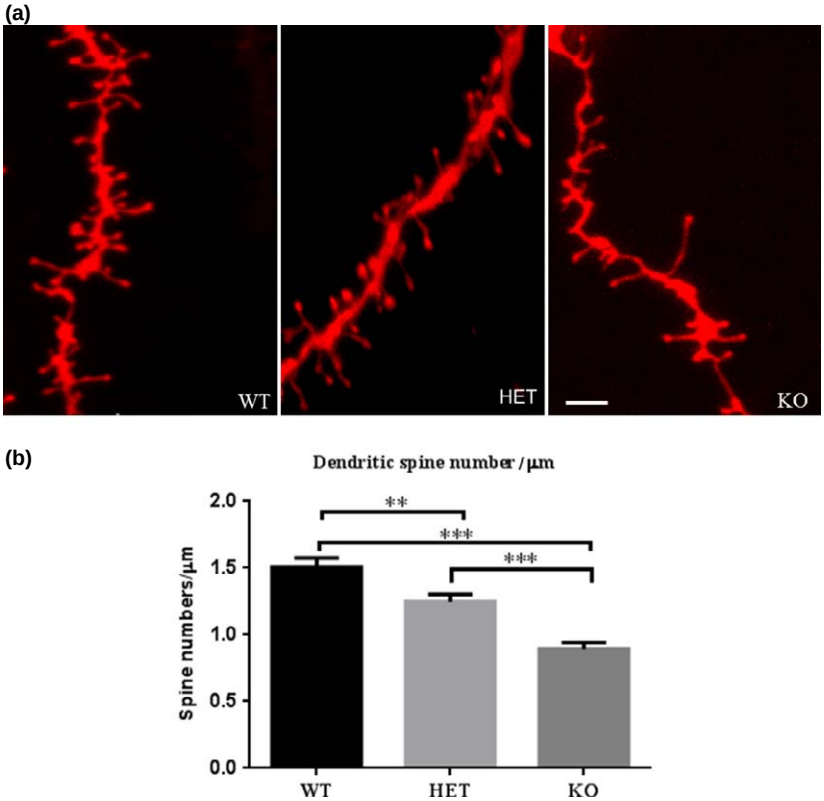

Fig. 6 Representative dendritic segments of CA1 apical pyramidal cells (scale bar = 2 μm) and quantification analysis of dendritic spine numbers in wild-type (WT), heterozygous (HET) and knockout (KO). DIL dye showed that the total number of dendritic spines was reduced in drebrin-KO and HET mice as compared to the WT mice. (a) Representative dendritic segments 34 of CA1 apical pyramidal cells (scale bar = 2 lm) and (b) quantification analysis of dendritic spine numbers in wild-type (WT), heterozygous (HET) and knockout (KO). $^{**}p < 0.01$, $^{***}p < 0.001$.

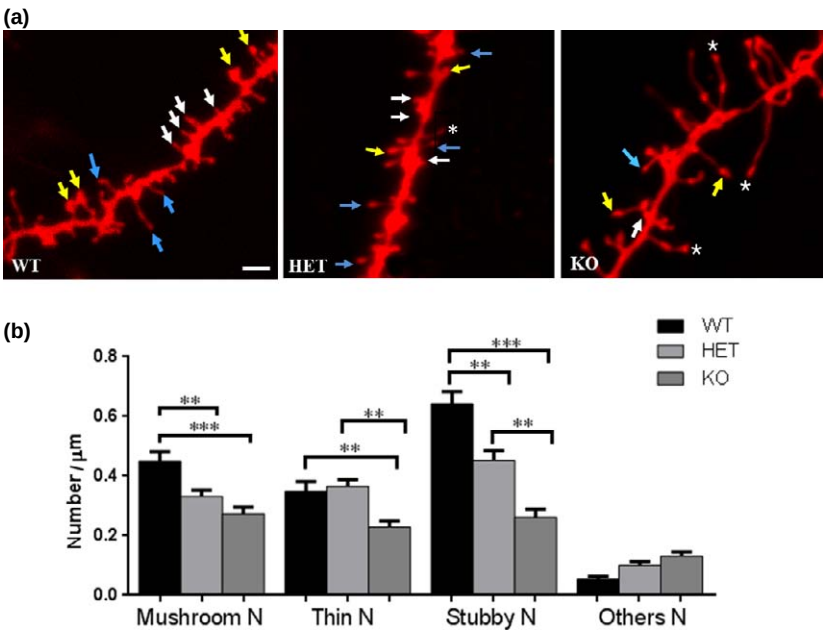

Fig. 7 Spine morphology analysis. (a) Representative dendritic segments on CA1 hippocampal neurons: White arrows indicate stubby spines, yellow arrows indicate mushroom spines, blue arrows indicate thin spines and asterisks indicate abnormal spines. (Scale bar = 2 μm). (b) The quantification of the type of dendritic spines demonstrates morphological changes in WT, heterozygous (HET) and drebrin knockout (KO) mice. $^{**}p < 0.01$, $^{***}p < 0.001$.

represent a key finding of the current study, further proving the fact that dopamine receptors are major molecular regulators of memory formation and maintenance (Rinaldi *et al.* 2007; Vijayraghavan *et al.* 2007; Takahashi *et al.* 2012). Our data might thus contribute to the identification of the key molecular players that underlie the pronounced deficits in memory function during contextual fear conditioning studies as described for other mouse models of drebrin depletion (Kojima *et al.* 2010).

It has been previously described that D1R can form not only homo-oligomers (O'Dowd *et al.* 2011) but also D1R–D2R hetero-oligomers (O'Dowd *et al.* 2012) that are co

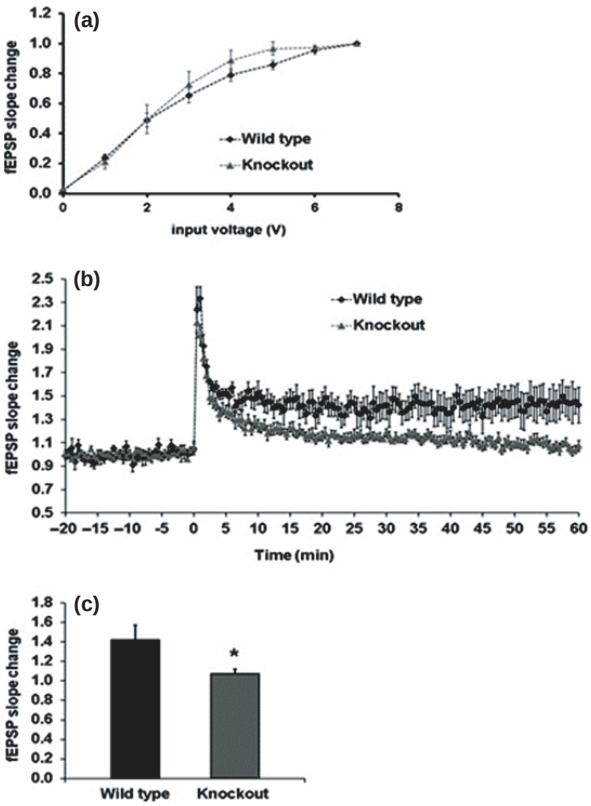

Fig. 8 (a) Drebrin depletion (knockout, KO) did not alter basal hippocampal synaptic transmission in hippocampal slices, compared with control wild-type (WT) mice, as examined by measuring input/output field-slope responses. (b) Temporal courses of averaged field excitatory post-synaptic potentials (fEPSPs) slopes obtained before and after application of electrical stimulation inducing synaptic strengthening in hippocampal slices of WT and KO mice. (c) The statistically significant reduction in synaptic potentiation due to DREBRIN depletion is more apparent when the late phases of synaptic strengthening are examined (as measured 1 h after delivering stimulation known to induce synaptic potentiation). *$p < 0.05$.

activated on the cell surface (So *et al.* 2005). Moreover, these hetero-oligomers have even been linked to regulation by calcium signaling in the brain (George and O'Dowd 2007). Herein, we show that D1R and D2R receptors are in fact co-localized in the same protein complexes, giving rise to hetero-oligomers with approximate molecular weights of 550 kDa as determined using BN-PAGE, co-IP, and antibody shift assays. Immunostaining of D1R on hippocampal section demonstrated that immunoreactivity for the D1R on dendritic spines was significantly decreased in drebrin-KO mouse hippocampal neurons but comparable to WT in the shaft region.

It has also been reported that D1R and D2R are involved in dendritic spine morphogenesis. D1R and D2R receptor KO mice presented dystrophic changes in prefrontal cortical pyramidal cell dendrites (Wang *et al.* 2009). It is known that, through D1R and D2R, dopamine facilitates dendritic spine formation as studied in cultured medium striatal spiny neurons (Fasano *et al.* 2013).

In addition to decreased dopamine receptors, reduced levels in 5-HT1$_A$R and 5-HT7R receptor containing complexes were observed in drebrin-deficient mice. It has been previously shown that 5-HT1$_A$R- and 5-HT7R-deficient mice present with cognitive deficits (Sarnyai *et al.* 2000; Bert *et al.* 2008; Roberts and Hedlund 2012) and the corresponding receptor complex levels have been associated with memory in rodents (Heo *et al.* 2011). Therefore, at least one or more of the abovementioned receptor complex reductions may underlie the memory deficits described in mice with deletion of drebrin and probably in human disorders with DBN deficiency (Shim and Lubec 2002; Counts *et al.* 2012).

It has been demonstrated that drebrin is linked to dendritic spine morphogenesis and maturation of cultured hippocampal neurons (Ivanov *et al.* 2009), and in an immunocytochemical study it was shown that spine head size depends on drebrin levels in mouse cerebral cortex (Kobayashi *et al.* 2007). So far, however, there is no information on dendritic spine morphology in the drebrin-KO mouse. The overall lamination and dendritic arborization of CA1 pyramidal neurons appeared normal in the drebrin-KO mice (Appendix S4, S5) but spine density was significantly decreased and dendritic spine morphology was considerably changed in drebrin-KO mice as compared to WT mice. Interestingly, some of the morphological features observed in our work resemble the abnormal spine morphology described in non-syndromic mentally retarded infants (Chen *et al.* 2013) and dendritic abnormalities reported in disorders associated with mental retardation (Kaufmann and Moser 2000).

Molecular cross-talk between neuronal drebrin and cofilin is believed to be part of the activity-dependent cytoskeleton-modulating pathway by competitively binding to F-actin, and recent research has shown that drebrin inhibits actin-severing by cofilin in dendritic spines (Grintsevich and Reisler 2014). In addition, cofilin is also involved in learning and memory. Interestingly, cofilin regulates dendritic spine morphology and post-synaptic parameters such as late long-term potentiation (Rust *et al.* 2010), properties that resemble our observations described above in the drebrin-KO. Thus, we checked cofilin expression levels by western blotting and immunohistochemical analysis using cofilin 1 antibody in all genotypes of hippocampus. However, the expression levels of cofilin 1 were unchanged in drebrin-KO mice as compared to WT and HET in hippocampus (Appendix S6a).

Taken together, receptor complex level changes of dopamine receptors D1R, D2R, 5-HT1$_A$R, and 5-HT7R paralleled reduction in dendritic spine numbers and morphology and a complex containing the D1R and D2R was characterized. These findings show for the first time that receptor complex levels and dendritic spine changes in genetic deletion of drebrin paralleled inhibited memory-related high-frequency-

induced synaptic strengthening and, thus, these findings are important for the interpretation of previous work and the design of future work in neurobiology and neuropathology of drebrin.

Acknowledgments and conflict of interest disclosure

We are highly indebted to the Verein "Unser Kind" for partial financial assistance and to Sabine Rauscher, Core Facility Imaging, Medical University of Vienna, 1090 Vienna, Austria, for supervising the morphological technologies. The authors have no conflicts of interest to declare.

All experiments were conducted in compliance with the ARRIVE guidelines.

Supporting information

Additional supporting information may be found in the online version of this article at the publisher's web-site:

Appendices S1–S7. Supplementary Materials and methods.

References

Adrian M., Kusters R., Wierenga C. J., Storm C., Hoogenraad C. C. and Kapitein L. C. (2014) Barriers in the brain: resolving dendritic spine morphology and compartmentalization. *Front. Neuroanat.* **8**, 142.

Aoki C., Kojima N., Sabaliauskas N., Shah L., Ahmed T. H., Oakford J., Ahmed T., Yamazaki H., Hanamura K. and Shirao T. (2009) Drebrin a knockout eliminates the rapid form of homeostatic synaptic plasticity at excitatory synapses of intact adult cerebral cortex. *J. Comp. Neurol.* **517**, 105–121.

Bailey C. H., Kandel E. R. and Si K. (2004) The persistence of long-term memory: a molecular approach to self-sustaining changes in learning-induced synaptic growth. *Neuron* **44**, 49–57.

Bert B., Fink H., Rothe J., Walstab J. and Bonisch H. (2008) Learning and memory in 5-HT(1A)-receptor mutant mice. *Behav. Brain Res.* **195**, 78–85.

Bliss T. V. and Collingridge G. L. (1993) A synaptic model of memory: long-term potentiation in the hippocampus. *Nature* **361**, 31–39.

Bliss T. V. and Lomo T. (1973) Long-lasting potentiation of synaptic transmission in the dentate area of the anaesthetized rabbit following stimulation of the perforant path. *J. Physiol.* **232**, 331–356.

Chen Y., Rex C. S., Rice C. J., Dube C. M., Gall C. M., Lynch G. and Baram T. Z. (2010) Correlated memory defects and hippocampal dendritic spine loss after acute stress involve corticotropin-releasing hormone signaling. *Proc. Natl Acad. Sci. USA* **107**, 13123–13128.

Chen Y., Kramar E. A., Chen L. Y., Babayan A. H., Andres A. L., Gall C. M., Lynch G. and Baram T. Z. (2013) Impairment of synaptic plasticity by the stress mediator CRH involves selective destruction of thin dendritic spines via RhoA signaling. *Mol. Psychiatry* **18**, 485–496.

Colgan L. A. and Yasuda R. (2014) Plasticity of dendritic spines: subcompartmentalization of signaling. *Annu. Rev. Physiol.* **76**, 365–385.

Counts S. E., He B., Nadeem M., Wuu J., Scheff S. W. and Mufson E. J. (2012) Hippocampal drebrin loss in mild cognitive impairment. *Neurodegener. Dis.* **10**, 216–219.

Fasano C., Bourque M. J., Lapointe G., Leo D., Thibault D., Haber M., Kortleven C., Desgroseillers L., Murai K. K. and Trudeau L. E. (2013) Dopamine facilitates dendritic spine formation by cultured striatal medium spiny neurons through both D1 and D2 dopamine receptors. *Neuropharmacology* **67**, 432–443.

George S. R. and O'Dowd B. F. (2007) A novel dopamine receptor signaling unit in brain: heterooligomers of D1 and D2 dopamine receptors. *ScientificWorldJournal* **7**, 58–63.

Goellner B. and Aberle H. (2012) The synaptic cytoskeleton in development and disease. *Dev. Neurobiol.* **72**, 111–125.

Golden S. A., Christoffel D. J., Heshmati M. *et al.* (2013) Epigenetic regulation of RAC1 induces synaptic remodeling in stress disorders and depression. *Nat. Med.* **19**, 337–344.

Grintsevich E. E. and Reisler E. (2014) Drebrin inhibits cofilin-induced severing of F-actin. *Cytoskeleton (Hoboken)* **71**, 472–483.

Harigaya Y., Shoji M., Shirao T. and Hirai S. (1996) Disappearance of actin-binding protein, drebrin, from hippocampal synapses in Alzheimer's disease. *J. Neurosci. Res.* **43**, 87–92.

Hatanpaa K., Isaacs K. R., Shirao T., Brady D. R. and Rapoport S. I. (1999) Loss of proteins regulating synaptic plasticity in normal aging of the human brain and in Alzheimer disease. *J. Neuropathol. Exp. Neurol.* **58**, 637–643.

Hayashi K. and Shirao T. (1999) Change in the shape of dendritic spines caused by overexpression of drebrin in cultured cortical neurons. *J. Neurosci.* **19**, 3918–3925.

Hayashi K., Ishikawa R., Ye L. H., He X. L., Takata K., Kohama K. and Shirao T. (1996) Modulatory role of drebrin on the cytoskeleton within dendritic spines in the rat cerebral cortex. *J. Neurosci.* **16**, 7161–7170.

Heo S., Patil S. S., Jung G., Hoger H. and Lubec G. (2011) A serotonin receptor 1A containing complex in hippocampus of PWD/PhJ mice is linked to training effects in the Barnes maze. *Behav. Brain Res.* **216**, 389–395.

Hering H. and Sheng M. (2001) Dendritic spines: structure, dynamics and regulation. *Nat. Rev. Neurosci.* **2**, 880–888.

Holtmaat A. and Svoboda K. (2009) Experience-dependent structural synaptic plasticity in the mammalian brain. *Nat. Rev. Neurosci.* **10**, 647–658.

Ivanov A., Esclapez M., Pellegrino C., Shirao T. and Ferhat L. (2009) Drebrin A regulates dendritic spine plasticity and synaptic function in mature cultured hippocampal neurons. *J. Cell Sci.* **122**, 524–534.

Kandel E. R. (2001) The molecular biology of memory storage: a dialogue between genes and synapses. *Science* **294**, 1030–1038.

Kandel E. R. (2012) The molecular biology of memory: cAMP, PKA, CRE, CREB-1, CREB-2, and CPEB. *Mol. Brain* **5**, 14.

Kaufmann W. E. and Moser H. W. (2000) Dendritic anomalies in disorders associated with mental retardation. *Cereb. Cortex* **10**, 981–991.

Kim E. J., Monje F. J., Li L., Hoger H., Pollak D. D. and Lubec G. (2012) Alzheimer's disease risk factor lymphocyte-specific protein tyrosine kinase regulates long-term synaptic strengthening, spatial learning and memory. *Cell. Mol. Life Sci.* **70**, 743–759.

Kobayashi C., Aoki C., Kojima N., Yamazaki H. and Shirao T. (2007) Drebrin a content correlates with spine head size in the adult mouse cerebral cortex. *J. Comp. Neurol.* **503**, 618–626.

Kojima N., Hanamura K., Yamazaki H., Ikeda T., Itohara S. and Shirao T. (2010) Genetic disruption of the alternative splicing of drebrin gene impairs context-dependent fear learning in adulthood. *Neuroscience* **165**, 138–150.

Lin R., Karpa K., Kabbani N., Goldman-Rakic P. and Levenson R. (2001) Dopamine D2 and D3 receptors are linked to the actin cytoskeleton via interaction with filamin A. *Proc. Natl Acad. Sci. USA* **98**, 5258–5263.

Merriam E. B., Lumbard D. C., Viesselmann C., Ballweg J., Stevenson M., Pietila L., Hu X. and Dent E. W. (2011) Dynamic microtubules promote synaptic NMDA receptor-dependent spine enlargement. *PLoS ONE* **6**, e27688.

Merriam E. B., Millette M., Lumbard D. C., Saengsawang W., Fothergill T., Hu X., Ferhat L. and Dent E. W. (2013) Synaptic regulation of microtubule dynamics in dendritic spines by calcium, F-actin, and drebrin. *J. Neurosci.* **33**, 16471–16482.

Mogha A., Guariglia S. R., Debata P. R., Wen G. Y. and Banerjee P. (2012) Serotonin 1A receptor-mediated signaling through ERK and PKCalpha is essential for normal synaptogenesis in neonatal mouse hippocampus. *Transl. Psychiatry* **2**, e66.

Monje F. J., Kim E. J., Pollak D. D., Cabatic M., Li L., Baston A. and Lubec G. (2012) Focal adhesion kinase regulates neuronal growth, synaptic plasticity and hippocampus-dependent spatial learning and memory. *Neurosignals* **20**, 1–14.

Nwabuisi-Heath E., LaDu M. J. and Yu C. (2012) Simultaneous analysis of dendritic spine density, morphology and excitatory glutamate receptors during neuron maturation in vitro by quantitative immunocytochemistry. *J. Neurosci. Methods* **207**, 137–147.

O'Dowd B. F., Ji X., Alijaniaram M., Nguyen T. and George S. R. (2011) Separation and reformation of cell surface dopamine receptor oligomers visualized in cells. *Eur. J. Pharmacol.* **658**, 74–83.

O'Dowd B. F., Ji X., Nguyen T. and George S. R. (2012) Two amino acids in each of D1 and D2 dopamine receptor cytoplasmic regions are involved in D1-D2 heteromer formation. *Biochem. Biophys. Res. Commun.* **417**, 23–28.

Rammes G., Starker L. K., Haseneder R., Berkmann J., Plack A., Zieglgansberger W., Ohl F., Kochs E. F. and Blobner M. (2009) Isoflurane anaesthesia reversibly improves cognitive function and long-term potentiation (LTP) via an up-regulation in NMDA receptor 2B subunit expression. *Neuropharmacology* **56**, 626–636.

Redondo R. L., Okuno H., Spooner P. A., Frenguelli B. G., Bito H. and Morris R. G. (2010) Synaptic tagging and capture: differential role of distinct calcium/calmodulin kinases in protein synthesis-dependent long-term potentiation. *J. Neurosci.* **30**, 4981–4989.

Rinaldi A., Mandillo S., Oliverio A. and Mele A. (2007) D1 and D2 receptor antagonist injections in the prefrontal cortex selectively impair spatial learning in mice. *Neuropsychopharmacology* **32**, 309–319.

Roberts A. J. and Hedlund P. B. (2012) The 5-HT(7) receptor in learning and memory. *Hippocampus* **22**, 762–771.

Rust M. B., Gurniak C. B., Renner M. *et al.* (2010) Learning, AMPA receptor mobility and synaptic plasticity depend on n-cofilin-mediated actin dynamics. *EMBO J.* **29**, 1889–1902.

Sarnyai Z., Sibille E. L., Pavlides C., Fenster R. J., McEwen B. S. and Toth M. (2000) Impaired hippocampal-dependent learning and functional abnormalities in the hippocampus in mice lacking serotonin(1A) receptors. *Proc. Natl Acad. Sci. USA* **97**, 14731–14736.

Schubert V. and Dotti C. G. (2007) Transmitting on actin: synaptic control of dendritic architecture. *J. Cell Sci.* **120**, 205–212.

Schwenk F., Baron U. and Rajewsky K. (1995) A cre-transgenic mouse strain for the ubiquitous deletion of loxP-flanked gene segments including deletion in germ cells. *Nucleic Acids Res* **23**, 5080–5081.

Sekino Y., Kojima N. and Shirao T. (2007) Role of actin cytoskeleton in dendritic spine morphogenesis. *Neurochem. Int.* **51**, 92–104.

Shim K. S. and Lubec G. (2002) Drebrin, a dendritic spine protein, is manifold decreased in brains of patients with Alzheimer's disease and Down syndrome. *Neurosci. Lett.* **324**, 209–212.

Shirao T. (1995) The roles of microfilament-associated proteins, drebrins, in brain morphogenesis: a review. *J. Biochem.* **117**, 231–236.

Shirao T. and Gonzalez-Billault C. (2013) Actin filaments and microtubules in dendritic spines. *J. Neurochem.* **126**, 155–164.

Shirao T., Kojima N., Terada S. and Obata K. (1990) Expression of three drebrin isoforms in the developing nervous system. *Neurosci. Res. Suppl.* **13**, S106–S111.

Shirao T., Hayashi K., Ishikawa R., Isa K., Asada H., Ikeda K. and Uyemura K. (1994) Formation of thick, curving bundles of actin by drebrin A expressed in fibroblasts. *Exp. Cell Res.* **215**, 145–153.

Simon W., Hapfelmeier G., Kochs E., Zieglgansberger W. and Rammes G. (2001) Isoflurane blocks synaptic plasticity in the mouse hippocampus. *Anesthesiology* **94**, 1058–1065.

So C. H., Varghese G., Curley K. J., Kong M. M., Alijaniaram M., Ji X., Nguyen T., O'Dowd B. F. and George S. R. (2005) D1 and D2 dopamine receptors form heterooligomers and cointernalize after selective activation of either receptor. *Mol. Pharmacol.* **68**, 568–578.

Takahashi H., Sekino Y., Tanaka S., Mizui T., Kishi S. and Shirao T. (2003) Drebrin-dependent actin clustering in dendritic filopodia governs synaptic targeting of postsynaptic density-95 and dendritic spine morphogenesis. *J. Neurosci.* **23**, 6586–6595.

Takahashi H., Mizui T. and Shirao T. (2006) Down-regulation of drebrin A expression suppresses synaptic targeting of NMDA receptors in developing hippocampal neurones. *J. Neurochem.* **97**(Suppl 1), 110–115.

Takahashi H., Yamazaki H., Hanamura K., Sekino Y. and Shirao T. (2009) Activity of the AMPA receptor regulates drebrin stabilization in dendritic spine morphogenesis. *J. Cell Sci.* **122**, 1211–1219.

Takahashi H., Yamada M. and Suhara T. (2012) Functional significance of central D1 receptors in cognition: beyond working memory. *J. Cereb. Blood Flow Metab.* **32**, 1248–1258.

Urbanska M., Swiech L. and Jaworski J. (2012) Developmental plasticity of the dendritic compartment: focus on the cytoskeleton. *Adv. Exp. Med. Biol.* **970**, 265–284.

Vastagh C., Gardoni F., Bagetta V., Stanic J., Zianni E., Giampa C., Picconi B., Calabresi P. and Di Luca M. (2012) N-methyl-D-aspartate (NMDA) receptor composition modulates dendritic spine morphology in striatal medium spiny neurons. *J. Biol. Chem.* **287**, 18103–18114.

Vijayraghavan S., Wang M., Birnbaum S. G., Williams G. V. and Arnsten A. F. (2007) Inverted-U dopamine D1 receptor actions on prefrontal neurons engaged in working memory. *Nat. Neurosci.* **10**, 376–384.

Wang H. D., Stanwood G. D., Grandy D. K. and Deutch A. Y. (2009) Dystrophic dendrites in prefrontal cortical pyramidal cells of dopamine D1 and D2 but not D4 receptor knockout mice. *Brain Res.* **1300**, 58–64.

Welinder C. and Ekblad L. (2011) Coomassie staining as loading control in Western blot analysis. *J. Proteome Res.* **10**, 1416–1419.

Wong G. T., Chang R. C. and Law A. C. (2013) A breach in the scaffold: the possible role of cytoskeleton dysfunction in the pathogenesis of major depression. *Ageing Res. Rev.* **12**, 67–75.

Yoshida H., Kanamaru C., Ohtani A., Li F., Senzaki K. and Shiga T. (2011) Subtype specific roles of serotonin receptors in the spine formation of cortical neurons in vitro. *Neurosci. Res.* **71**, 311–314.

